EBERHARD KARLS UNIVERSITÄT TÜBINGEN

FACULTY OF SCIENCE

Josephson Junctions & Superconducting Quantum Interference Devices (SQUIDs)

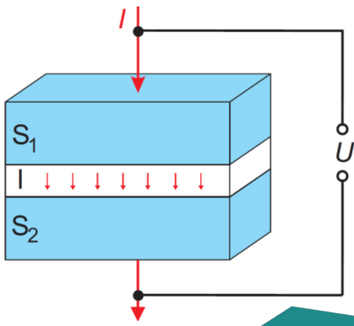

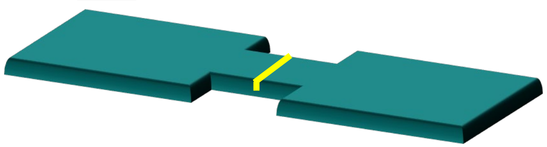

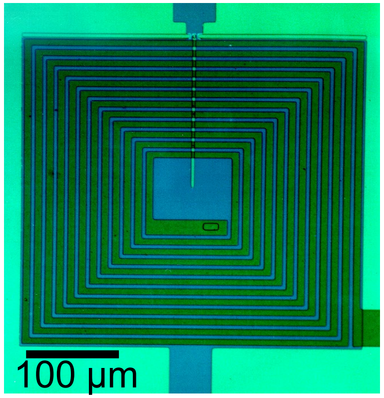

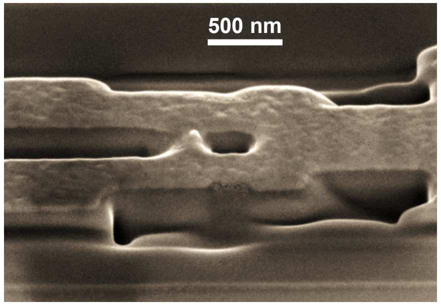

Dieter Koelle

Physikalisches Institut, Center for Quantum Science (CQ) and Center for Light-Matter Interaction, Sensors & Analytics (LISA+)

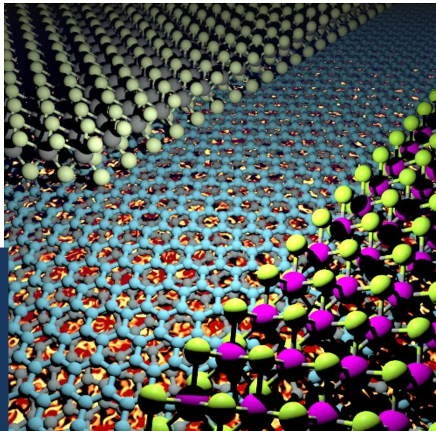

SuperQUMAP

European School on Superconductivity & Magnetism in Quantum Materials,

21-25 April 2024, Gandia (Valencia, Spain)


Baden-
Württemberg
Tübingen (population ~90,000)

EBERHARD KARLS UNIVERSITÄT TÜBINGEN

FACULTY OF SCIENCE

Part 1: Basic Properties of Josephson Junctions

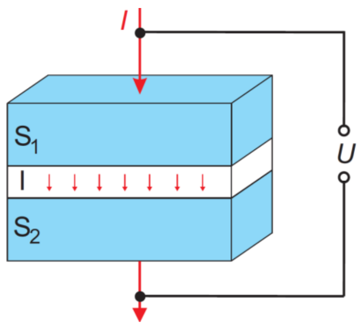

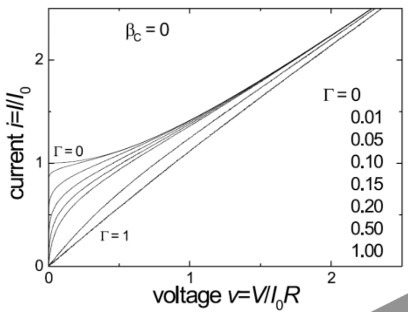

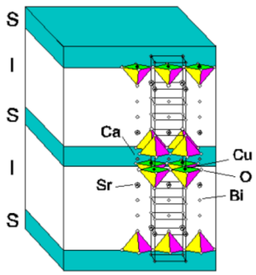

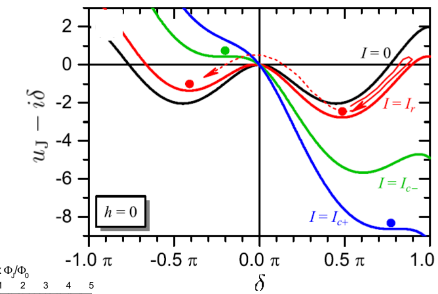

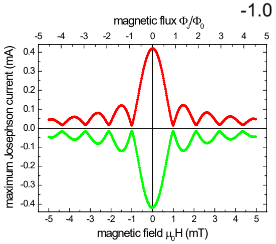

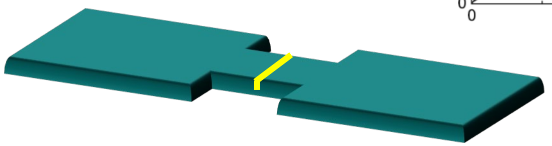

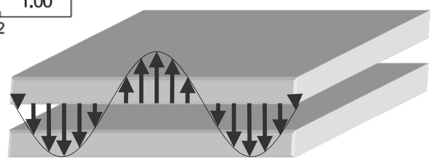

Dieter Koelle

Physikalisches Institut, Center for Quantum Science (CQ) and Center for Light-Matter Interaction, Sensors & Analytics (LISA⁺)

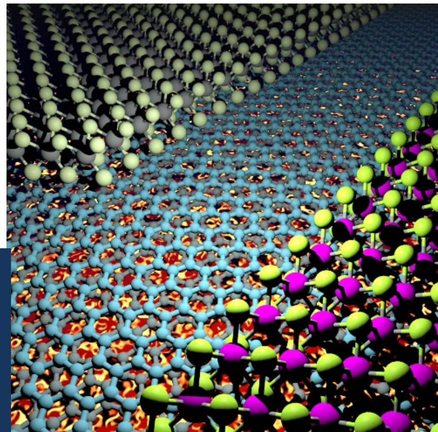

SuperQUMAP

European School on Superconductivity & Magnetism in Quantum Materials, 21-25 April 2024, Gandia (Valencia, Spain)

Motivation

Josephson junction (JJ) = two weakly coupled superconductors („weak link“)

quantum mechanical coupling of the superconductor wave functions

⇨ insights into basic properties of superconductors

e.g. phase-sensitive experiments on the order parameter symmetry of unconventional superconductors, based on interference effects

⇨ JJ is the key element in superconducting electronics

large variety of devices for many applications, e.g.

- voltage standards,
- SQUID magnetometers,
- radiation detectors,
- qubits,
- ultrafast processors,
- ...

EBERHARD KARLS
UNIVERSITÄT
TÜBINGEN

Outline

1. **Macroscopic Wave Function**
2. **Josephson Relations & Consequences**
3. **Josephson Junction in a Magnetic Field**
4. **Resistively & Capacitively Shunted Junction (RCSJ) model**
5. **Fluctuations in Josephson Junctions**
6. **Classification of JJs – Ground States: 0- π-, φ-Junctions**

Books:

A. Barone & G. Paterno, *Physics & Applications of the Josephson Effect*, J. Wiley & Sons (1982)

K.K. Likharev, *Dynamics of Josephson Junctions and Circuits*, Gordon & Breach (1986)

T.P. Orlando, K.A. Delin, *Foundations of Applied Superconductivity*, Addison-Wesley (1991)

W. Buckel, R. Kleiner, *Superconductivity*, Wiley-VCH, 3rd ed. (2016)

Reviews:

K.K. Likharev, *Superconducting weak links*, Rev. Mod. Phys. **51**, 101 (1979)

A.A. Golubov, M.Yu. Kupriyanov, E. Il‘ichev, *The current phase relation in Josephson junctions*, Rev. Mod. Phys. **76**, 411 (2004)

A.I. Buzdin, *Proximity effects in superconductor-ferromagnet heterostructures*, Rev. Mod. Phys. **77**, 935 (2005)

EBERHARD KARLS UNIVERSITÄT TÜBINGEN

Macroscopic Wave Function

a single (macroscopic) wave function describes the state of all Cooper pairs in a superconductor
→ highly correlated, coherent many-particle quantum state

superconducting charge carriers: Cooper pairs (mobile electrons correlated in momentum *k*-space)

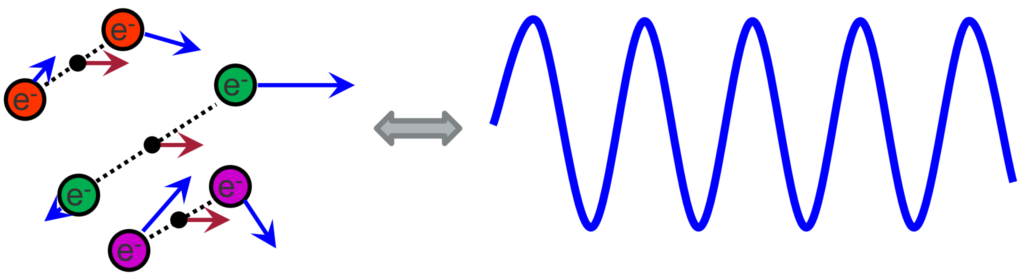

macroscopic wave function

$$\boxed{\Psi = \Psi_0 \cdot e^{i\varphi}}$$

phase φ
determined by carrier velocity $\boldsymbol{v}_\mathrm{s}$
& vector potential $\boldsymbol{A}$
(connected to magnetic field via relation for magnetic induction (flux density) $\boldsymbol{B} = \boldsymbol{\nabla} \times \boldsymbol{A}$

amplitude $\Psi_0 = \sqrt{n_\mathrm{s}}$
n_s: Cooper pair density

$$\boxed{\hbar \boldsymbol{\nabla} \varphi = m_\mathrm{s} \boldsymbol{v}_\mathrm{s} + q_\mathrm{s} \boldsymbol{A}}$$

Cooper pair charge $q_\mathrm{s} = 2e$
and mass $m_\mathrm{s} = 2m_e$

Macroscopic Wave Function

a single (macroscopic) wave function
describes the state of all Cooper pairs in a superconductor
→ highly correlated, coherent many-particle quantum state

Cooper pairs
highly correlated
motion

supercurrent density: $$\boxed{\boldsymbol{j}_\mathrm{s} = q_\mathrm{s} n_\mathrm{s} \boldsymbol{v}_\mathrm{s} = \frac{q_\mathrm{s} n_\mathrm{s}}{m_\mathrm{s}} \left(\hbar \boldsymbol{\nabla} \varphi - q_\mathrm{s} \boldsymbol{A} \right)}$$

Macroscopic Wave Function

with the definition of the **gauge-invariant phase gradient**

$$\boldsymbol{\nabla}\phi \equiv \boldsymbol{\nabla}\varphi - \frac{q_\mathrm{s}}{\hbar}\boldsymbol{A} \quad \text{or} \quad \boxed{\boldsymbol{\nabla}\phi \equiv \boldsymbol{\nabla}\varphi - \frac{2\pi}{\Phi_0}\boldsymbol{A}}$$

with $q_s = 2e$ and magnetic flux quantum $\Phi_0 \equiv \frac{h}{2e}$

$$\boldsymbol{j}_\mathrm{s} = \frac{q_\mathrm{s}\hbar}{m_s} n_\mathrm{s}\boldsymbol{\nabla}\phi \quad \text{i.e.} \quad \boxed{\boldsymbol{j}_\mathrm{s} \propto n_\mathrm{s}\boldsymbol{\nabla}\phi}$$

integration of $\boldsymbol{\nabla}\phi \equiv \boldsymbol{\nabla}\varphi - \frac{2\pi}{\Phi_0}\boldsymbol{A}$ ⇨ **gauge-invariant phase**

$$\boxed{\phi(\boldsymbol{r}) = \varphi(\boldsymbol{r}) - \frac{2\pi}{\Phi_0}\int_{\boldsymbol{r}_0}^{\boldsymbol{r}} \boldsymbol{A}\mathrm{d}\boldsymbol{r}}$$

Weakly Coupled Superconductors

consider now two superconductors S_1, S_2 with macroscopic wave functions

$$\Psi_i = \Psi_{0,i} \cdot e^{i\varphi_i} \qquad (i = 1, 2)$$

What is the relation between the wave functions Ψ_i (phases φ_i) if the two superconductors are coupled via a weak link?
(e.g. via insulating (I) tunnel barrier in a SIS junction)

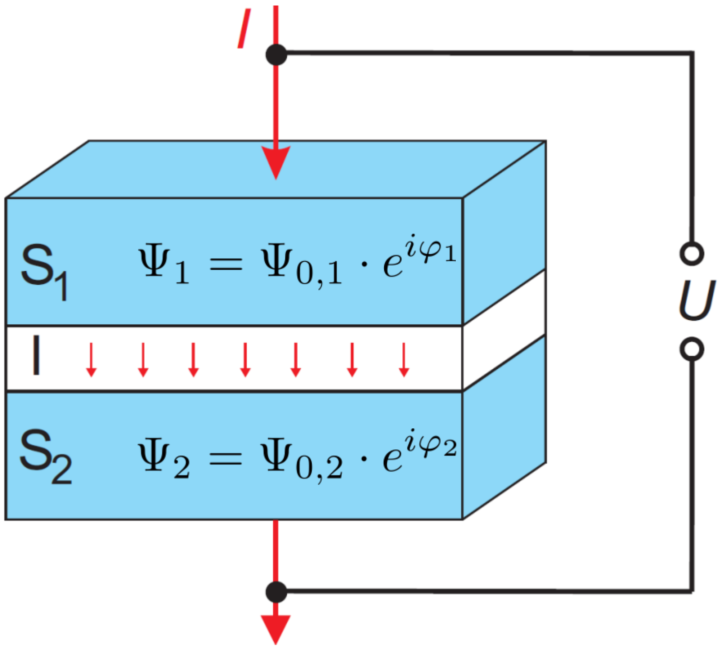

finite coupling ⟺ overlap of the wave functions Ψ_i

⇒ supercurrent through weak link (across barrier)

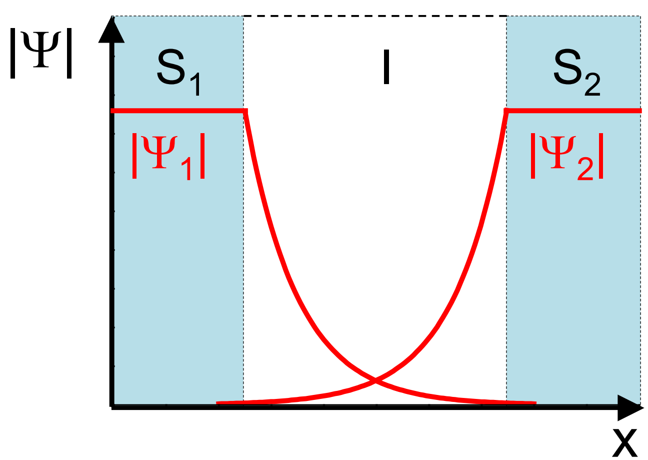

Outline

I. Macroscopic Wave Function

II. Josephson Relations & Consequences

III. Josephson Junction in a Magnetic Field

IV. Resistively & Capacitively Shunted Junction (RCSJ) model

V. Fluctuations in Josephson Junctions

VI. Classification of JJs – Ground States: 0- π-, φ-Junctions

Josephson Relations

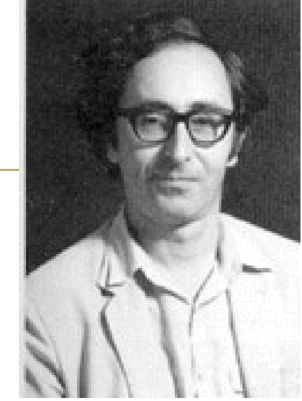

B. D. Josephson
Nobel prize physics 1973

connect phase of the wave functions
to current *I* and voltage *U* across weak link

derivation by solving Schrödinger Eq. for two coupled quantum mechanical systems → Feynman

Alternative: following general arguments by Landau & Lifschitz

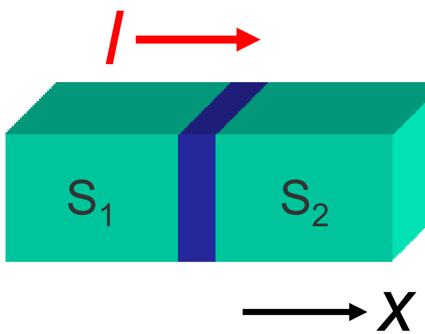

assume

- barrier in (y,z) plane
- constant current density in (y,z)
- constant phase gradient and n_s in the S_1, S_2 electrodes

B.D. Josephson, *Possible new effects in superconductive tunneling*, Phys. Lett. **1**, 251 (1962)
R.P. Feynman, R.B. Leighton, M. Sands, *Feynman Lectures on Physics* **3**, Addison-Wesley (1965)
L.D. Landau, E.M. Lifschitz, *Lehrbuch der Theoretischen Physik* ***IX***, Akademie-Verlag (1980)
W. Buckel, R. Kleiner, *Superconductivity*, Wiley-VCH, 3rd ed. (2016)

Josephson Relations

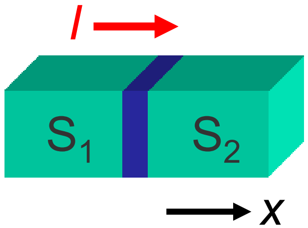

for current I along x and cross section A_J=const

$$j_s(x) = I/A_J = const$$

i.e., because of $\boldsymbol{j}_s \propto n_s \nabla\phi$ ⇨ $n_s(x) \cdot \frac{\partial\phi}{\partial x}(x) = const$

⇨ **change in n_s at weak link has to be compensated by change in $\partial\phi/\partial x$**

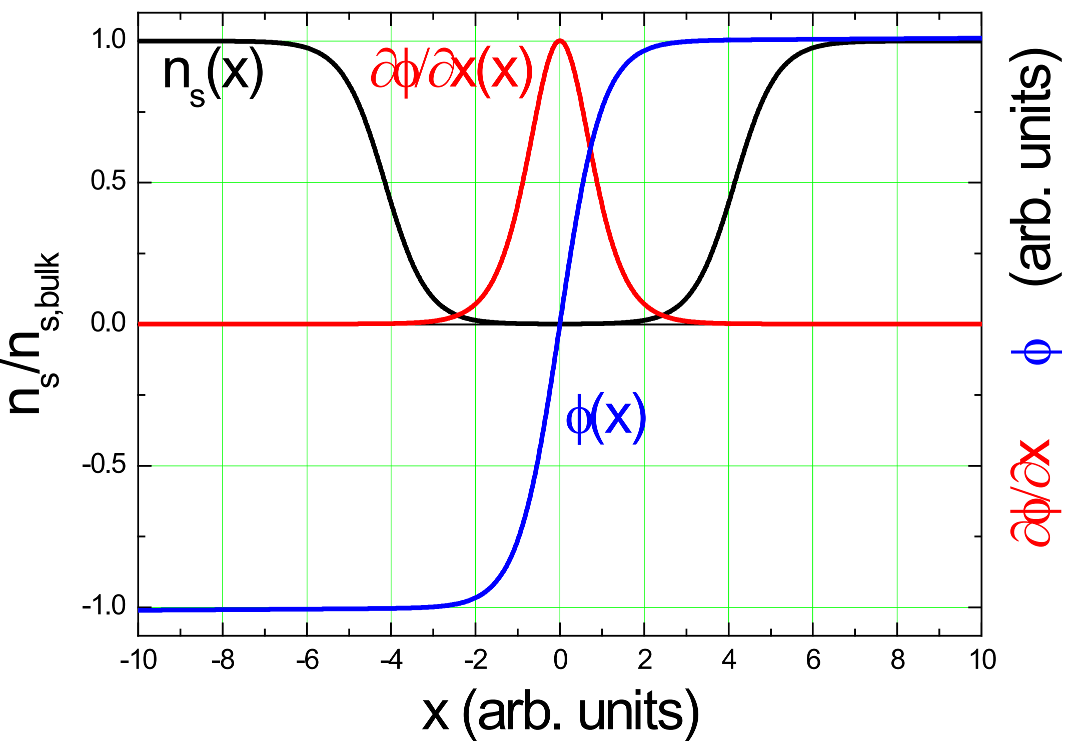

suppressed n_s at barrier
→ dip in $n_s(x)$

⇨ peak in $\partial\phi/\partial x$

⇨ $\phi(x)$ makes a step

Josephson Relations

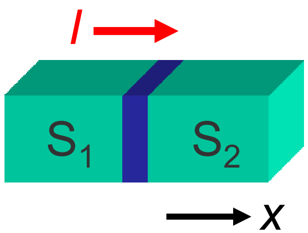

weak link is characterized by a **phase difference**

$$\boxed{\delta \equiv \phi_2 - \phi_1 = \varphi_2 - \varphi_1 - \frac{2\pi}{\Phi_0}\int_1^2 A_x \mathrm{d}x}$$

integral across barrier

⇨ analogous to $\boldsymbol{j}_\mathrm{s} \propto \boldsymbol{\nabla}\phi$ in the bulk superconductor,
j_s across the weak link is a function of the phase difference

$$\boldsymbol{j}_\mathrm{s} = \boldsymbol{j}_\mathrm{s}(\delta)$$

Josephson Relations

Question: what is the functional dependence of $j_s(\delta)$?

⇨ from simple considerations:

- phases ϕ_i in the electrodes are defined modulo 2π
  (phase change of $2\pi n$ (n: integer) does not change Ψ_i)

  ⇨ j_s = 2π-periodic function of δ

$$j_\mathrm{s} = \sum_n j_{0n} \sin n\delta + \sum_n \tilde{j}_{0n} \cos n\delta \qquad (n = 1, 2, \ldots)$$

- time reversal symmetry: $j_\mathrm{s}(\delta) = -j_\mathrm{s}(-\delta)$
  (both, currents and phases ($\sim\omega t$) change sign upon time reversal)

  ⇨ excludes cosine terms

- rapid convergence of sin-series (e.g. for conventional SIS junctions)

$$\boxed{j_\mathrm{s} = j_0 \sin\delta}$$

1. Josephson relation (current-phase relation = CPR)

Josephson Relations

Question: what is the evolution of δ in time ?

take time derivative of gauge-invariant phase difference $\delta = \varphi_2 - \varphi_1 - \frac{2\pi}{\Phi_0}\int_1^2 \boldsymbol{A}\cdot \mathrm{d}\boldsymbol{l}$

$$\frac{\partial \delta}{\partial t} = \frac{\partial \varphi_2}{\partial t} - \frac{\partial \varphi_1}{\partial t} - \frac{2\pi}{\Phi_0}\frac{\partial}{\partial t}\int_1^2 \boldsymbol{A}\cdot \mathrm{d}\boldsymbol{l}$$

with energy-phase relation $-\hbar\frac{\partial \varphi}{\partial t} = \frac{\mu_0 \lambda_\mathrm{L}^2}{2n_\mathrm{s}}\boldsymbol{j}_\mathrm{s}^2 + q_\mathrm{s}\tilde{\phi}$ (derived from Schrödinger equation for n_s=const in the electrodes)

with London penetration depth $\lambda_\mathrm{L} = \left(\frac{m_\mathrm{s}}{\mu_0 q_\mathrm{s}^2 n_\mathrm{s}}\right)^{1/2}$

and electrochemical potential $\tilde{\phi}$ related to electric field $\boldsymbol{E} = -\frac{\partial \boldsymbol{A}}{\partial t} - \boldsymbol{\nabla}\tilde{\phi}$

$$\frac{\partial \delta}{\partial t} = -\frac{1}{\hbar}\left(\frac{\mu_0 \lambda_\mathrm{L}^2}{2n_\mathrm{s}}\underbrace{\left[\boldsymbol{j}_\mathrm{s}^2(2) - \boldsymbol{j}_\mathrm{s}^2(1)\right]}_{=0 \text{ (current continuity)}} + q_\mathrm{s}\left[\tilde{\phi}_2 - \tilde{\phi}_1\right]\right) - \frac{2\pi}{\Phi_0}\frac{\partial}{\partial t}\int_1^2 \boldsymbol{A}\cdot \mathrm{d}\boldsymbol{l}$$

$$\frac{\partial \delta}{\partial t} = \frac{2\pi}{\Phi_0}\int_1^2 \underbrace{\left(-\boldsymbol{\nabla}\tilde{\phi} - \frac{\partial \boldsymbol{A}}{\partial t}\right)}_{= \text{ electric field } \boldsymbol{E}}\cdot \mathrm{d}\boldsymbol{l} \quad \Rightarrow \quad \frac{\partial \delta}{\partial t} \equiv \boxed{\dot{\delta} = \frac{2\pi}{\Phi_0}U}$$

2. Josephson relation (voltage-phase relation)

voltage across junction

T.P. Orlando, K.A. Delin, *Foundations of Applied Superconductivity*, Addison-Wesley (1991)

Consequences of Josephson Relations

1. zero voltage state (static case) $U = 0 \Rightarrow \delta = const = \delta_0$

$\Rightarrow$ $j_s = j_0 \sin\delta_0$ $\Rightarrow$ maximum supercurrent density across junction:

$\sin\delta_0 = 1 \Rightarrow \boxed{j_{s,max} = j_0}$ critical current density

$\Rightarrow$ $j_0 \ll j_{c,deparing}$ $\Rightarrow$ „weak link“

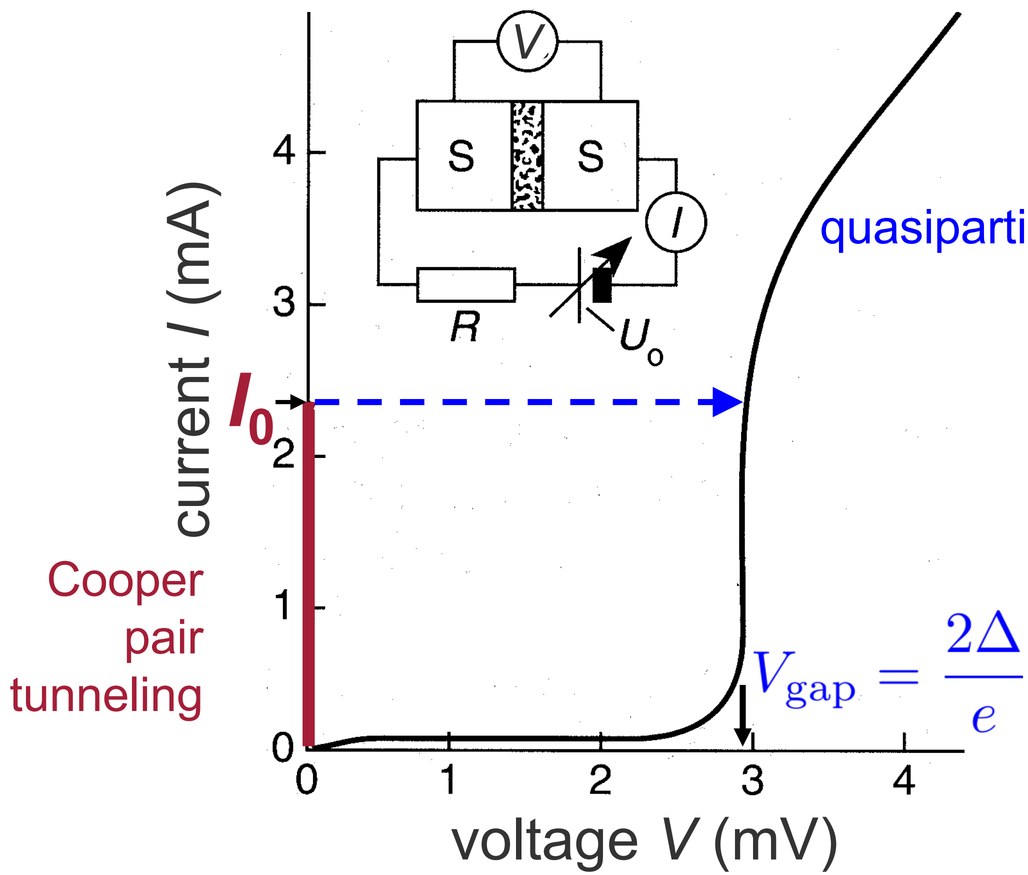

Δ: energy gap in the quasiparticle density of states

Consequences of Josephson Relations

2. finite voltage state (dynamic case) $U \neq 0$

for $U = const$ integrate 2nd Josephson Eq. $\delta(t) = \delta_0 + 2\pi \frac{U}{\Phi_0} t$

insert into 1st Josephson Eq. $j_s = j_0 \sin\{\delta_0 + 2\pi f_J t\}$

⇨ Cooper pair current across junction oscillating with the **Josephson frequency**

$$\boxed{f_J \equiv \frac{U}{\Phi_0} \approx 483.6 \, \frac{\text{GHz}}{\text{mV}} \cdot U}$$

⇨ **quantum interference of the wave functions across the barrier**

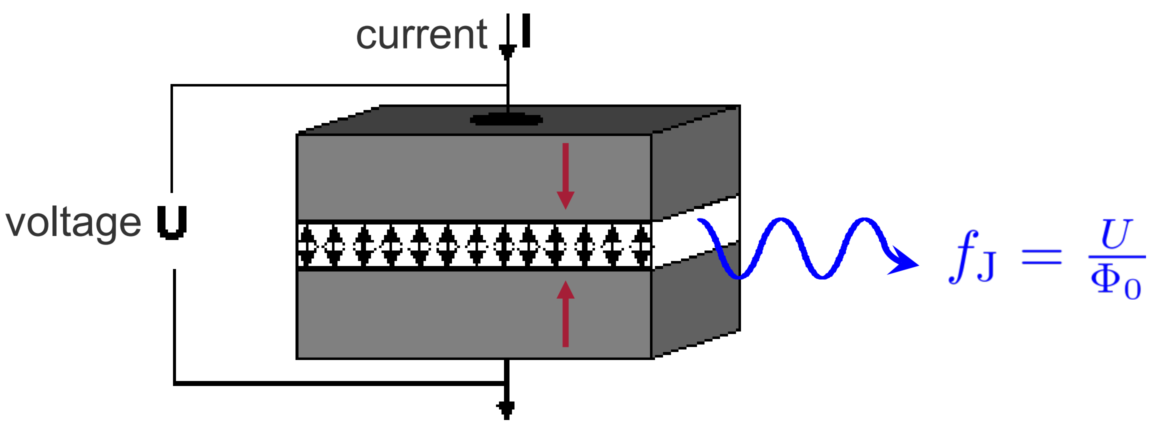

Outline

I. Macroscopic Wave Function

II. Josephson Relations & Consequences

III. Josephson Junction in a Magnetic Field

IV. Resistively & Capacitively Shunted Junction (RCSJ) model

V. Fluctuations in Josephson Junctions

VI. Classification of JJs – Ground States: 0- π-, φ-Junctions

Josephson Junction in a Magnetic Field

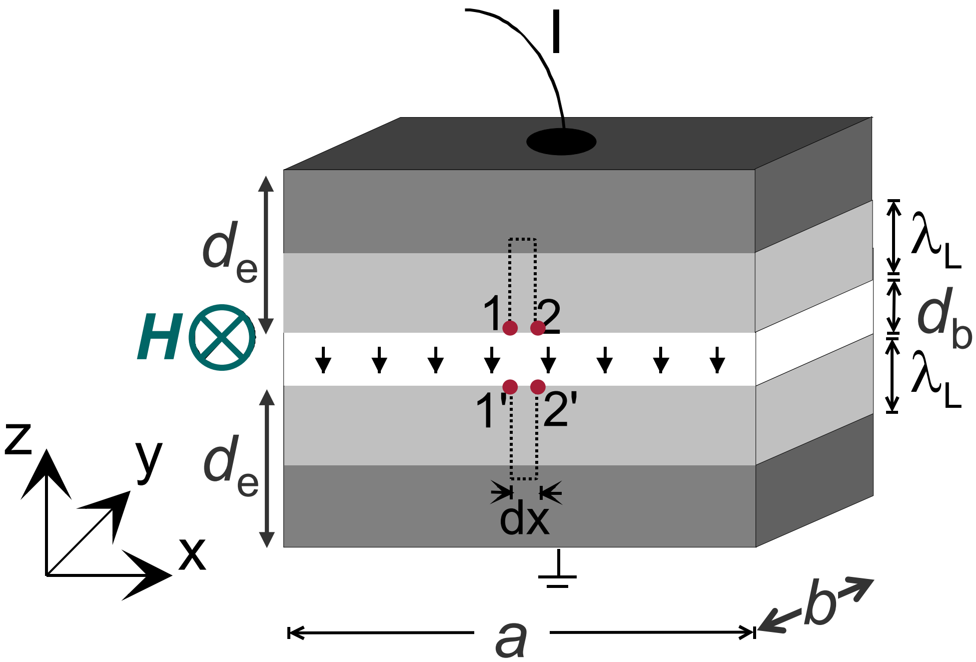

field *H* applied in the JJ plane
(rectangular barrier)

magnetic flux density ***B*** penetrates into electrodes
→ effective magnetic thickness:

$$d_{\mathrm{eff}} \approx d_{\mathrm{b}} + 2\lambda_{\mathrm{L}}$$

for identical electrode materials with thickness $d_{\mathrm{e}} \gtrsim 2\lambda_{\mathrm{L}}$

for different electrode materials with thickness $d_{e,i}$:

$$d_{\mathrm{eff}} \equiv d_{\mathrm{b}} + \lambda_{\mathrm{L},1} \tanh \frac{d_{\mathrm{e},1}}{\lambda_{\mathrm{L},1}} + \lambda_{\mathrm{L},2} \tanh \frac{d_{\mathrm{e},2}}{\lambda_{\mathrm{L},2}}$$

Josephson Junction in a Magnetic Field

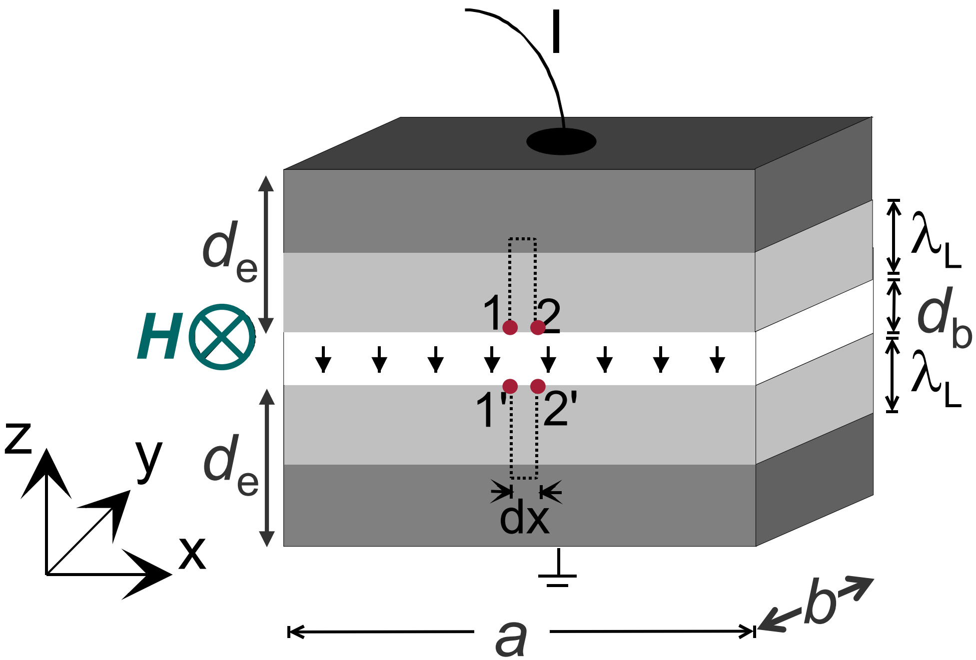

relation between *B* and δ ?

$$\boldsymbol{B} = \boldsymbol{\nabla} \times \boldsymbol{A}$$

$$\delta = \varphi_2 - \varphi_1 - \frac{2\pi}{\Phi_0} \int_1^2 \boldsymbol{A} \cdot \mathrm{d}\boldsymbol{l}$$

from $\boldsymbol{j}_\mathrm{s} = \frac{q_\mathrm{s} n_\mathrm{s}}{m_\mathrm{s}} \left(\hbar \boldsymbol{\nabla} \varphi - q_\mathrm{s} \boldsymbol{A} \right)$

$$\boldsymbol{\nabla} \varphi = \frac{2\pi}{\Phi_0} \left(\mu_0 \lambda_\mathrm{L}^2 \boldsymbol{j}_\mathrm{s} + \boldsymbol{A} \right)$$

with $\mu_0 \lambda_\mathrm{L}^2 = \frac{m_\mathrm{s}}{q_\mathrm{s}^2 n_\mathrm{s}}$

integrate $\boldsymbol{\nabla} \varphi$ along dotted lines in the two electrodes

path 2→1: $$\varphi(1) - \varphi(2) = \frac{2\pi}{\Phi_0} \mu_0 \lambda_\mathrm{L}^2 \int_2^1 \boldsymbol{j}_\mathrm{s} \, \mathrm{d}\boldsymbol{l} + \frac{2\pi}{\Phi_0} \int_2^1 \boldsymbol{A} \, \mathrm{d}\boldsymbol{l}$$

path 1´→2´: $$\varphi(2') - \varphi(1') = \frac{2\pi}{\Phi_0} \mu_0 \lambda_\mathrm{L}^2 \int_{1'}^{2'} \boldsymbol{j}_\mathrm{s} \, \mathrm{d}\boldsymbol{l} + \frac{2\pi}{\Phi_0} \int_{1'}^{2'} \boldsymbol{A} \, \mathrm{d}\boldsymbol{l}$$

Josephson Junction in a Magnetic Field

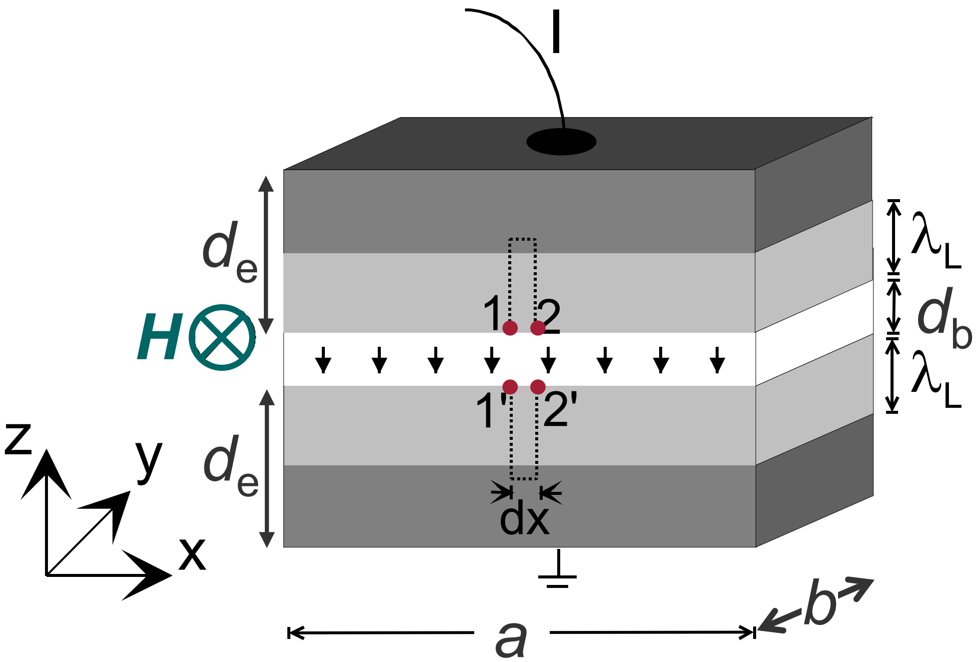

sum up both Eqs. and add
on both sides integrals across barrier

$$\frac{2\pi}{\Phi_0}\int_1^{1'} \boldsymbol{A}\,\mathrm{d}\boldsymbol{l} + \frac{2\pi}{\Phi_0}\int_{2'}^{2} \boldsymbol{A}\,\mathrm{d}\boldsymbol{l}$$

magnetic flux through integration path

$$\overbrace{\varphi(2')-\varphi(2)-\frac{2\pi}{\Phi_0}\int_2^{2'} \boldsymbol{A}\,\mathrm{d}\boldsymbol{l}}^{\delta(x+\mathrm{d}x)} - \left(\overbrace{\varphi(1')-\varphi(1)-\frac{2\pi}{\Phi_0}\int_1^{1'} \boldsymbol{A}\,\mathrm{d}\boldsymbol{l}}^{\delta(x)}\right) = \frac{2\pi}{\Phi_0}\overbrace{\oint \boldsymbol{A}\,\mathrm{d}\boldsymbol{l}}^{\Phi = B d_{\mathrm{eff}}\mathrm{d}x} + \frac{2\pi}{\Phi_0}\mu_0\lambda_L^2\left(\underbrace{\int_2^1 \boldsymbol{j}_s\,\mathrm{d}\boldsymbol{l} + \int_{1'}^{2'} \boldsymbol{j}_s\,\mathrm{d}\boldsymbol{l}}_{\approx 0}\right)$$

for thick enough electrodes
in the Meissner state

magnetic field induces a gradient of δ along the JJ

$$\frac{\partial\delta}{\partial x} = \frac{2\pi}{\Phi_0} B d_{\mathrm{eff}}$$

Josephson Junction in a Magnetic Field

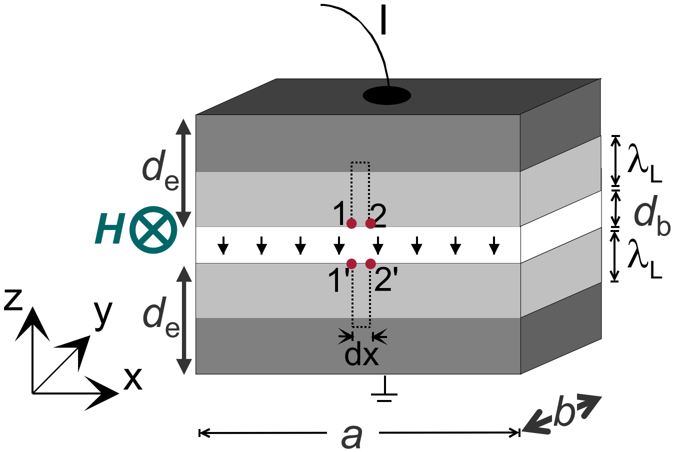

General case: applied field $\boldsymbol{H}$ can be screened by supercurrents flowing across the JJ

with Ampere's law $\nabla \times \boldsymbol{B} = \mu_0 \boldsymbol{j}$

for our geometry $\boldsymbol{B} = B_y \hat{\boldsymbol{e}}_y$: $\frac{\partial B_y(x)}{\partial x} = \mu_0 j_z(x)$

combined with $\frac{\partial \delta}{\partial x} = \frac{2\pi}{\Phi_0} B_y d_{\mathrm{eff}}$ $\Rightarrow$ $\frac{\partial^2 \delta}{\partial x^2} = \frac{2\pi}{\Phi_0} d_{\mathrm{eff}} \frac{\partial B_y}{\partial x} = \frac{1}{\lambda_J^2} \frac{j_z(x)}{j_0} = \frac{1}{\lambda_J^2} \sin \delta(x)$

Ferrel-Prange Eq.

with the Josephson length $\lambda_J \equiv \left(\frac{\Phi_0}{2\pi \mu_0 d_{\mathrm{eff}} j_0} \right)^{1/2}$

for small applied fields: $\frac{\partial^2 \delta}{\partial x^2} = \frac{1}{\lambda_J^2} \delta(x)$ $\Rightarrow$ $\delta(x) = \delta(0) e^{-\frac{x}{\lambda_J}}$

$\left(\frac{\partial \delta}{\partial x} \ll \frac{1}{\lambda_J} \right)$

$\Rightarrow$ $B_y(x) = B_y(0) e^{-\frac{x}{\lambda_J}}$

λ_J is the characteristic length over which a JJ can screen external magnetic fields
(similar to λ_L in a bulk superconductor)

Short JJ in a Magnetic Field

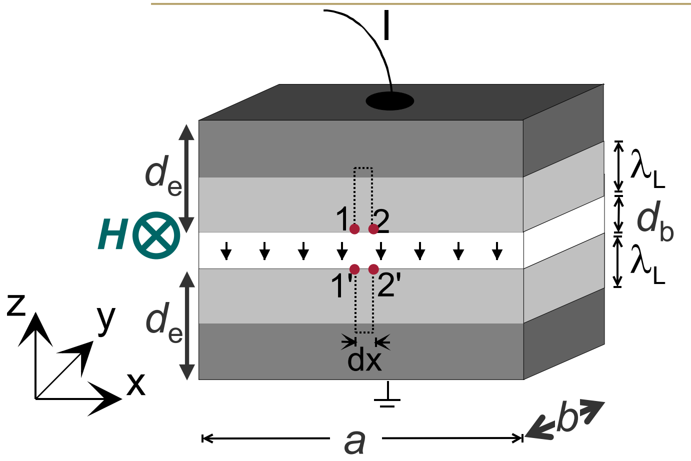

„short junction“ limit:
size of JJ along direction ⊥***H***

$$\boxed{a \lesssim 4\lambda_J}$$

⇒ magnetic field penetrates JJ homogeneously along the barrier

$$B(x) = const$$

⇒ magnetic flux in the JJ:

$$\boxed{\Phi_J = B\, d_{\text{eff}}\, a}$$

integration of $\frac{\partial \delta}{\partial x} = \frac{2\pi}{\Phi_0} B d_{\text{eff}}$ along x ⇒ $\delta(x) = \delta_0 + \frac{2\pi}{\Phi_0} B d_{\text{eff}} x$

δ(x) grows linearly along barrier
(slope determined by $B=\mu_0 H$)

Short JJ in a Magnetic Field

$\delta(x) = \delta_0 + \frac{2\pi}{\Phi_0} B d_{\mathrm{eff}} x$ inserted into 1st Josephson relation:

$$j_s(x) = j_0 \sin\left\{\delta(0) + \frac{2\pi}{\Phi_0} B\, d_{\mathrm{eff}} \cdot x\right\}$$

⇨ ***j*$_s$(*x*) oscillates with a wavelength** $= \frac{\Phi_0}{B d_{\mathrm{eff}}} = a \frac{\Phi_0}{\Phi_J}$

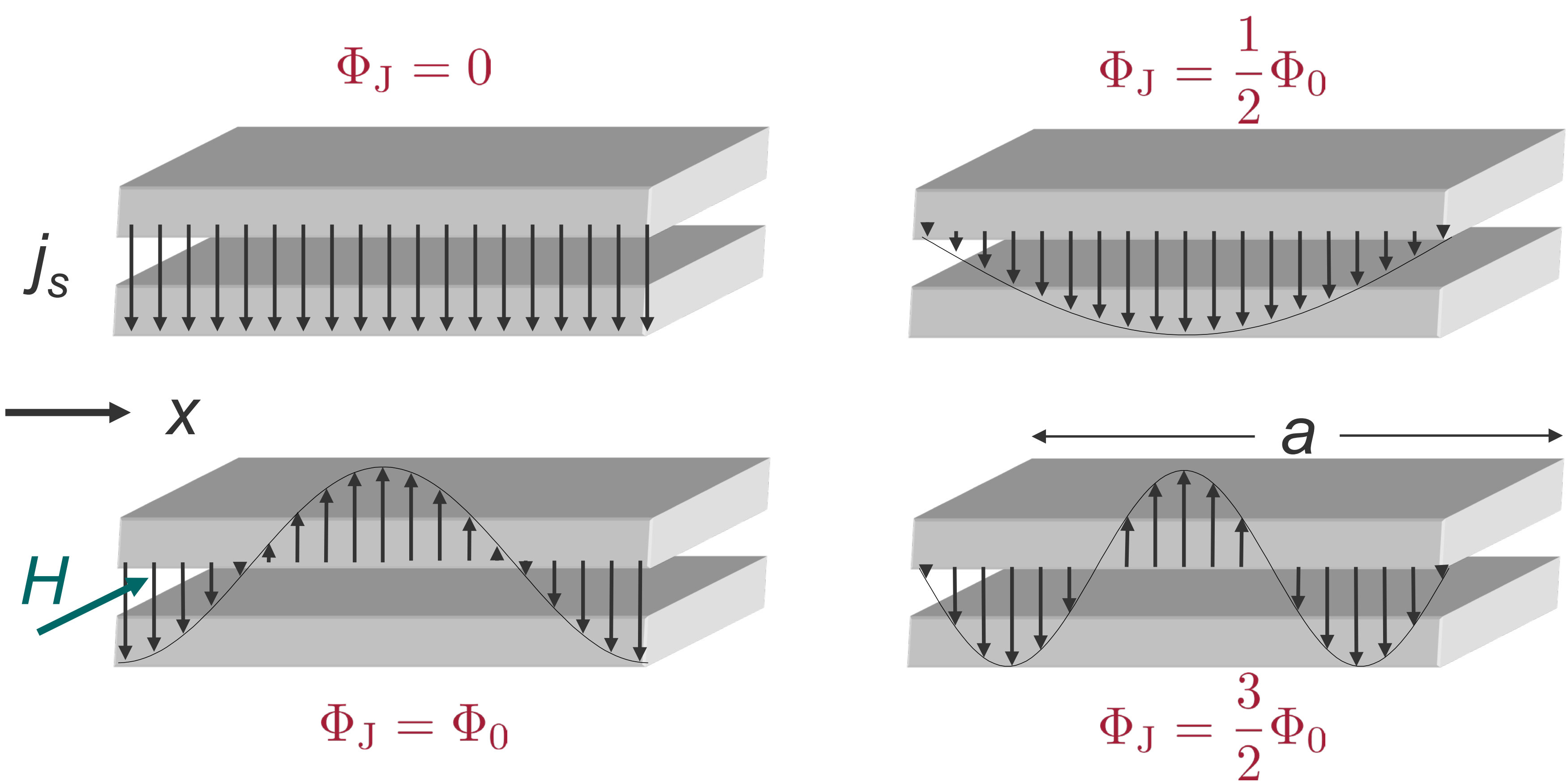

Short JJ in a Magnetic Field

total supercurrent I_s through the JJ → integrate $j_s(x)$ over JJ area $A_\mathrm{J} = ab$

$$I_\mathrm{s}(\Phi_\mathrm{J}, \delta_0) = \int_0^b \mathrm{d}y \int_0^a \mathrm{d}x j_0 \sin\delta(x) = -j_0 \cdot b \cdot \left.\frac{\cos\left(\delta_0 + \frac{2\pi}{\Phi_0} B d_\mathrm{eff} x\right)}{\left(\frac{2\pi}{\Phi_0} B d_\mathrm{eff}\right)}\right|_0^a$$

$\Phi_\mathrm{J} = B\, d_\mathrm{eff}\, a$

$$= \underbrace{j_0 \cdot b \cdot a}_{I_0} \cdot \frac{\sin \pi \frac{\Phi_J}{\Phi_0}}{\pi \frac{\Phi_J}{\Phi_0}} \cdot \sin(\delta_0 + \pi \frac{\Phi_J}{\Phi_0})$$

for given I_s, Φ_J → δ_0 adjusts accordingly

maximum supercurrent I_c through the JJ:

→ $\sin(\delta_0 + \pi \frac{\Phi_\mathrm{J}}{\Phi_0}) = \pm 1$

$$\boxed{I_c(\Phi_\mathrm{J}) = I_0 \cdot \left| \frac{\sin \pi \frac{\Phi_\mathrm{J}}{\Phi_0}}{\pi \frac{\Phi_\mathrm{J}}{\Phi_0}} \right|}$$

Fraunhofer pattern

(analogous to diffraction at single slit in optics)

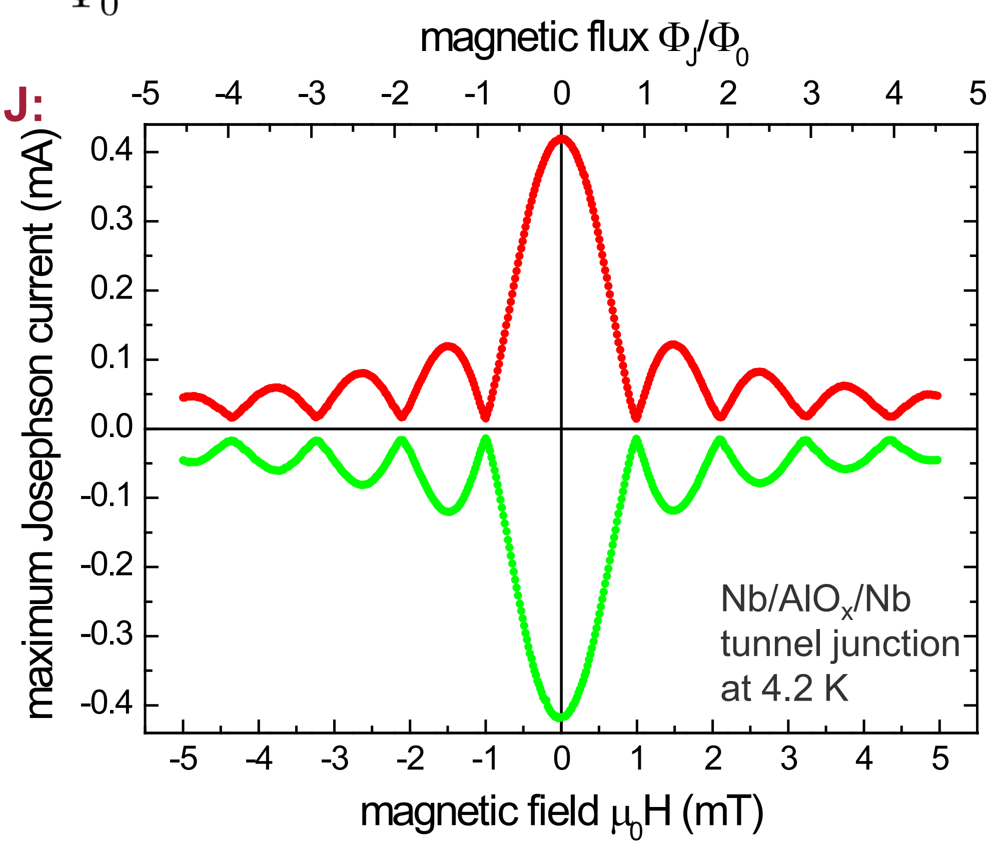

Outline

RCSJ Model & Washboard Potential

resistively and capacitively shunted junction (RCSJ)

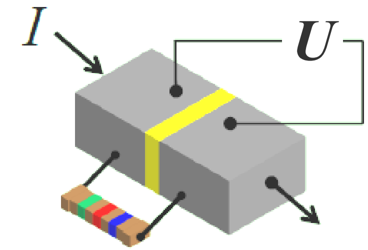

simple model to describe dynamics of JJs
→ current voltage characteristics (IVC)

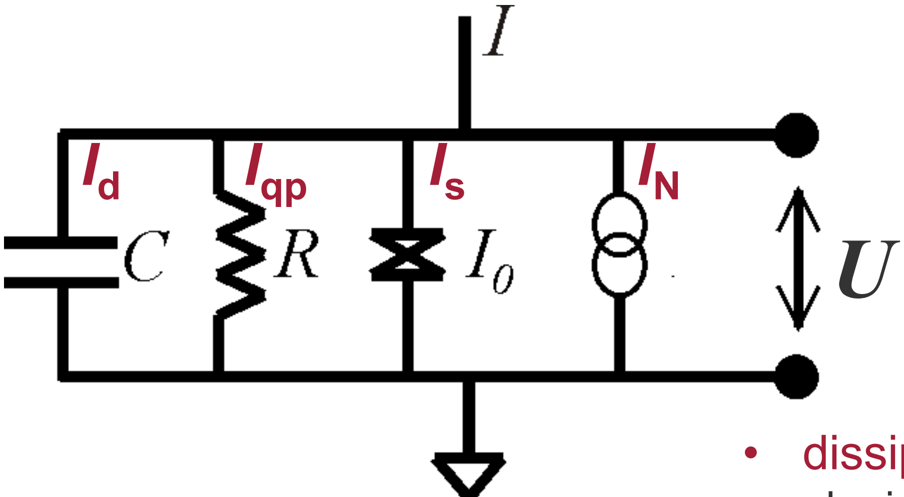

- Josephson current $I_\mathrm{s} = I_0 \sin\delta$
- displacement current across junction capacitance C $I_\mathrm{d} = C\dot{U}$
- dissipative (quasiparticle) current ohmic current through shunt resistor R $I_\mathrm{qp} = U/R$
- current noise source $I_\mathrm{N}(t)$ thermal noise of shunt resistor R at temperature T, with spectral density $S_I(f) = \frac{4k_BT}{R}$

W.C. Stewart, *Current-voltage characteristics of Josephson junctions*, Appl. Phys. Lett. **12**, 277 (1968)
D.E. McCumber, *Effect of ac impedance on dc voltage-current characteristics of Josephson junctions*, J. Appl. Phys. **39**, 3113 (1968)

RCSJ Model & Washboard Potential

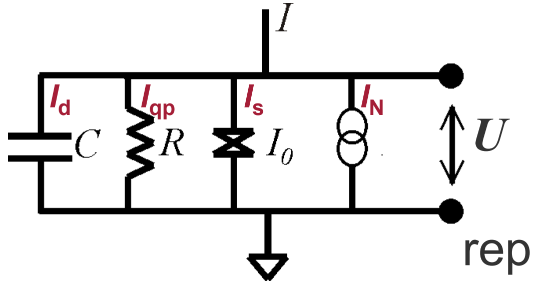

from Kirchoff's law:

$$I + I_N(t) = I_0 \sin\delta + \frac{U}{R} + C\dot{U}$$

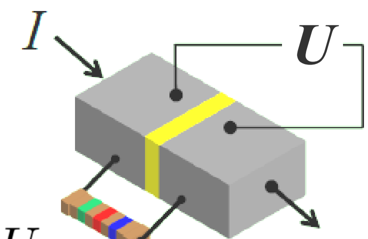

replace $U \rightarrow \dot{\delta}$ via 2nd Josephson relation $\dot{\delta} = \frac{2\pi}{\Phi_0} U$

Eq. of motion for δ :

$$\boxed{I + I_N(t) = I_0 \sin\delta + \frac{\Phi_0}{2\pi R}\,\dot{\delta} + \frac{\Phi_0 C}{2\pi}\,\ddot{\delta}}$$

finite voltage contains high-frequency Josephson oscillations → experimentally detected voltage: $V \equiv \langle U \rangle = \frac{1}{t_{av}} \int_0^{tav} \mathrm{d}t\, U(t)$

averaged over time $t_{av} \gg \frac{1}{f_J}$

solution of Eq. of motion (numerical simulations)

$\delta(t) \Rightarrow \dot{\delta}(t) \propto U(t) \Rightarrow V$ for given bias current *I*

current-voltage characteristics (IVC)

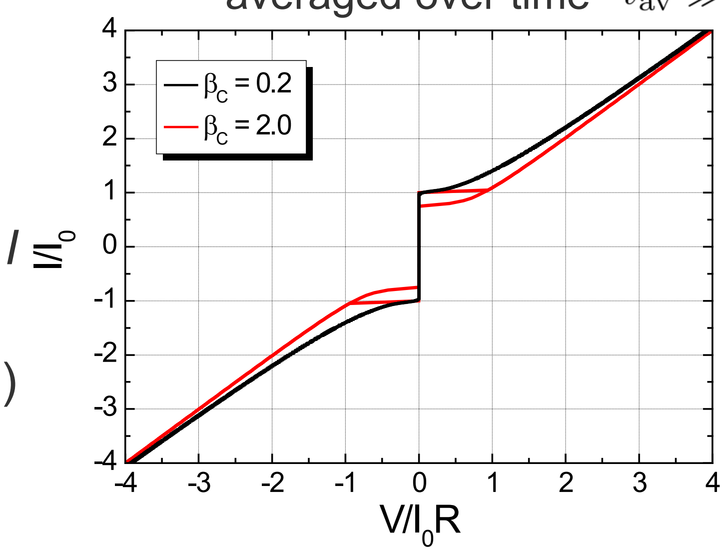

RCSJ Model & Washboard Potential

rearrange Eq. of motion for δ (for simplicity we set T=0, i.e. I_N=0)

$$\frac{\Phi_0}{2\pi} C\ddot{\delta} + \frac{\Phi_0}{2\pi}\frac{1}{R}\dot{\delta} = -I_0 \sin\delta + I \equiv -\frac{2\pi}{\Phi_0}\frac{\partial U_\mathrm{J}}{\partial \delta}$$

with the **tilted washboard potential** $U_\mathrm{J} \equiv E_\mathrm{J}\{1 - \cos\delta - i\,\delta\}$

Josephson coupling energy $E_\mathrm{J} \equiv \frac{I_0 \Phi_0}{2\pi}$ normalized bias current $i \equiv \frac{I}{I_0}$

analogous system: point-like particle in the tilted washboard potential

$$m\ddot{x} + \xi\dot{x} = -\frac{\partial\{W(x) - F_\mathrm{d}x\}}{\partial x}$$

mass	m	C	capacitance
friction coeff.	ξ	$1/R$	conductance
force	F_d	I	current
velocity	$\dot{x}$	$\dot{\delta}\frac{\Phi_0}{2\pi} = U$	voltage

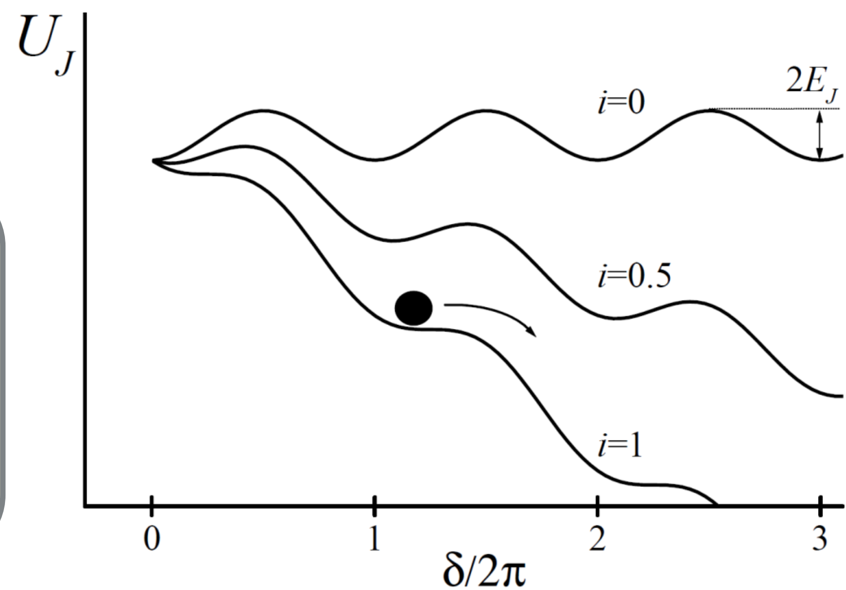

RCSJ Model & Washboard Potential

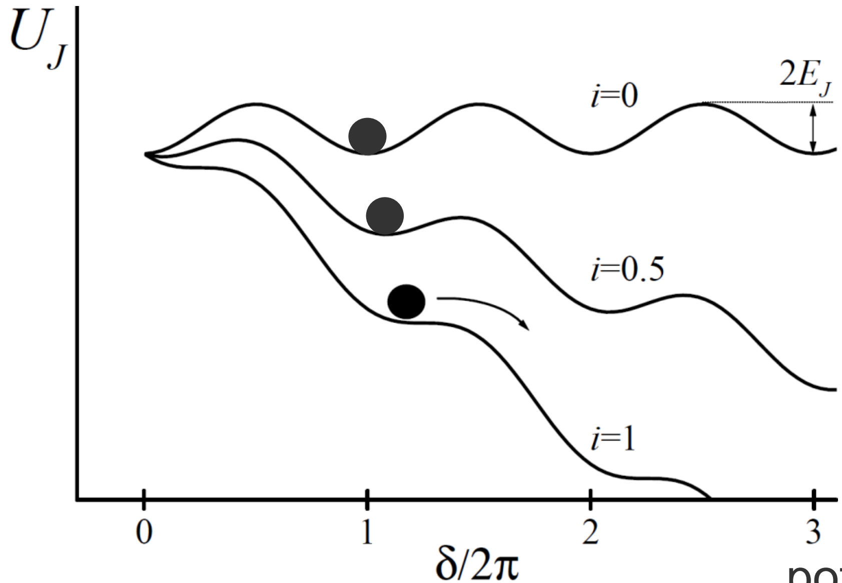

static case:

„particle“ is trapped in potential minimum

$$\langle\dot{\delta}\rangle \propto V = 0$$

dynamic case:

„particle“ rolls down the tilted potential

$$\langle\dot{\delta}\rangle \propto V \neq 0$$

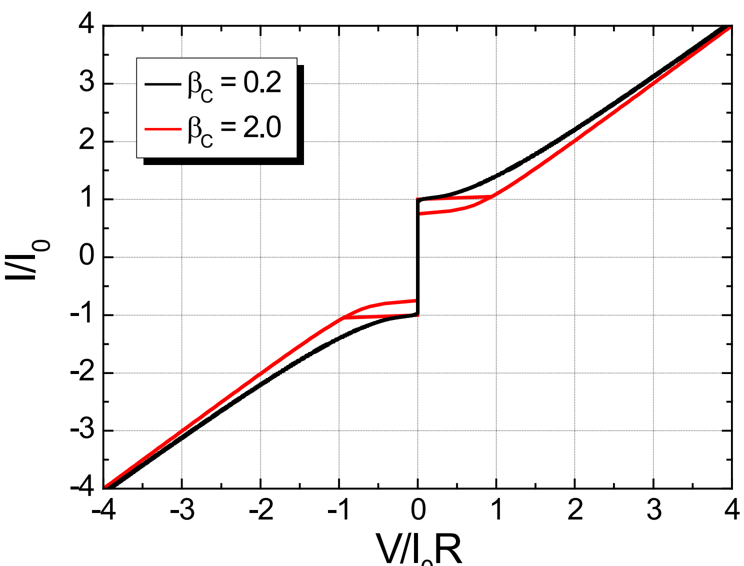

potential minima disappear at $i = 1 \Leftrightarrow I = I_0$

i.e. when critical current I_0 is reached

for large tilt $F_\mathrm{d} \gg \dfrac{\partial W(x)}{\partial x}$ ⇨ $\dot{x} = \dfrac{F_\mathrm{d}}{\xi}$

i.e. for $I \gg I_0$ ⇨ $V = I\,R$

Effect of Damping in the RCSJ Model

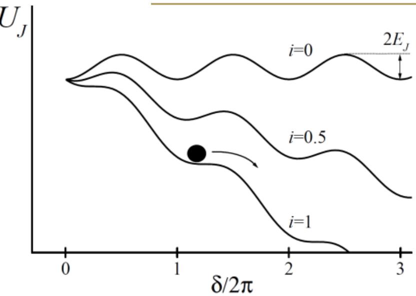

normalized Eq. of motion

$$\boxed{\beta_C \ddot{\delta} + \dot{\delta} + \sin\,\delta = i + i_N}$$

$$i \equiv \frac{I}{I_0}\,,\; i_{\rm N} \equiv \frac{I_{\rm N}}{I_0}$$

characteristic voltage

(I_0R product) $V_{\rm c} \equiv I_0 R$

characteristic frequency

$$\omega_{\rm c} \equiv \frac{2\pi}{\Phi_0} I_0 R$$

with Stewart-McCumber parameter $\boxed{\beta_C \equiv \frac{2\pi}{\Phi_0} I_0 R^2 C}$

normalized time $\tau \equiv t\omega_{\rm c}$

decrasing I from $I>I_0$:

strong damping: friction term $\dot{\delta}$ dominates,
i.e. $\beta_{\rm C} \ll 1$

particle gets retrapped at $I=I_0$

⇨ non-hysteretic IVC

weak damping: inertial term $\ddot{\delta}$ dominates,
i.e. $\beta_{\rm C} \gg 1$

particle gets retrapped at $I=I_r<I_0$

⇨ hysteretic IVC

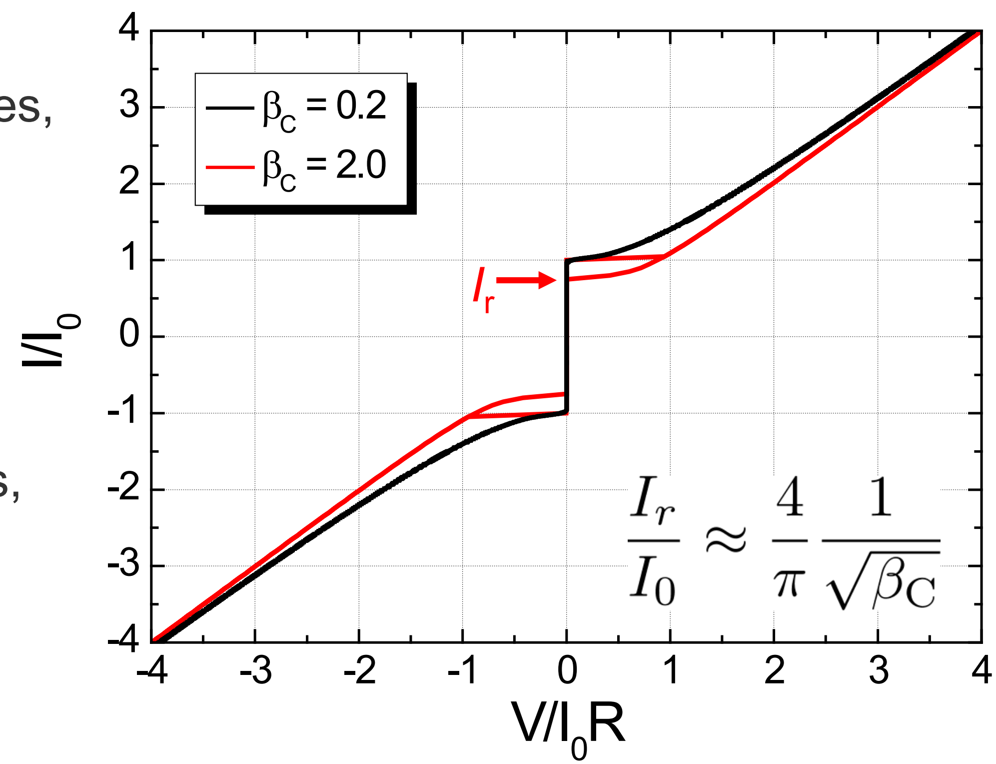

Microwave Absorption: Shapiro Steps

apply alternating current in addition to dc current $I_{\mathrm{tot}} = I + I_{\mathrm{ac}} \sin \omega_{\mathrm{ac}} t$

⇨ **regimes of constant voltage V_n in the IVC = Shapiro steps**

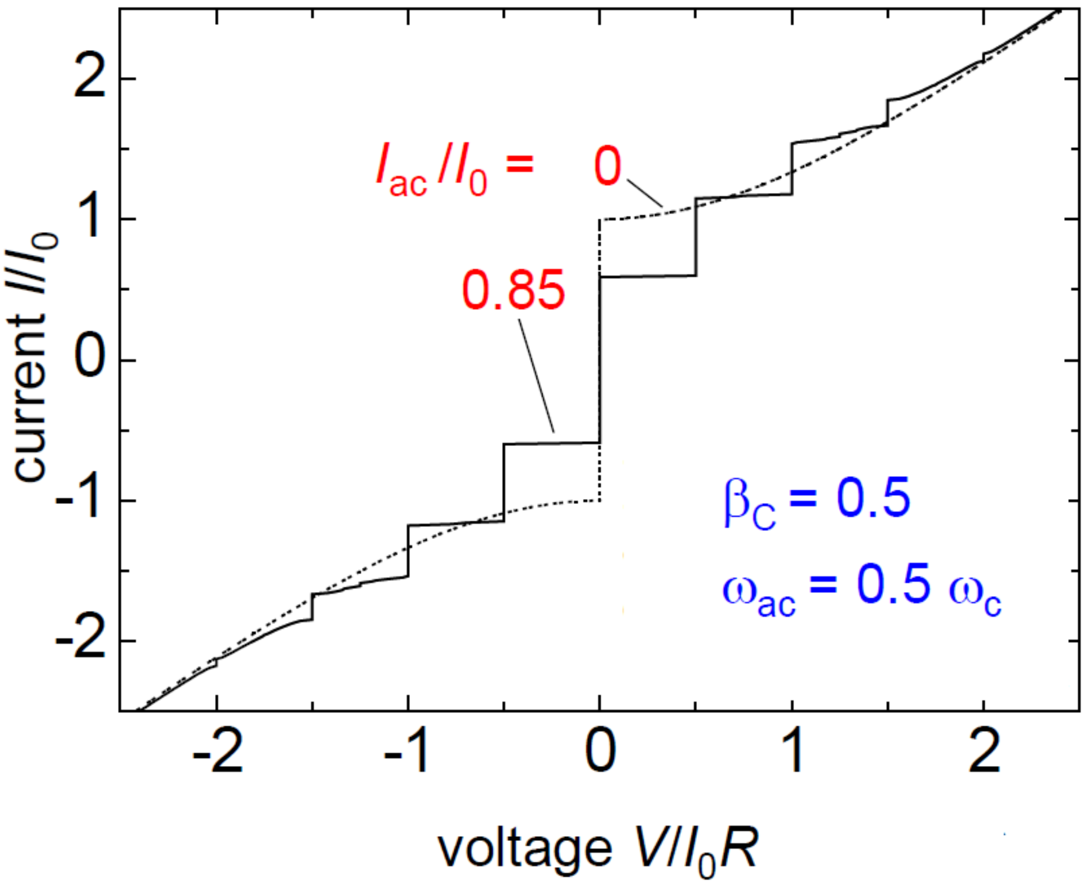

Microwave Absorption: Shapiro Steps

illustrative interpretation with particle in tilted washboard potential

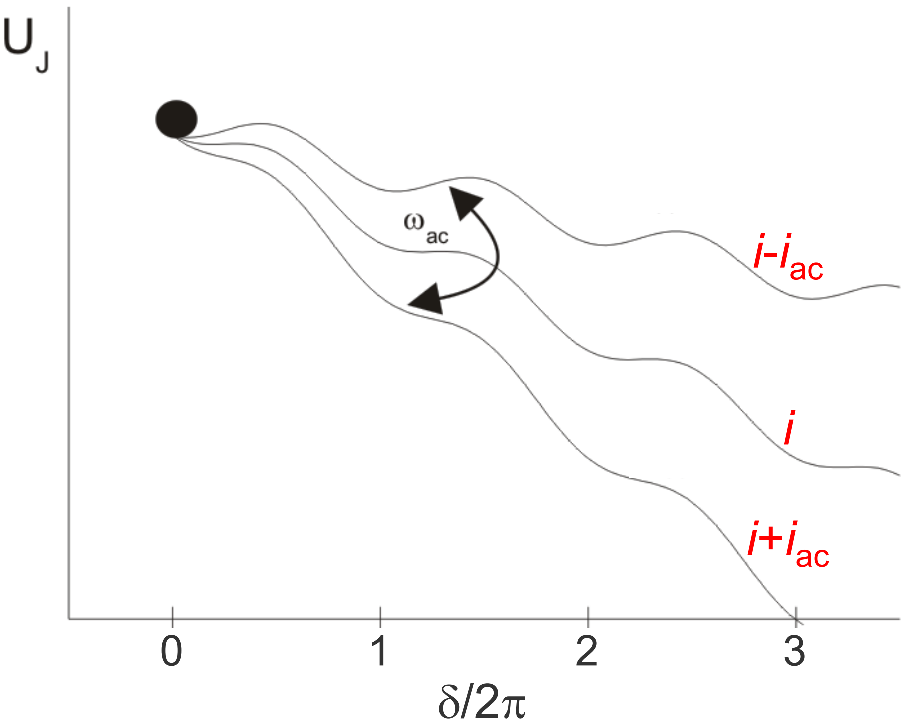

motion of the „particle“ synchronizes with the external drive

⇨ change of δ by $2\pi\, n$ $\quad (n = 1, 2, \ldots)$

per excitation period $T_{\mathrm{ac}} = 1/f_{\mathrm{ac}}$

$f_{\mathrm{ac}} = 2\pi\omega_{\mathrm{ac}}$

⇨ velocity $\dot{\delta}_n = \dfrac{2\pi n}{T_{\mathrm{ac}}} = 2\pi n f_{\mathrm{ac}}$

stable within some intervall of applied dc current *I*

⇨ steps of constant voltage V_n on IVC at $V_n = \dfrac{\Phi_0}{2\pi}\dot{\delta}_n = n\Phi_0 f_{\mathrm{ac}}$

⇨ equidistant Shapiro steps with separation

$$\Delta V = V_{n+1} - V_n = \Phi_0 f_{\mathrm{ac}} \approx \frac{1\,\mathrm{mV}}{483.6\,\mathrm{GHz}} \cdot f_{\mathrm{ac}}$$

Josephson Normal: Voltage Standard

irradiation of microwaves on Josephson junctions
(typically: f = 70 GHz → $n \cdot 0.144$ mV)

$$V_n = n\Phi_0 f_{\mathrm{ac}}$$

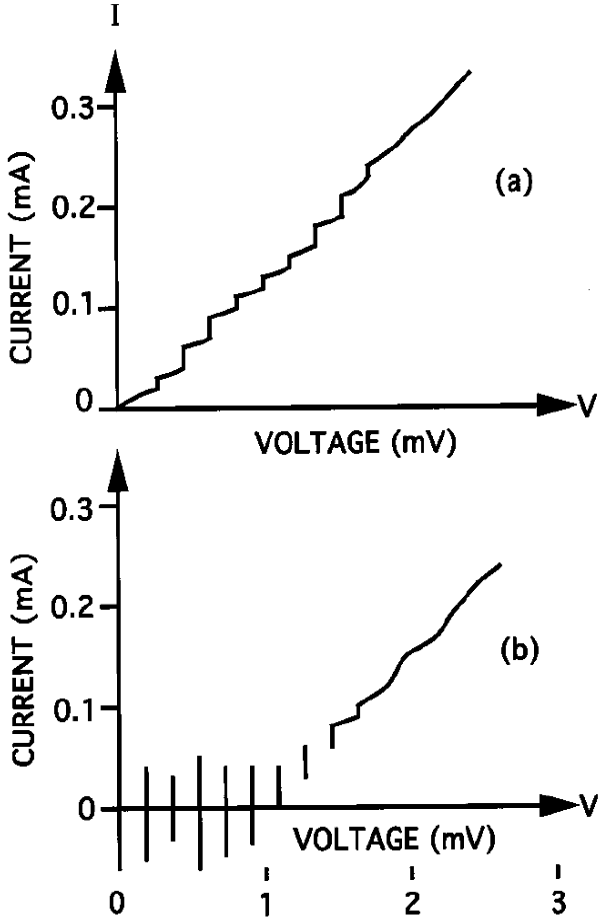

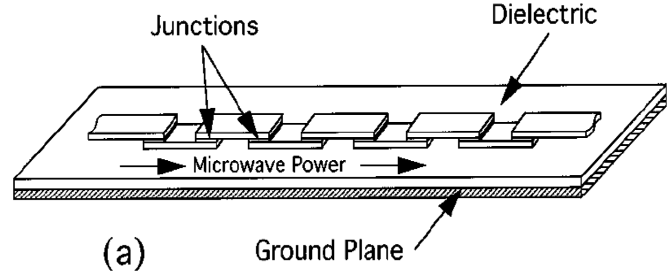

20.000 Josephson junctions

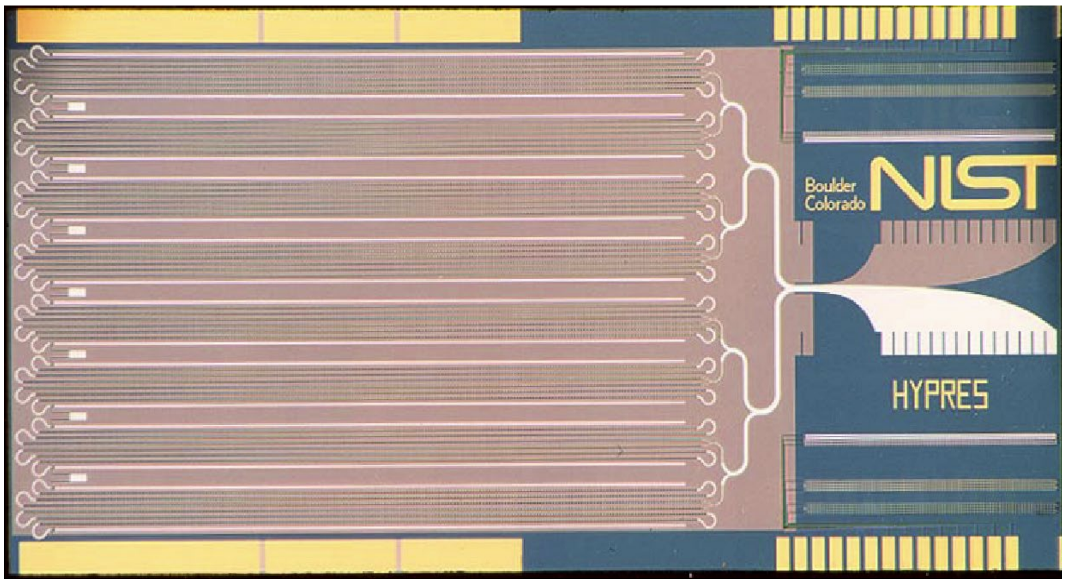

reproducible voltages with relative uncertainty
< 1 : 10^{10}, corresponds to 1 nV at 10 V)

Outline

Fluctuations in Josephson Junctions

- **Thermal noise**

What is the effect of finite temperature *T* ?

for a JJ described within the RCSJ model:

$$\frac{\Phi_0}{2\pi}C\ddot{\delta}+\frac{\Phi_0}{2\pi}\frac{1}{R}\dot{\delta}=-I_0\sin\delta+I+I_\mathrm{N}\equiv-\frac{2\pi}{\Phi_0}\frac{\partial U_\mathrm{J}}{\partial\delta}$$

noise current acts as a stochastic force → Langevin Eq.

induces fluctuating tilt of the washboard potential

$$U_\mathrm{J}\equiv E_\mathrm{J}\{1-\cos\delta-(i+i_\mathrm{N})\,\delta\}\qquad i_\mathrm{N}\equiv I_\mathrm{N}/I_0$$

Fluctuations in Josephson Junctions

for $I \lesssim I_0$ fluctuations can lead to $I + I_\mathrm{N}(t) > I_0$ ⇨ voltage pulses $U(t)$ with $V>0$

⇨ thermal smearing (noise rounding) of IVCs

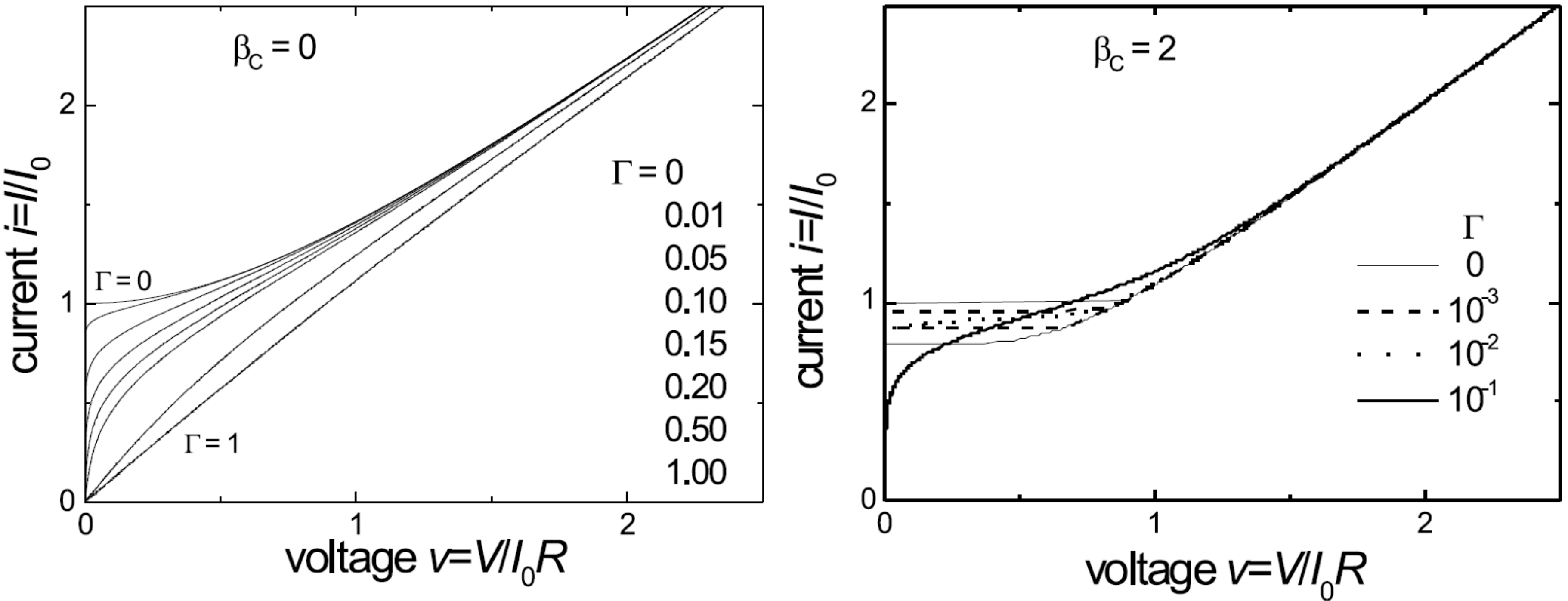

quantified by thermal noise parameter $\Gamma \equiv \dfrac{k_\mathrm{B}T}{E_\mathrm{J}}$

E_J: Josephson coupling energy = amplitude of washboard potential

Fluctuations in Josephson Junctions

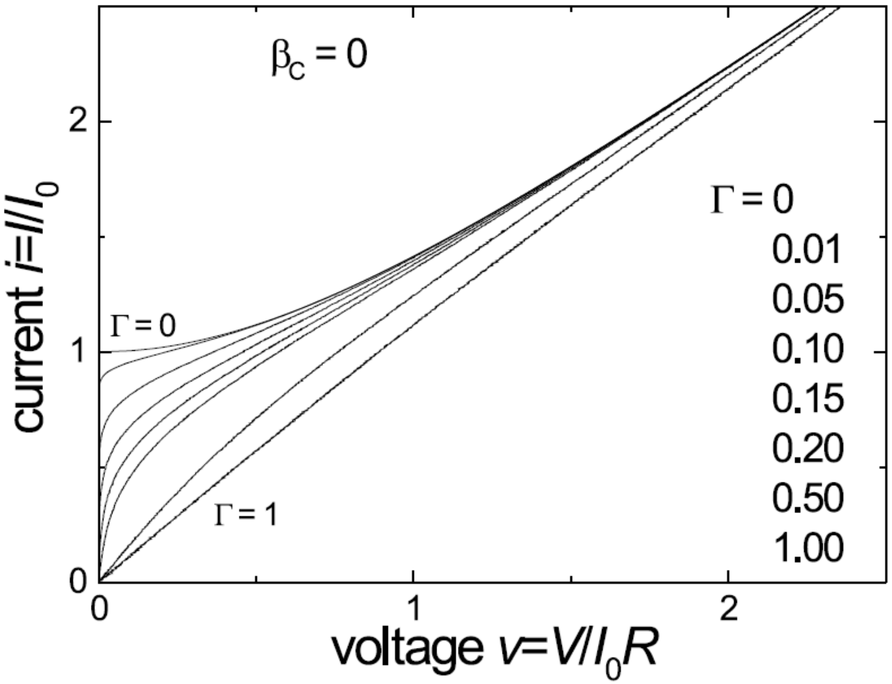

$$\Gamma = \frac{2\pi k_\mathrm{B} T}{I_0 \Phi_0} = \frac{2\pi k_\mathrm{B} T/\Phi_0}{I_0} = \frac{I_\mathrm{th}}{I_0}$$

thermal fluctuations „destroy“ Josephson coupling

regime of small thermal fluctuations:

$$\Gamma \ll 1$$

corresponds to $I_0 \gg I_\mathrm{th} = \frac{2\pi}{\Phi_0} k_\mathrm{B} T \propto T$

significant suppression of „measurable I_c already at Γ=10^{-2} !

for T= 4.2 K: I_{th} ~ 0.18 μA
for T = 77 K: I_{th} ~ 2.3 μA

EBERHARD KARLS UNIVERSITÄT TÜBINGEN

Fluctuations in Josephson Junctions

• Low-frequency excess noise: 1/*f* noise

description of tunnel junctions by parameter fluctuations rather than Langevin force

origin:

fluctuations in I_0 due to trapping and release of electrons at defects in the tunnel barrier (change barrier height, and hence I_0, (also R))

single trap:

random switching of I_0 between two values with difference δI_0 and effective lifetime τ

⇨ random telegraph signal (RTS)

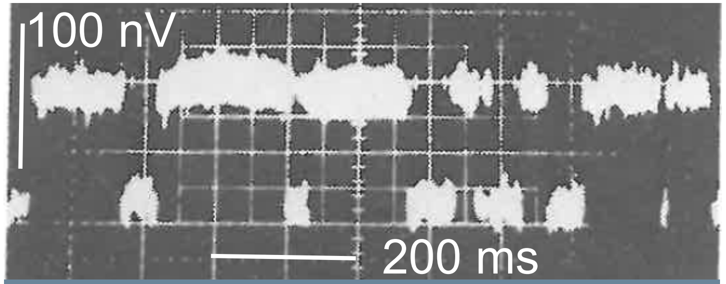

R. Gross, B. Mayer, Physica C **180**, 235 (1991)

$V(t)$ of grain boundary junction at I=1.2 I_0

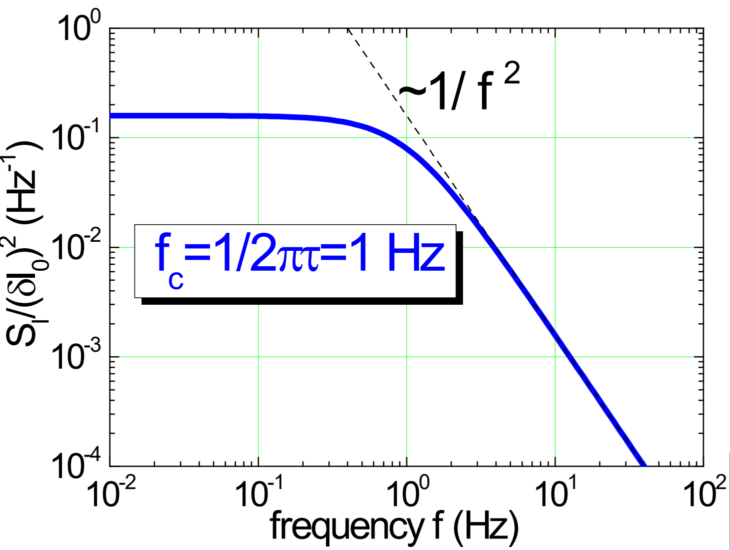

with Lorentzian spectral density

$$S_I(f) = \frac{(\delta I_0)^2 \cdot \tau}{1 + (2\pi\tau \cdot f)^2}$$

with $\tau^{-1} \equiv \tau_1^{-1} + \tau_2^{-1}$ for mean life times τ_1=τ_2 in the two states

C.T. Rogers & R.A. Burman, *Composition of 1/f noise in metal-insulator-metal tunnel junctions*, Phys. Rev. Lett. **53**, 1272 (1984)

Fluctuations in Josephson Junctions

for thermally activated trapping processes

$$\tau = \tau_0 \exp\left(\frac{E}{k_\mathrm{B}T}\right)$$

with τ_0=const, and activation energy E

e.g. τ_0=0.1 s, and E=1.8 meV for Nb-AlO$_x$-Nb tunnel JJs

B. Savo, F.C. Wellstood, J. Clarke, Appl. Phys. Lett. **50**, 1757 (1987)

superposition of several (or many) traps

$$S(f) \propto \int dE\, D(E) \left[\frac{\tau_0\, e^{\frac{E}{k_\mathrm{B}T}}}{1 + (2\pi f \tau_0)^2\, e^{\frac{2E}{k_\mathrm{B}T}}}\right]$$

distribution function

peak at $\tilde{E} \equiv k_\mathrm{B}T \ln\{\frac{1}{2\pi f \tau_0}\}$

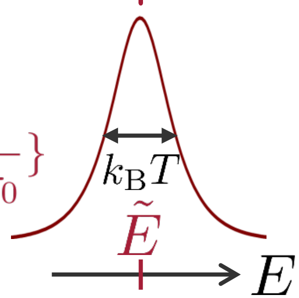

for given T, only traps contribute with

$$\tilde{E} - k_\mathrm{B}T \lesssim E \lesssim \tilde{E} + k_\mathrm{B}T$$

for broad distribution $D(E)$ with respect to $k_\mathrm{B}T$:

take $D(\tilde{E})$ out of the integral

$$\boxed{S(f) \propto k_\mathrm{B}T\, D(\tilde{E})\, \frac{1}{f}}$$

P. Dutta, P.M. Horn, *Low-frequency fluctuations in solids: 1/f noise*, Rev. Mod. Phys. **53**, 497 (1981); M.B. Weissman, *1/f noise and other slow, nonexponential kinetics in condensed matter*, Rev.Mod.Phys. **60**, 537 (1988)

Fluctuations in Josephson Junctions

superposition of several (or many) traps

the superposition of only few traps already yields $S(f) \propto \frac{1}{f}$

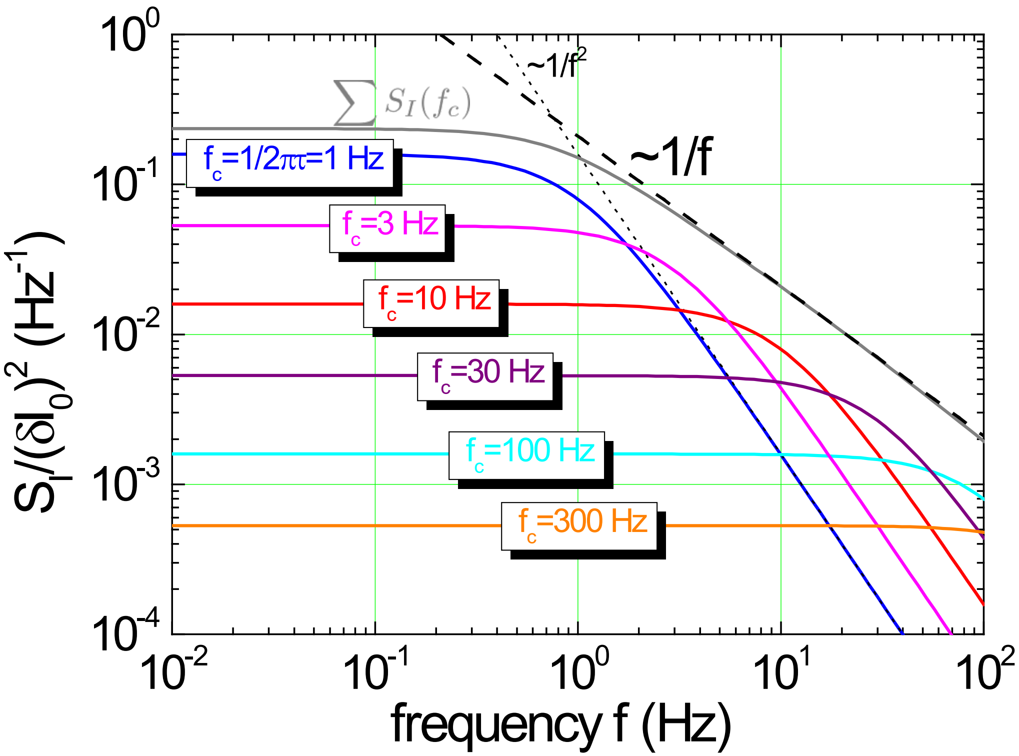

P. Dutta, P.M. Horn, *Low-frequency fluctuations in solids: 1/f noise*, Rev. Mod. Phys. **53**, 497 (1981); M.B. Weissman, *1/f noise and other slow, nonexponential kinetics in condensed matter*, Rev.Mod.Phys. **60**, 537 (1988)

Outline

Types of Josephson Junctions

planar sandwich-type JJ

(SIS, SNS, SFS, SINIS, SIFS, …, SAlFS)

barrier

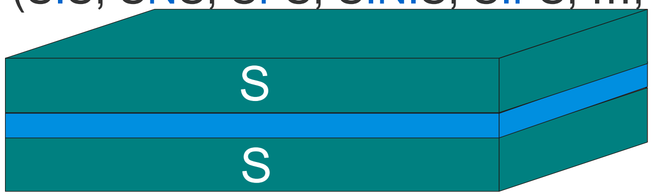

insulator (I), normal conductor (N), ferromagnet (F), alterferromagnet (AlF)

point contact

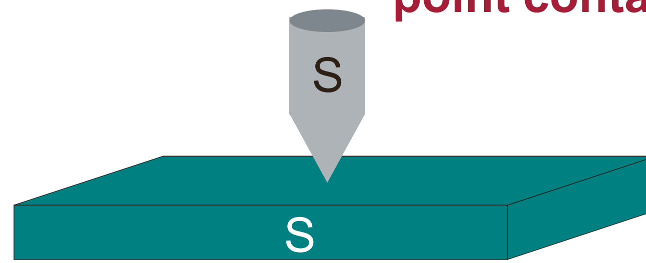

irradiation-induced barrier JJ (e.g. ion beam)

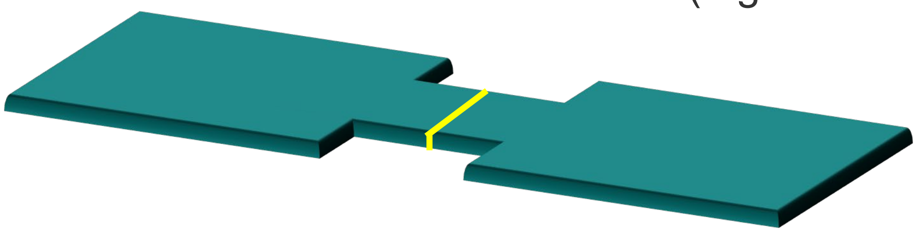

constriction junction (Dayem bridge)

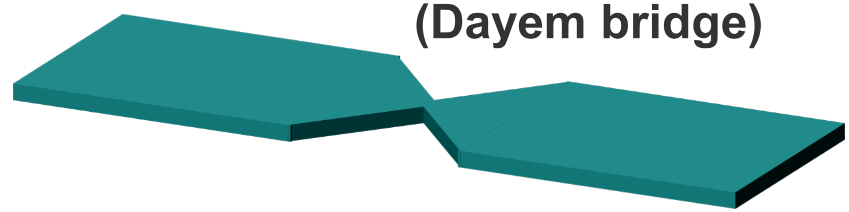

grain boundary junction (cuprates)

(bicrystal, biepitaxial, …)

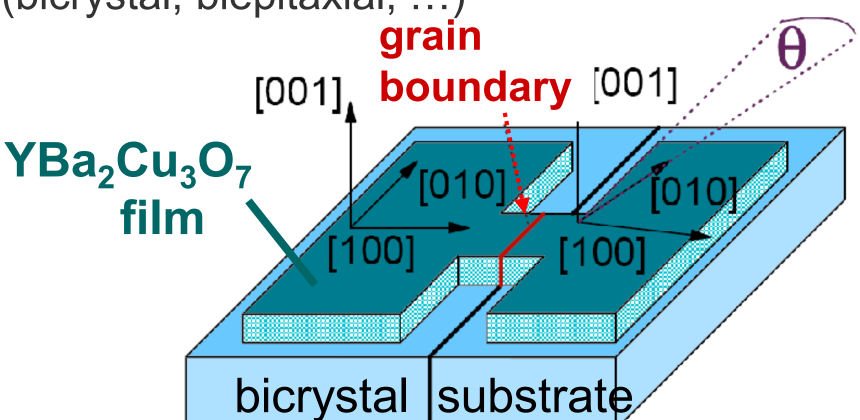

intrinsic Josephson junctions

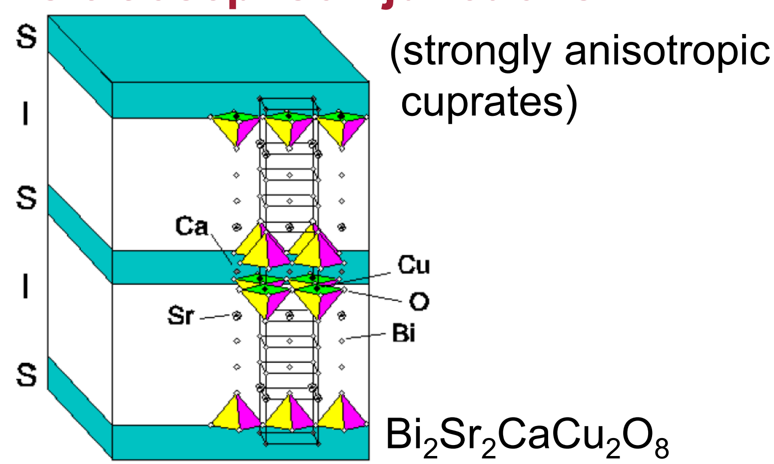

JJs with Different Ground States

The **Josephson energy $U_J(\delta)$** can be derived for any CPR, i.e. $I_s(\delta)$:
Increase current I_s in time t → change of $\delta(t)$ → finite voltage U

$$U_J(\delta) = \int_{t_0}^{t} I_s(\delta(\tilde t))\underbrace{U}_{=\frac{\Phi_0}{2\pi}\dot\delta(\tilde t)}\,\mathrm{d}\tilde t = \frac{\Phi_0}{2\pi}\int_{t_0}^{t} I_s(\tilde\delta(\tilde t))\,\underbrace{\dot\delta(\tilde t)\,\mathrm{d}\tilde t}_{=\mathrm{d}\tilde\delta} = \frac{\Phi_0}{2\pi}\int_{\delta_0}^{\delta} I_s(\tilde\delta)\,\mathrm{d}\tilde\delta$$

for $I_s = I_0 \sin\delta$ ⇒ $U_J(\delta) = \underbrace{E_J}_{=\frac{I_0\Phi_0}{2\pi}}(1-\cos\delta)$

CPR

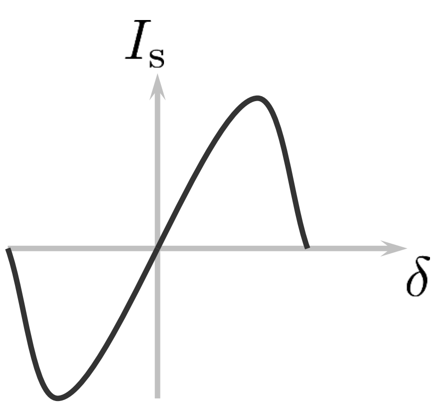

Josephson energy

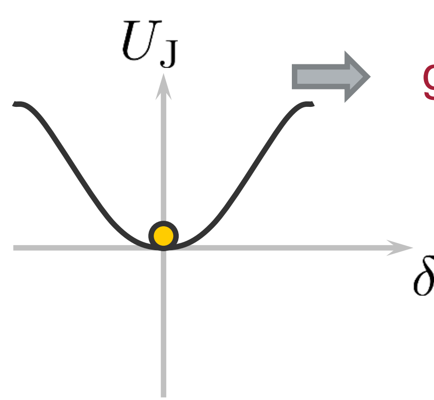

⇒ ground state phase:
δ=0 (for I=0)

⇒ **„0-JJ“**

EBERHARD KARLS UNIVERSITÄT TÜBINGEN

JJs with Different Ground States

CPR: $I_\mathrm{s} = I_0 \sin(\delta)$ → **ground state**: $\delta = 0$

CPR: $I_\mathrm{s} = I_0 \sin(\delta - \pi)$ → **ground state**: $\delta = \pi$

Experiment: V.V. Ryazanov *et al.*, Phys. Rev. Lett. **86**, 2427 (2001)

CPR: $I_\mathrm{s} = I_0 \sin(\delta - \varphi_0)$ → **ground state**: $\delta = \varphi_0$
(with $0 < \varphi_0 < \pi$)

Experiment: D.B. Szombati *et al.*, Nat. Phys. **12**, 568 (2016)

CPR: $I_\mathrm{s} = I_{0,1} \sin(\delta) + I_{0,2} \sin(2\delta)$
→ **ground state**: $\delta = \pm\varphi$

(with $0 < \varphi < \pi$ and $\varphi = \arccos(-\frac{I_{0,1}}{2I_{0,2}})$ for $-I_{0,2} > \frac{I_{0,1}}{2}$)

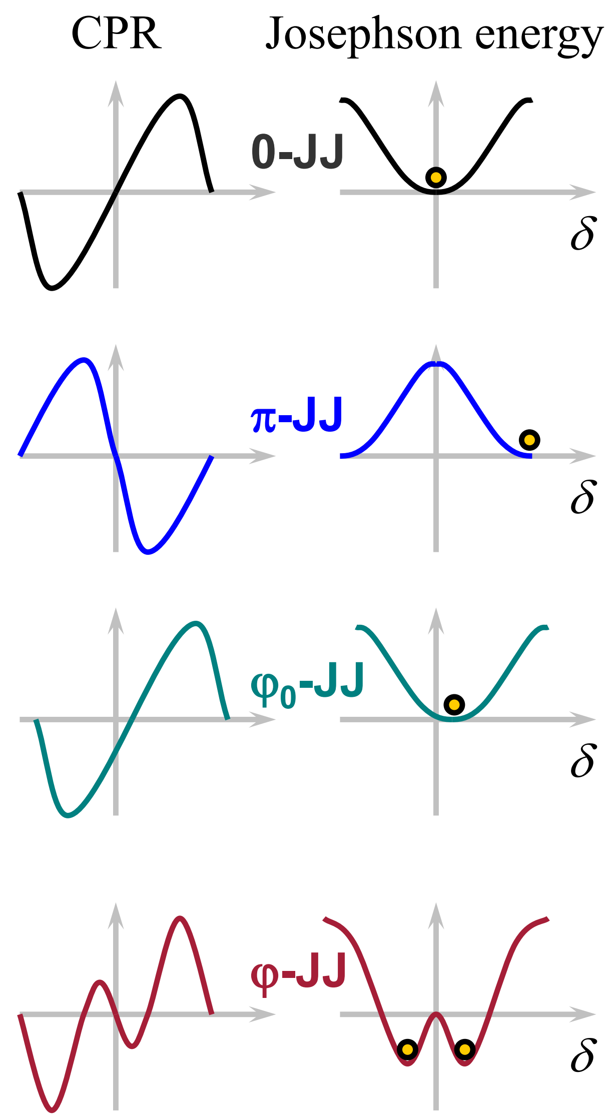

Theory: Yu.S. Barash *et al.*, Phys. Rev. B **52**, 665 (1995)
Y. Tanaka , S. Kashiwaya, Phys. Rev. B **53**, R11957 (1996)
A. Buzdin, A.E. Koshelev, Phys. Rev. B **67**, 220504(R) (2003)

JJs with Different Ground States

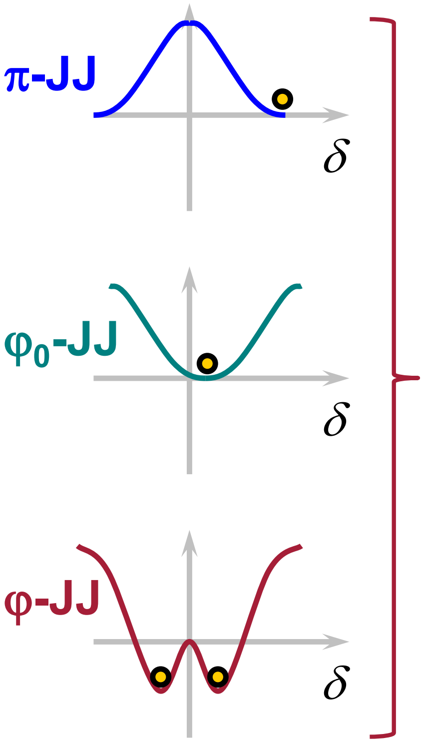

phase battery
phase shifter

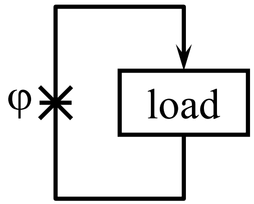

Self-biased RSFQ flip-flop:
integrated π-rings based on YBCO-Nb *s*-/*d*-wave JJs

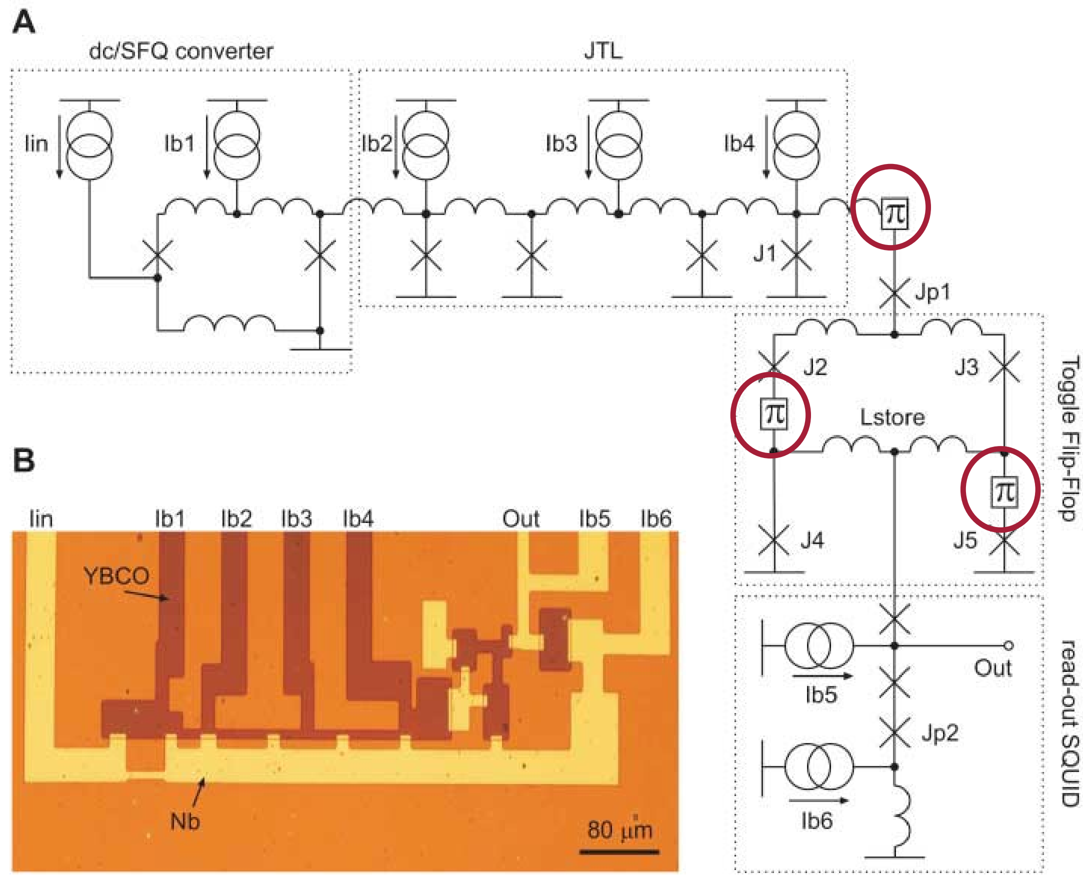

T. Ortlepp *et al.*, Science **312**, 1495 (2006)

RSFQ: rapid single flux quantum

EBERHARD KARLS UNIVERSITÄT TÜBINGEN

φ-JJ: Tunable Bistable System

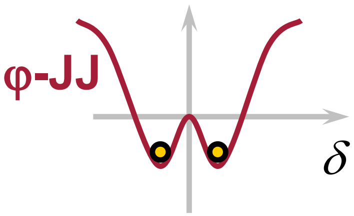

based on periodic 0-π JJs

A. Buzdin, A.E. Koshelev, PRB **67** (2003)

⇨ simplest case: **0-π JJ**

E. Goldobin *et al.*, Phys. Rev. Lett. **107**, 227001 (2011)

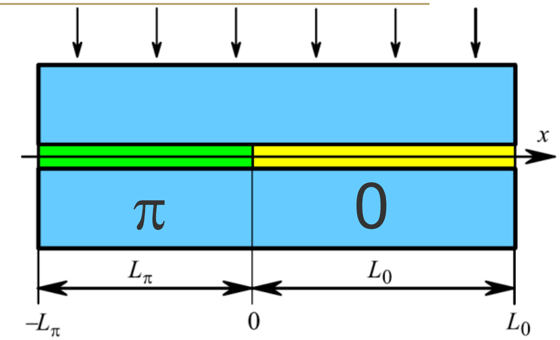

$$u_J \equiv \frac{U_J(\delta)}{E_J} = 1 - \cos(\delta) + \frac{\Gamma_0}{4}\{1 - \cos(2\delta)\} + \Gamma_h h \sin(\delta)$$

Γ_h : asymmetry parameter

$$\Gamma_0 \equiv \frac{2I_{0,2}}{I_{0,1}}$$

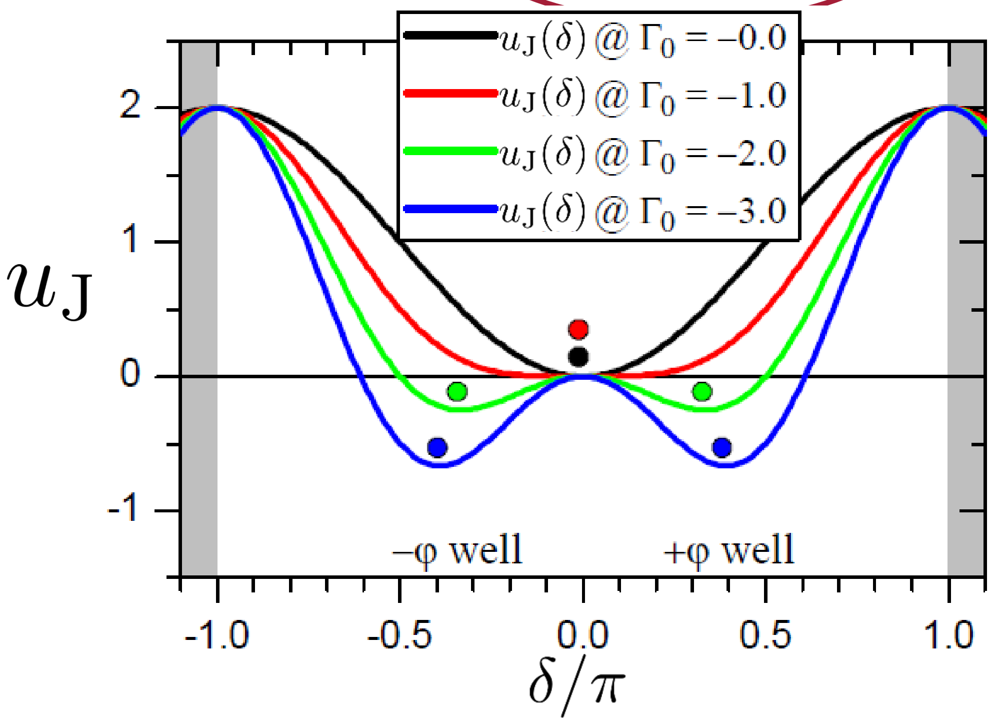

bistabe/two-level system for $-\Gamma_0$>1

EBERHARD KARLS UNIVERSITÄT TÜBINGEN

φ-JJ: Tunable Bistable System

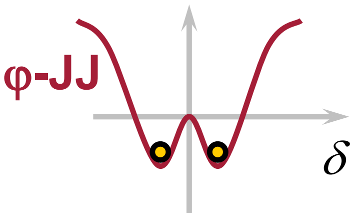

simplest case: **0-π JJ**

E. Goldobin *et al.*, Phys. Rev. Lett. **107**, 227001 (2011)

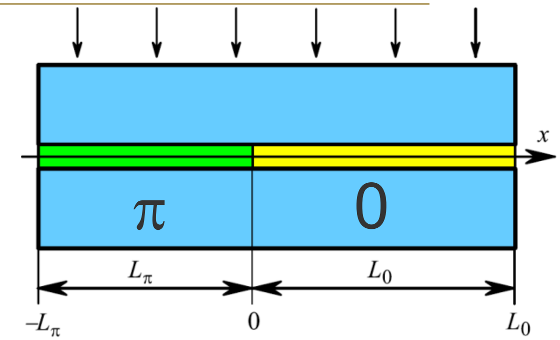

$$u_J \equiv \frac{U_J(\delta)}{E_J} = 1 - \cos(\delta) + \frac{\Gamma_0}{4}\{1 - \cos(2\delta)\} + \Gamma_h h \sin(\delta)$$

Γ_h : asymmetry parameter

$$\Gamma_0 \equiv \frac{2I_{0,2}}{I_{0,1}}$$

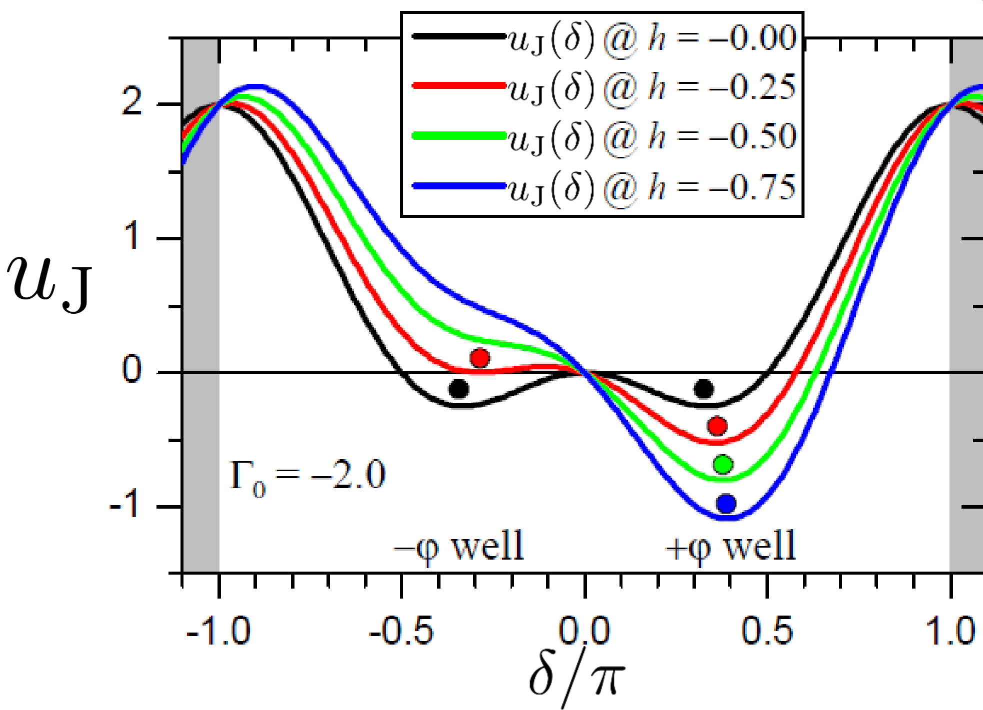

tunable by magnetic field

lifts degeneracy of double-well potential

φ-JJ: Two Critical Currents

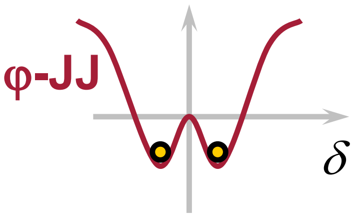

experimental realization:
Nb-AlO$_x$-Cu$_{0.4}$Ni$_{0.6}$-Nb SIFS JJ
with step in the F layer

H. Sickinger *et al.*, Phys. Rev. Lett. **109**, 107002 (2012)

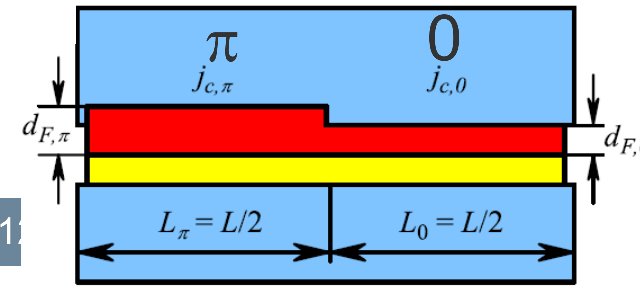

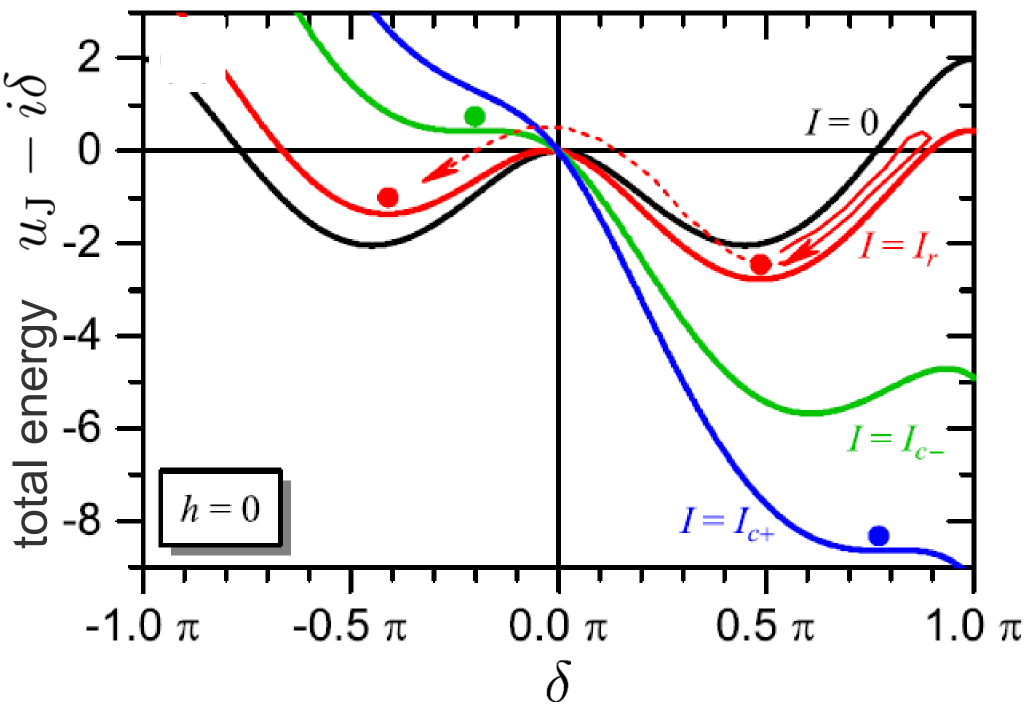

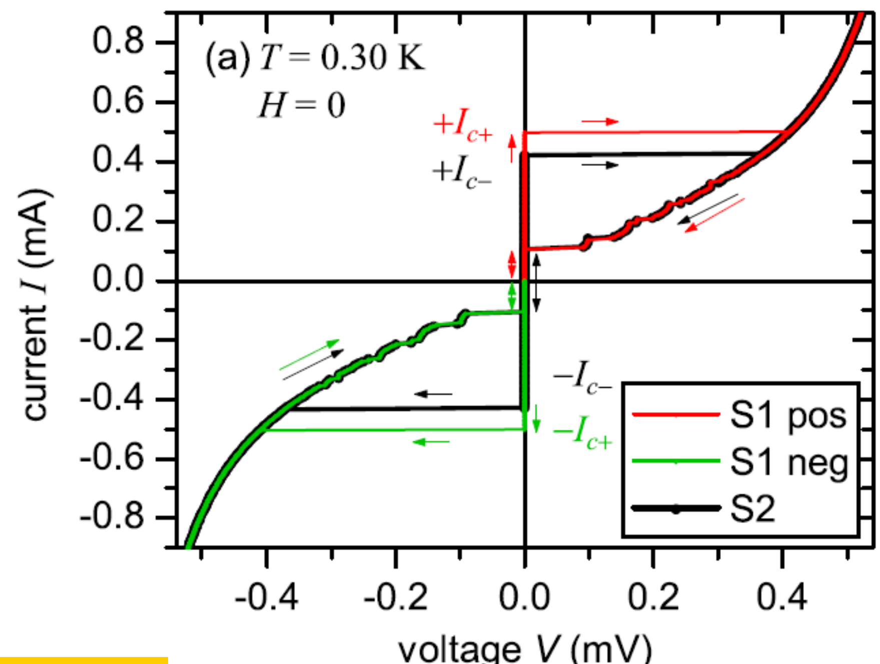

state detector!

φ-JJ Application: φ bit (memory cell)

Write in

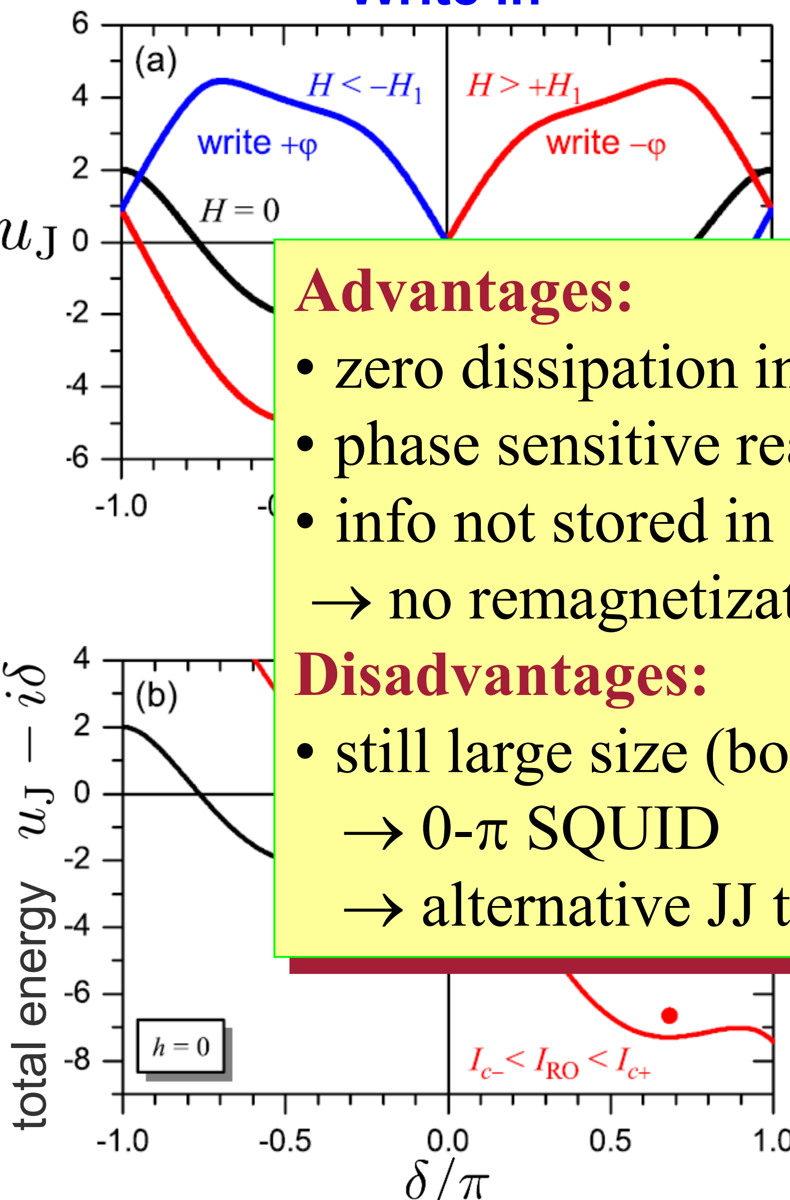

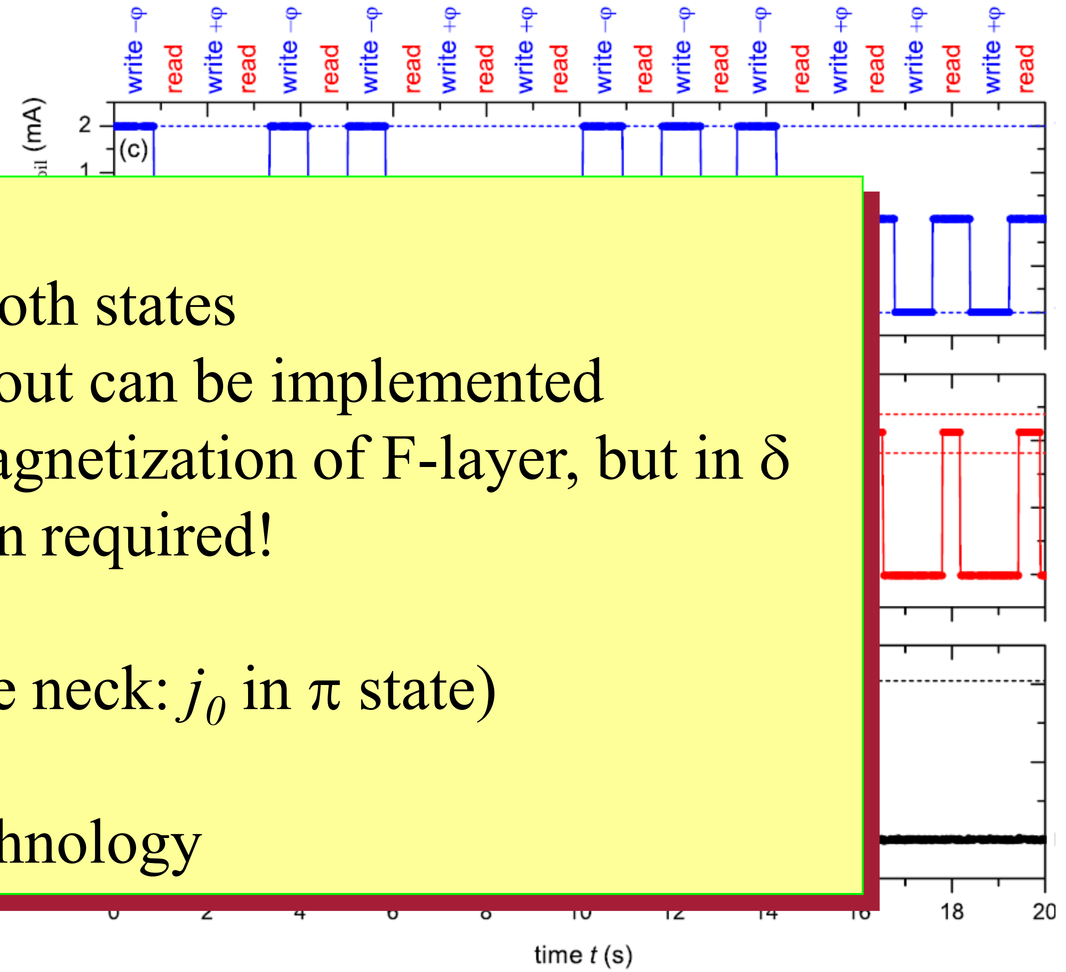

Advantages:

- zero dissipation in both states
- phase sensitive readout can be implemented
- info not stored in magnetization of F-layer, but in δ
  → no remagnetization required!

Disadvantages:

- still large size (bottle neck: j_0 in π state)
  → 0-π SQUID
  → alternative JJ technology

E. Goldobin et al., APL **102**, 242602 (2013)

Summary – part 1

Macroscopic Wave Function → coherent state of Cooper pairs

⇩

Weak coupling of two condensates

→Josephson Relations & Consequences (static & dynamic cases)

- Static case:

Josephson Junction in a Magnetic Field → $I_c(H)$ Fraunhofer pattern for short JJs

- Dynamic case:

Resistively & Capacitively Shunted Junction (RCSJ) model
→ I-V-characteristics (particle in the tilted washboard potential)

Fluctuations in Josephson Junctions → thermal noise & I_c fluctuations important for device applications , e.g. SQUIDS

Classification of JJs – Ground States: 0- π-, φ-Junctions
→ new applications: phase batteries, memory devices, qubits,..

EBERHARD KARLS UNIVERSITÄT TÜBINGEN

FACULTY OF SCIENCE

Part 2: Superconducting Quantum Interference Devices: Basic Properties & Applications of SQUIDs

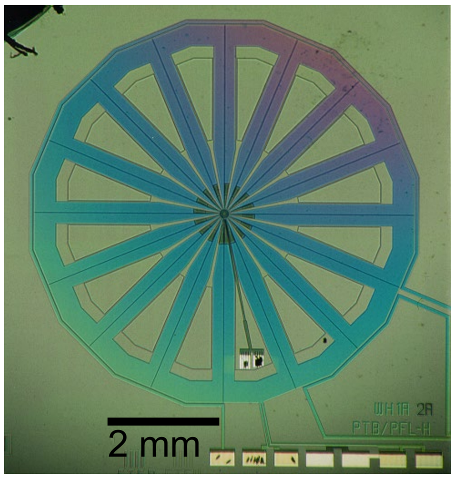

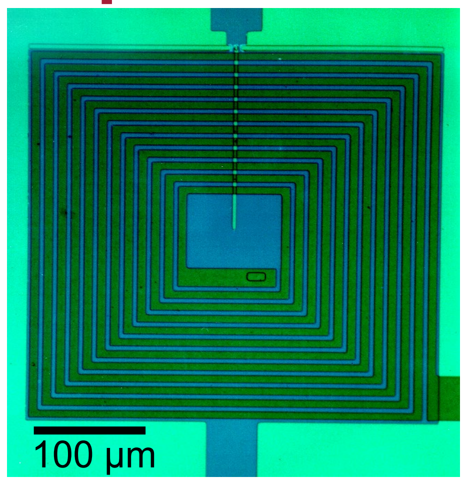

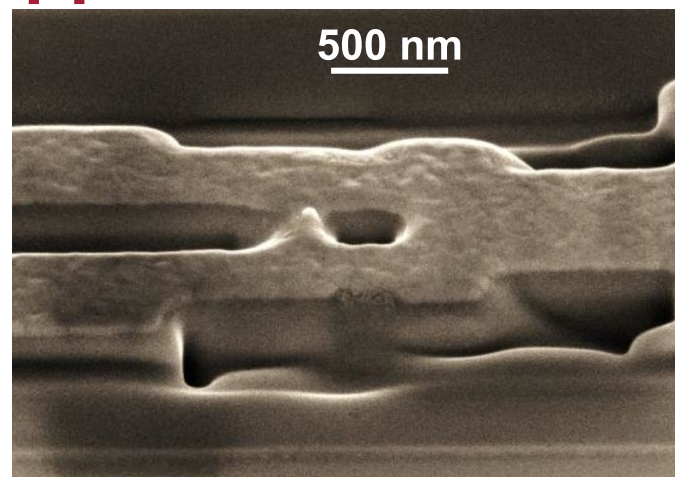

Dieter Koelle

Physikalisches Institut, Center for Quantum Science (CQ) and Center for Light-Matter Interaction, Sensors & Analytics (LISA⁺)

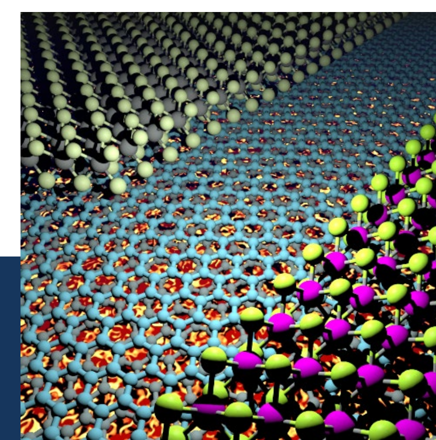

SuperQUMAP

European School on Superconductivity & Magnetism in Quantum Materials, 21-25 April 2024, Gandia (Valencia, Spain)

Outline

I. SQUIDs: Basics & principle of operation

II. Practical devices and readout

III. SQUID applications

a. Magnetometry, Susceptometry

b. Biomagnetism: MEG, low-field MRI

c. Scanning SQUID microscopy

d. magnetic nanoparticle (MNP) detection

The SQUID Handbook, ***Vol. I Fundamentals and Technology of SQUIDs and SQUID Systems***, J. Clarke, A. I. Braginski (eds.) Wiley-VCH, Weinheim (2004)

The SQUID Handbook, ***Vol. II Applications of SQUIDs and SQUID Systems***, J. Clarke, A. I. Braginski (eds.) Wiley-VCH, Weinheim (2006)

Direct current (dc) SQUID

combines
- fluxoid quantization in a superconducting ring
- Josephson effect in superconducting weak links

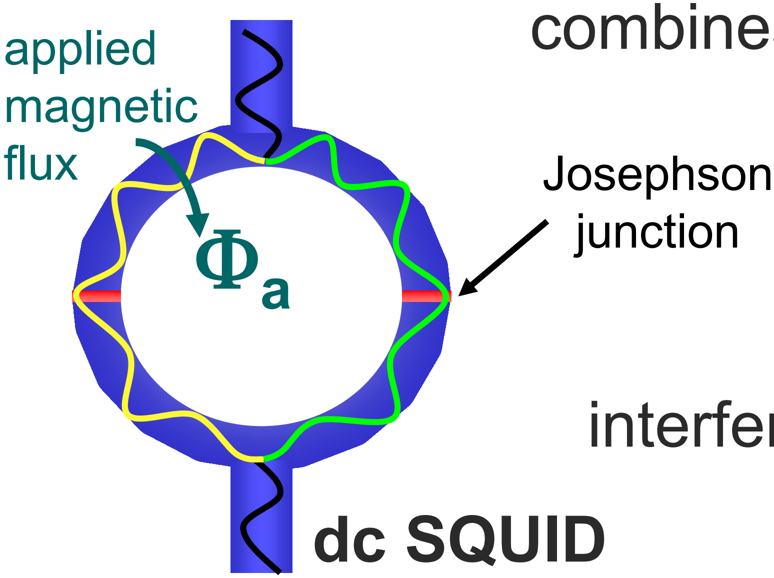

interference of superconductor wavefunction

$$\boxed{\Psi = \Psi_0 \cdot e^{i\varphi}}$$

→ 2 junctions intersect SQUID loop

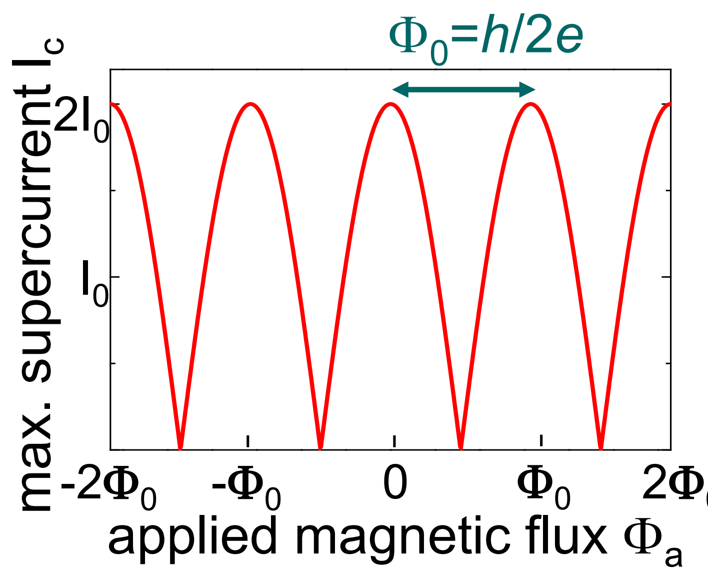

interference at double slit

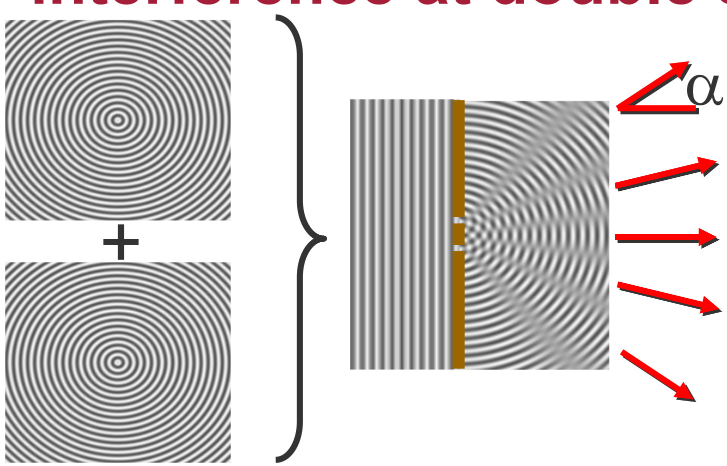

dc SQUID Basics: Fluxoid Quantization

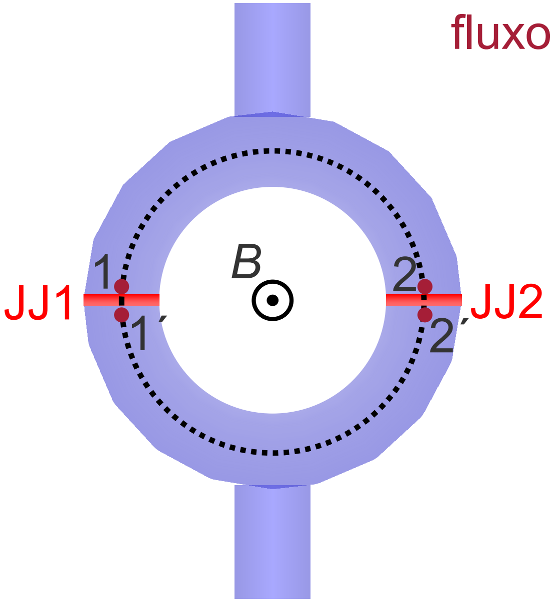

fluxoid quantization: $$2\pi n = \oint \nabla\varphi \, \mathrm{d}\boldsymbol{l} \qquad n = 1, 2, 3 \ldots$$

with the phase gradient in the ring segments

$$\nabla\varphi = \frac{2\pi}{\Phi_0}\left(\boldsymbol{A} + \mu_0 \lambda_\mathrm{L}^2 \boldsymbol{j}_\mathrm{s}\right)$$

and the phase difference across the junctions

$$\delta = \varphi_b - \varphi_a - \frac{2\pi}{\Phi_0}\int_a^b \boldsymbol{A}\, \mathrm{d}\boldsymbol{l}$$

calculation as for the determination of $\delta(x)$ in a single JJ in an applied magnetic field:

path 2→1: $$\int_2^1 \nabla\varphi \, \mathrm{d}\boldsymbol{l} = \frac{2\pi}{\Phi_0}\int_2^1 \boldsymbol{A}\, \mathrm{d}\boldsymbol{l} + \frac{2\pi}{\Phi_0}\mu_0\lambda_\mathrm{L}^2 \int_2^1 \boldsymbol{j}_\mathrm{s}\, \mathrm{d}\boldsymbol{l}$$

path 1´→2´: $$\int_{1'}^{2'} \nabla\varphi \, \mathrm{d}\boldsymbol{l} = \frac{2\pi}{\Phi_0}\int_{1'}^{2'} \boldsymbol{A}\, \mathrm{d}\boldsymbol{l} + \frac{2\pi}{\Phi_0}\mu_0\lambda_\mathrm{L}^2 \int_{1'}^{2'} \boldsymbol{j}_\mathrm{s}\, \mathrm{d}\boldsymbol{l}$$

path 1→1´: $$\int_1^{1'} \nabla\varphi \, \mathrm{d}\boldsymbol{l} = \varphi_{1'} - \varphi_1 = \delta_1 + \frac{2\pi}{\Phi_0}\int_1^{1'} \boldsymbol{A}\, \mathrm{d}\boldsymbol{l}$$

path 2´→2: $$\int_{2'}^{2} \nabla\varphi \, \mathrm{d}\boldsymbol{l} = -(\varphi_{2'} - \varphi_2) = -(\delta_2 + \frac{2\pi}{\Phi_0}\int_2^{2'} \boldsymbol{A}\, \mathrm{d}\boldsymbol{l})$$

dc SQUID Basics: Fluxoid Quantization

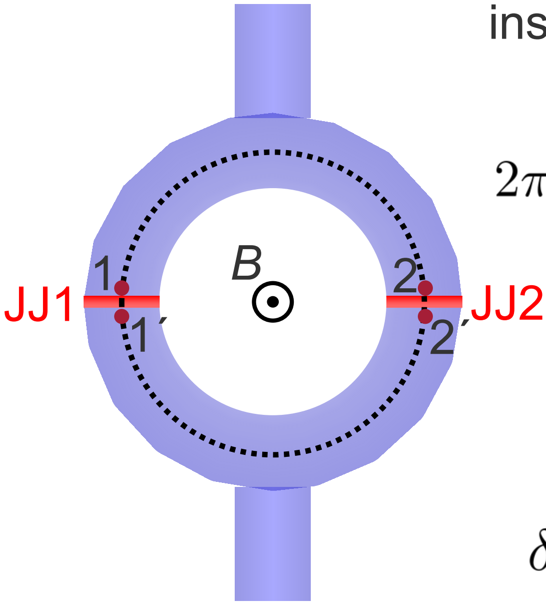

inserted into $2\pi n = \oint \nabla\varphi\, \mathrm{d}\boldsymbol{l}$ yields:

$$2\pi n = \delta_1 - \delta_2 + \frac{2\pi}{\Phi_0}\left\{\underbrace{\oint \boldsymbol{A}\,\mathrm{d}\boldsymbol{l}}_{=\int \boldsymbol{B}\,\mathrm{d}\boldsymbol{f} = \Phi} + \mu_0\lambda_\mathrm{L}^2\left(\int_2^1 \boldsymbol{j}_\mathrm{s}\,\mathrm{d}\boldsymbol{l} + \int_{1'}^{2'} \boldsymbol{j}_\mathrm{s}\,\mathrm{d}\boldsymbol{l}\right)\right\}$$

$$\int_2^1 + \int_{1'}^{2'} \equiv \oint_{C'}$$

$$\delta_2 - \delta_1 + 2\pi n = \frac{2\pi}{\Phi_0}\underbrace{\left\{\Phi + \mu_0\lambda_\mathrm{L}^2 \oint_{C'} \boldsymbol{j}_\mathrm{s}\,\mathrm{d}\boldsymbol{l}\right\}}_{\equiv\, \Phi_\mathrm{tot}\ \text{total flux}} \equiv \frac{2\pi}{\Phi_0}\Phi_\mathrm{tot}$$

dc SQUID Basics: Fluxoid Quantization

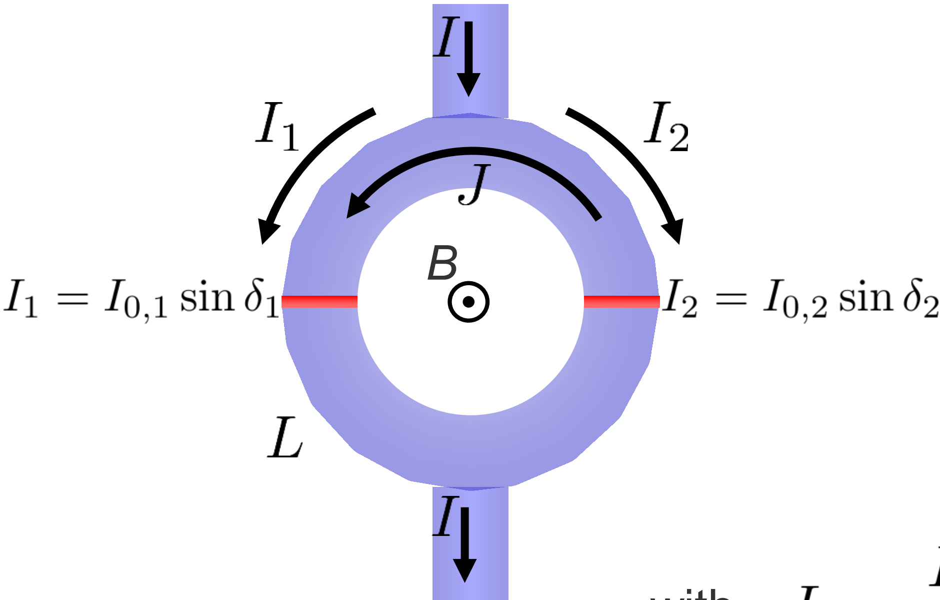

$$\Phi_{\mathrm{tot}} = \Phi_{\mathrm{a}} + LJ$$

applied flux

loop inductance

circulating current

with
$$I_1 = \frac{I}{2} + J$$
$$I_2 = \frac{I}{2} - J$$

$\Rightarrow$

circulating current:

$$J = \frac{I_1 - I_2}{2}$$

dc SQUID Basics: Static Case

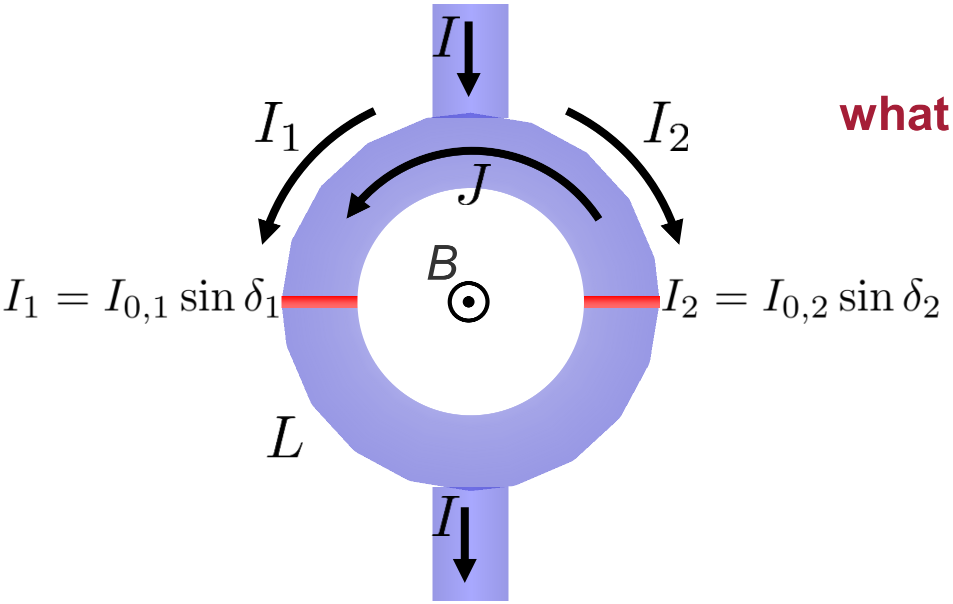

what is the maximum supercurrent $I_c(\Phi_a)$?

assume symmetric SQUID: $I_{0,1} = I_{0,2} = I_0$

with $\sin\alpha + \sin\beta = 2\cos(\frac{\beta-\alpha}{2}) \cdot \sin(\frac{\alpha+\beta}{2})$

$$I = I_1 + I_2 = I_0(\sin\delta_1 + \sin\delta_2) = 2I_0 \cos\left(\frac{\delta_2 - \delta_1}{2}\right) \cdot \sin\left(\frac{\delta_1 + \delta_2}{2}\right)$$

with $\delta_2 = \frac{2\pi}{\Phi_0}\Phi_{\text{tot}} + \delta_1 - 2\pi n$ $\quad I = 2I_0 \cos\left(\frac{\pi\Phi_{\text{tot}}}{\Phi_0} - \pi n\right) \cdot \sin\left(\frac{\pi\Phi_{\text{tot}}}{\Phi_0} + \delta_1 - \pi n\right)$

with $\cos(\alpha - \pi n) \cdot \sin(\beta - \pi n) = \cos(\alpha) \cdot \sin(\beta)$

$$I = 2I_0 \cos\left(\frac{\pi\Phi_{\text{tot}}}{\Phi_0}\right) \cdot \sin\left(\frac{\pi\Phi_{\text{tot}}}{\Phi_0} + \delta_1\right)$$

dc SQUID Basics: Static Case

now maximize by proper choice of δ_1: $$I = 2I_0 \cos\left(\frac{\pi\Phi_{\mathrm{tot}}}{\Phi_0}\right) \cdot \sin\left(\frac{\pi\Phi_{\mathrm{tot}}}{\Phi_0} + \delta_1\right)$$

with $\Phi_{\mathrm{tot}} = \Phi_{\mathrm{a}} + LJ$

$$\downarrow$$

$$J = \frac{I_1 - I_2}{2} = \frac{I_0}{2}(\sin\delta_1 - \sin\delta_2) = I_0 \sin\left(\frac{\pi\Phi_{\mathrm{tot}}}{\Phi_0}\right) \cdot \cos\left(\frac{\pi\Phi_{\mathrm{tot}}}{\Phi_0} + \delta_1\right)$$

⇨ must be solved self-consistently

⇨ simple analytic solutions for two limiting cases

dc SQUID Basics: Static Case

a) negligible inductance:

if maximum flux induced by screening current

$$\Phi_{\mathrm{J,max}} = I_0 L \ll \frac{\Phi_0}{2} \Longleftrightarrow \beta_L \equiv \frac{2LI_0}{\Phi_0} \ll 1$$ screening parameter

$$\Rightarrow \Phi_{\mathrm{tot}} \approx \Phi_{\mathrm{a}}$$

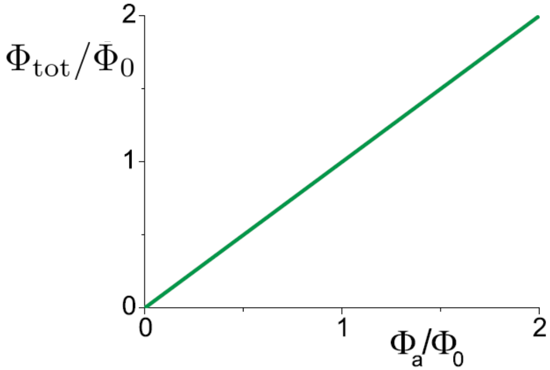

$$I \approx 2I_0 \cos\left(\frac{\pi\Phi_{\mathrm{a}}}{\Phi_0}\right) \cdot \sin\left(\frac{\pi\Phi_{\mathrm{a}}}{\Phi_0} + \delta_1\right)$$

maximum supercurrent I_c through the SQUID:

→ $\sin(\pi\frac{\Phi_{\mathrm{a}}}{\Phi_0} + \delta_1) = \pm 1$

$$\boxed{I_{\mathrm{c}} \approx 2I_0 \left|\cos\left(\frac{\pi\Phi_{\mathrm{a}}}{\Phi_0}\right)\right|}$$

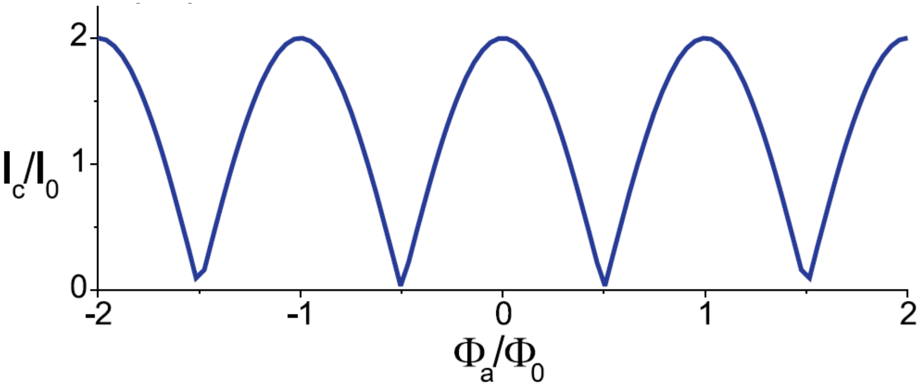

EBERHARD KARLS UNIVERSITÄT TÜBINGEN

dc SQUID Basics: Static Case

b) large inductance: $\beta_L \gg 1$

the applied flux is screened by the flux induced by *LJ*

to minimize magnetic energy $L|J| \leq \frac{\Phi_0}{2}$ ⇨ $|J| \leq \frac{\Phi_0}{2L} = \overbrace{\frac{\Phi_0}{2LI_0}}^{=\frac{1}{\beta_L} \ll 1} I_0 \ll I_0$

⇨ the effect of the induced circulating current *J* on δ_1, δ_2 is small: $\delta_2 - \delta_1 \approx 0$

⇨ $\Phi_{\mathrm{tot}} = \Phi_{\mathrm{a}} + LJ \approx n\Phi_0$

⇨ $J \approx -\frac{\Phi_{\mathrm{a}} - n\Phi_0}{L}$ i.e., for large *L*, *J* → 0

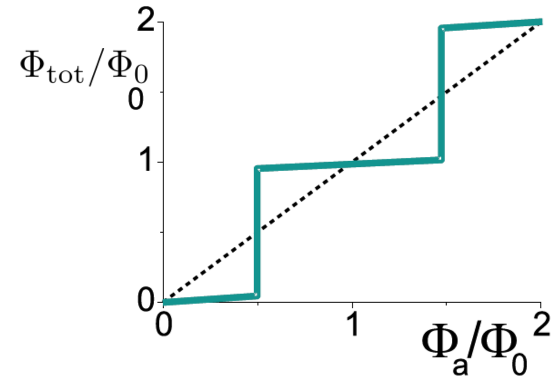

one finds for the maximum change of I_c

$$\Delta I_c \approx \frac{\Phi_0}{L} = \frac{2}{\beta_L} I_0 \ll 2I_0$$

or for the relative modulation depth

$$\frac{\Delta I_c}{2I_0} \approx \frac{\Phi_0}{2I_0 L} = \frac{1}{\beta_L} \ll 1$$

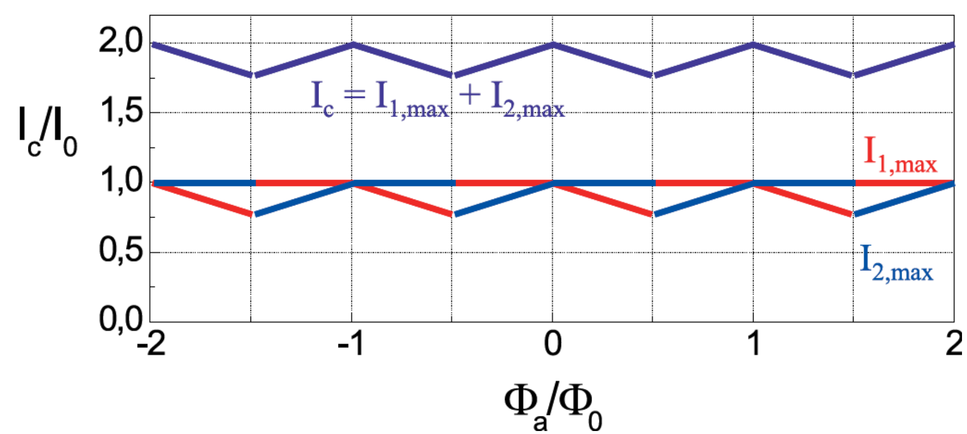

dc SQUID Basics: Static Case

General case:

from numerical simulations for

- symmetric dc SQUID
- at T=0 & sinusoidal CPR

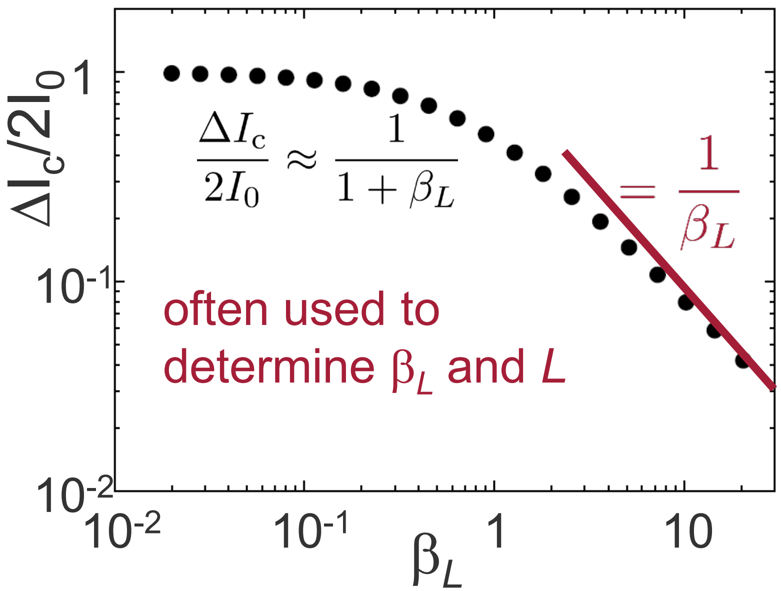

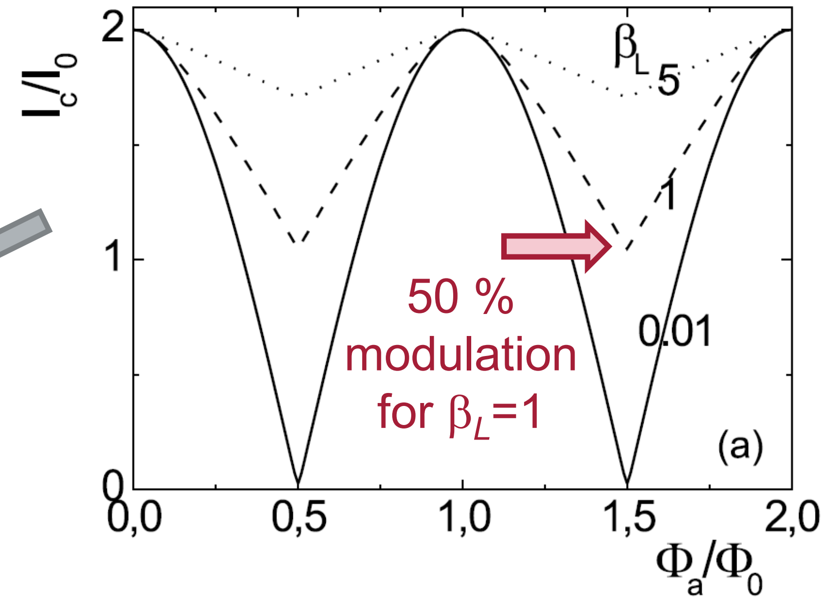

Caution: $I_c(\Phi_a)$ modified for asymmetric SQUIDs

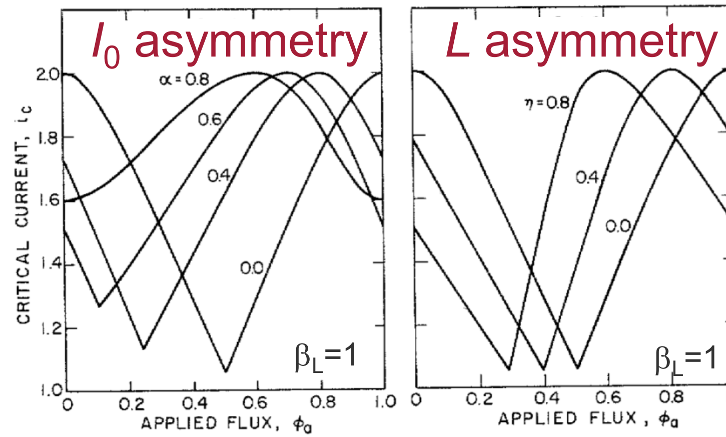

… and by thermal noise!

… and deviations from sinusoidal CPR!

J. R. Prance & M. D. Thompson, Appl. Phys. Lett. **122** (2023)
D. Jetter, B.Sc. Thesis, Univ. Tübingen (2019)

B. Chesca, R. Kleiner & D. Koelle, *SQUID Theory*, Ch. 2 in The SQUID Handbook, Vol. I

C.D. Tesche, J. Clarke, *dc SQUID: Noise and Optimization*, J. Low Temp. Phys. **29**, 301 (1977)

dc SQUID Basics: Dynamic Case

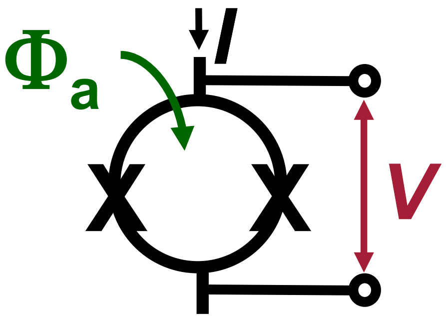

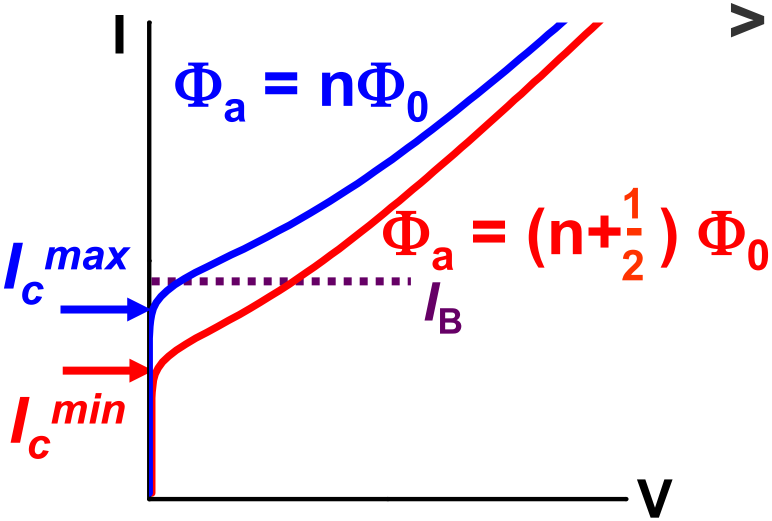

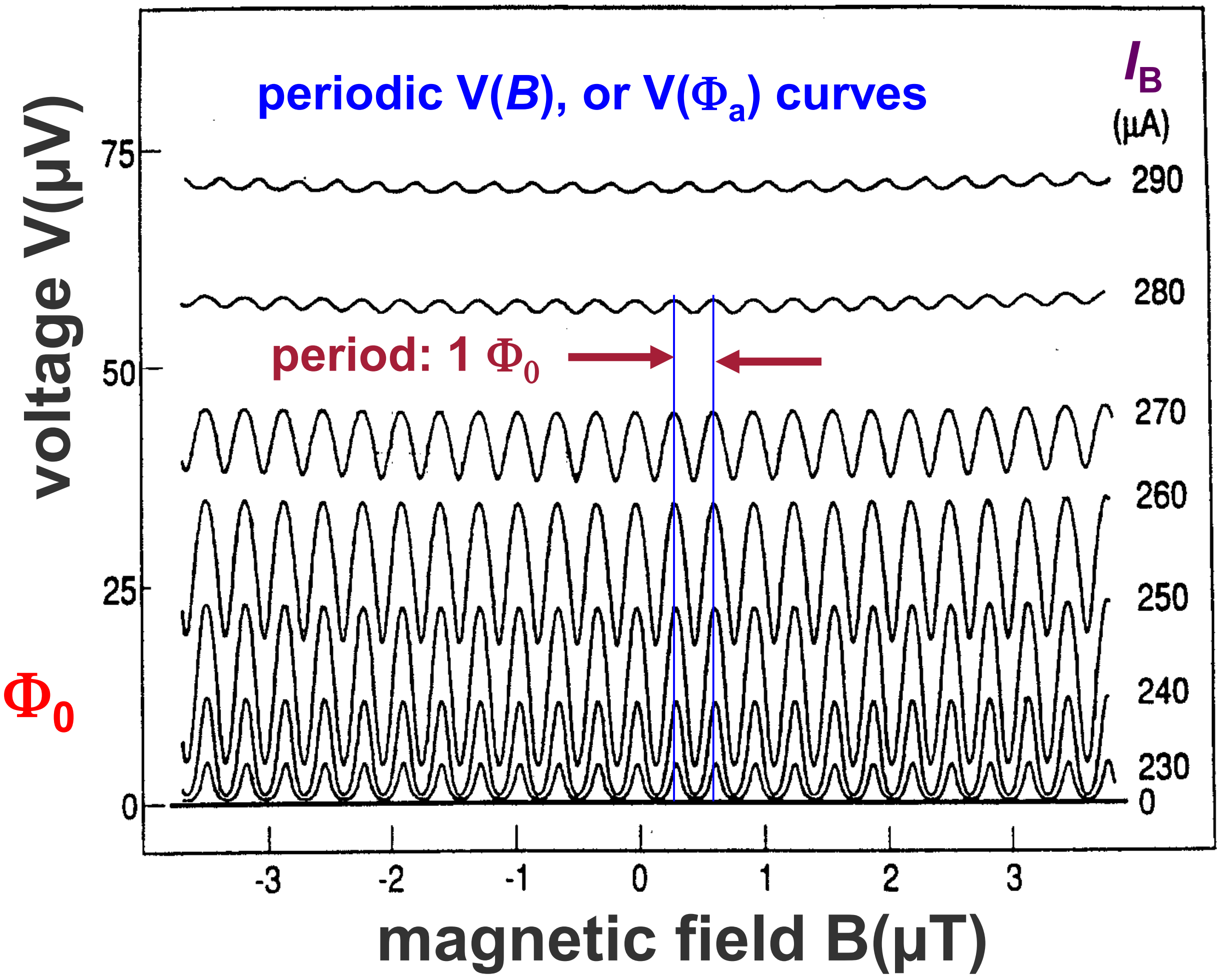

dc SQUID Basics: Dynmic Case

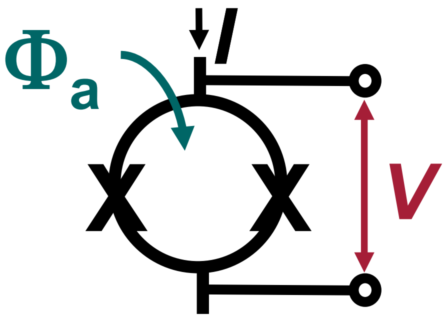

voltage vs applied flux $V(\Phi_a)$
(at I_B = const)

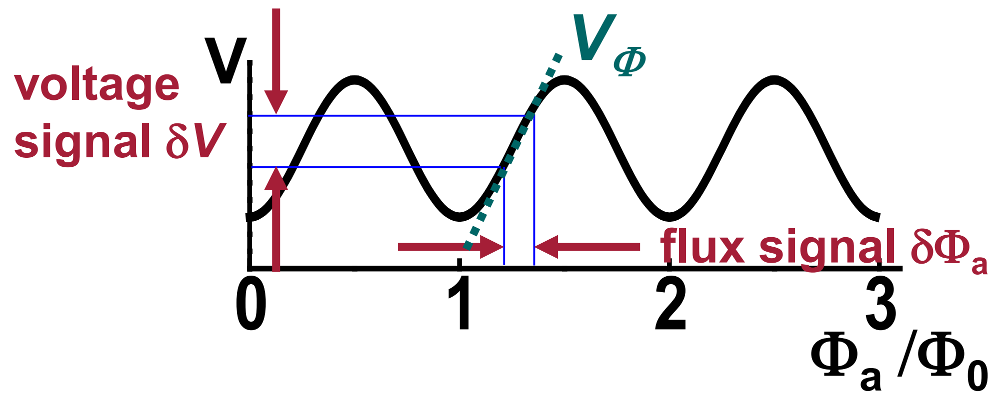

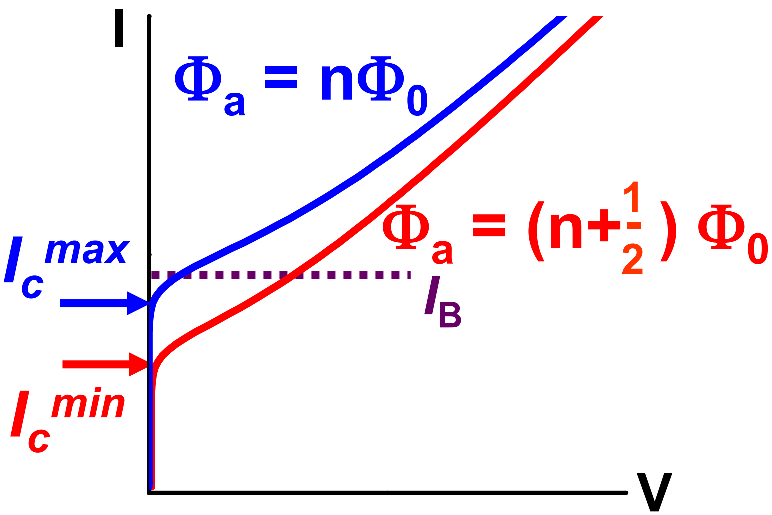

transfer function = maximum slope of $V(\Phi_a)$

$$\boxed{V_\Phi \approx R/L}$$

typical: $V_\Phi \approx 100\ \mu V/\Phi_0$

dc SQUID Basics: Dynmic Case

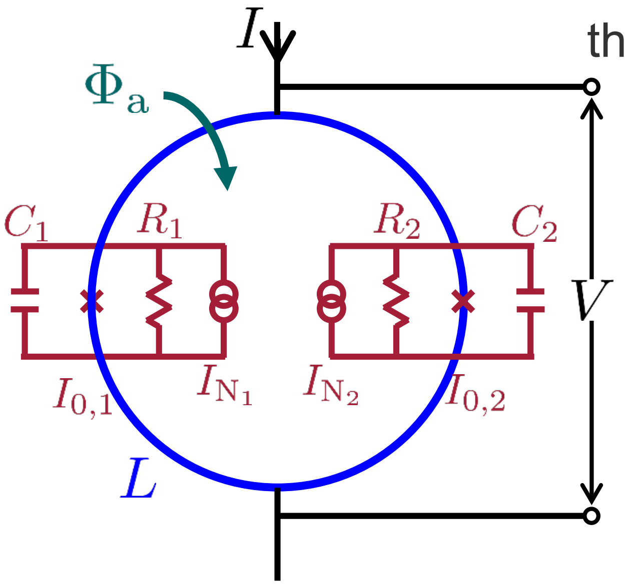

theoretical description based on RCSJ model

$$I_1 = \frac{I}{2} + J = I_{0,1}\sin\delta_1 + \frac{\Phi_0}{2\pi R_1}\dot{\delta}_1 + \frac{\Phi_0 C_1}{2\pi}\ddot{\delta}_1 + I_{N_1}$$

$$\Updownarrow$$

$$I_2 = \frac{I}{2} - J = I_{0,2}\sin\delta_2 + \frac{\Phi_0}{2\pi R_2}\dot{\delta}_2 + \frac{\Phi_0 C_2}{2\pi}\ddot{\delta}_2 + I_{N_2}$$

$$\delta_2 - \delta_1 = \frac{2\pi}{\Phi_0}(\Phi_a + LJ) = \frac{2\pi}{\Phi_0}\Phi_{tot} \qquad V = \frac{\Phi_0}{2\pi}\frac{\overline{\dot{\delta}_1} + \overline{\dot{\delta}_2}}{2}$$

asymmetry:

$$I_{0,1} = I_0(1-\alpha_I); \quad R_1 = R/(1-\alpha_R); \quad C_1 = C(1-\alpha_C)$$
$$I_{0,2} = I_0(1+\alpha_I); \quad R_2 = R/(1+\alpha_R); \quad C_2 = C(1+\alpha_C)$$

$$I_0 = (I_{0,1} + I_{0,2})/2$$
$$R = 2R_1R_2/(R_1 + R_2)$$
$$C = (C_1 + C_2)/2$$

normalization: currents i, j (I_0), voltage (I_0R), time ($\tau = \Phi_0/(2\pi I_0 R)$), magnetic flux ϕ (Φ_0)

$$i_1 = \frac{i}{2} + j = (1-\alpha_I)\sin\delta_1 + (1-\alpha_R)\dot{\delta}_1 + \beta_C(1-\alpha_C)\ddot{\delta}_1 + i_{N_1}$$

$$i_2 = \frac{i}{2} - j = (1+\alpha_I)\sin\delta_2 + (1+\alpha_R)\dot{\delta}_2 + \beta_C(1+\alpha_C)\ddot{\delta}_2 + i_{N_2}$$

$$\delta_2 - \delta_1 = 2\pi(\phi_a + \frac{\beta_L j}{2}) \qquad v = \frac{\overline{\dot{\delta}_1} + \overline{\dot{\delta}_2}}{2}$$

dc SQUID Basics: Dynamic Case
dc SQUID Potential

with normalized circulating current $\frac{J}{I_0} \equiv j = \frac{2}{\pi\beta_L}\left(\frac{\delta_2-\delta_1}{2} - \pi\phi_a\right)$

inserted into the normalized Eqs. of motion (for symmetric case):

$$\beta_C \ddot{\delta}_k + \dot{\delta}_k = -\frac{\partial u_{\mathrm{dcsquid}}}{\partial \delta_k} \qquad \text{(with } k = 1, 2\text{)}$$

with the 2-dim. dc SQUID potential

$$E_{\mathrm{J}} \equiv \frac{I_0\Phi_0}{2\pi}$$

$$E_{\mathrm{M}} = \frac{1}{2\pi}\frac{\Phi_0^2}{2L}$$

$$\frac{U_{dcsquid}}{E_{\mathrm{J}}} = u_{dcsquid} = \underbrace{\frac{2}{\pi}\frac{1}{\beta_L}\left(\frac{\delta_2-\delta_1}{2} - \pi\phi_a\right)^2}_{\text{magnetic energy}} \underbrace{- \cos\delta_1 - \cos\delta_2}_{\text{Josephson energy}} - i\,\frac{\delta_1+\delta_2}{2}$$

$$\beta_L = \frac{E_{\mathrm{J}}}{E_{\mathrm{M}}}$$

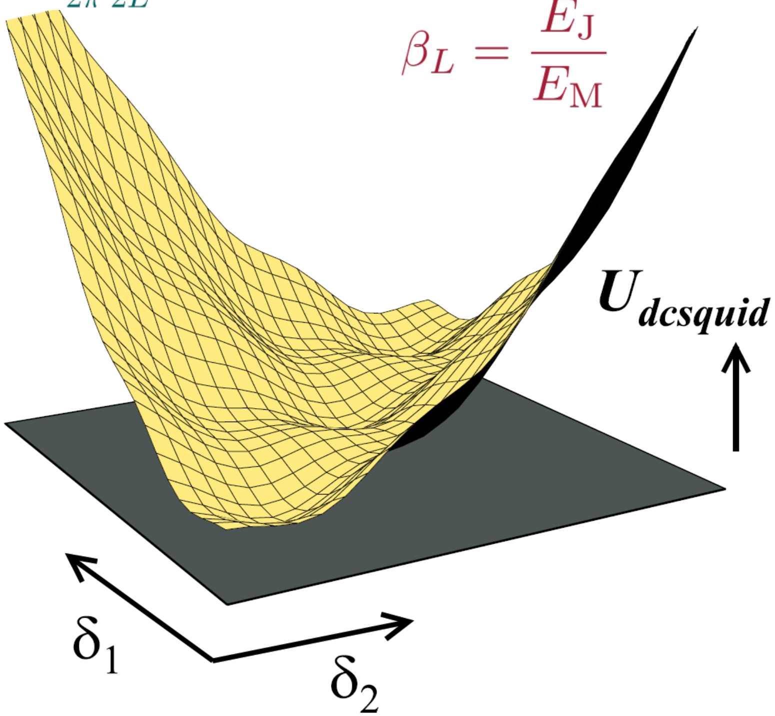

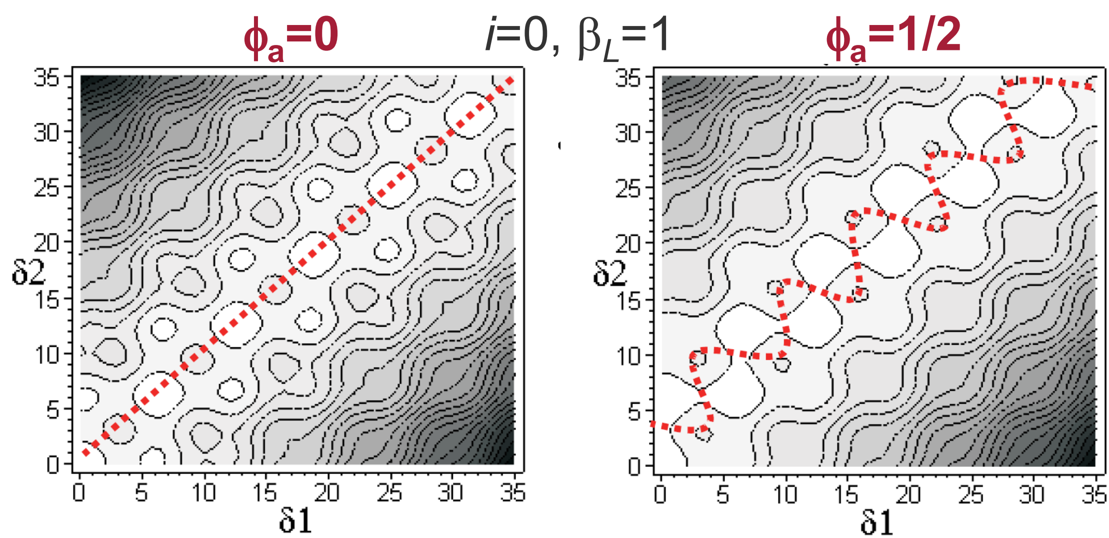

dc SQUID: noise

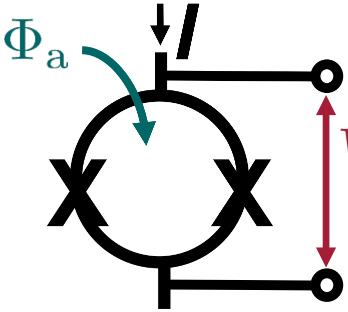

noise voltage $V_N(t)$ with spectral power density of voltage noise $S_V(f)$

$$V = V_{dc} + V_N$$

→ equivalent noise flux

$$\Phi_N(t) = \frac{V_N}{V_\Phi}$$

with equivalent spectral density of flux noise $\quad S_\Phi(f) = \frac{S_V}{V_\Phi^2}$

→ rms flux noise $S_\Phi^{1/2} = S_V^{1/2}/V_\Phi \quad$ units: $\Phi_0/\sqrt{\mathrm{Hz}}$

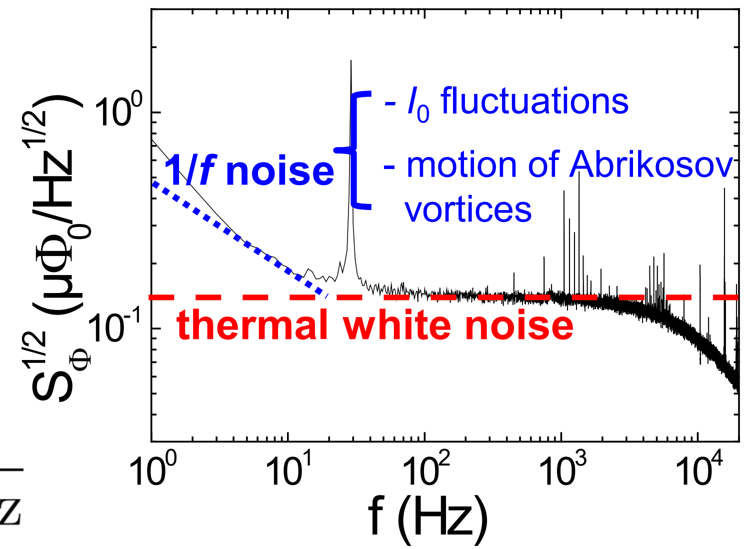

fluctuation energy $\quad \frac{\Phi_N^2}{2L}$

energy resolution $\quad \varepsilon = \frac{S_\Phi}{2L} \qquad$ units: $\mathrm{J}/\sqrt{\mathrm{Hz}}$

dc SQUID Basics: Thermal Fluctuations

thermal fluctuations at finite temperature T become important when $k_B T$ approaches

- the Josephson coupling energy $E_\mathrm{J} = \dfrac{I_0 \Phi_0}{2\pi}$ i.e. $\dfrac{k_\mathrm{B}T}{E_\mathrm{J}} = \Gamma = \dfrac{\frac{2\pi}{\Phi_0} k_\mathrm{B} T}{I_0} = \dfrac{I_\mathrm{th}}{I_0} \to 1$

- the characteristic magnetic energy $E_\mathrm{M} = \dfrac{E_\mathrm{J}}{\beta_L} = \dfrac{1}{2\pi}\dfrac{\Phi_0^2}{2L}$

  i.e. $\dfrac{k_\mathrm{B}T}{E_\mathrm{M}} = \Gamma\beta_L = \dfrac{L}{\Phi_0^2/(4\pi k_\mathrm{B}T)} = \dfrac{L}{L_\mathrm{th}} \to 1$

regime of small thermal fluctuations:

$$\Gamma \ll 1 \quad \Longrightarrow \quad I_0 \gg I_\mathrm{th} = \frac{2\pi}{\Phi_0} k_\mathrm{B} T \propto T$$

for T= 4.2 K: I_th ~ 0.18 μA
for T = 77 K: I_th ~ 2.3 μA

$$\Gamma\beta_L \ll 1 \quad \Longrightarrow \quad L \ll L_\mathrm{th} = \frac{\Phi_0^2}{4\pi k_\mathrm{B} T} \propto \frac{1}{T}$$

for T= 4.2 K: L_th ~ 5.9 pH
for T = 77 K: L_th ~ 320 pH

$$\Leftrightarrow L I_\mathrm{th} \ll \frac{\Phi_0}{2}$$

dc SQUID: thermal „white“ noise

analysis based on numerical simulations (RCSJ model: solve coupled Langevin Eqs.)

in the limit of small thermal fluctuations (at ~ 4 K):

transfer function $V_\Phi \propto \frac{1}{1+\beta_L}$ optimum noise performance at $\beta_L \approx 1$

for $\beta_L \approx 1;\ \Gamma \approx 1/20:$

$$V_\Phi \approx \frac{R}{L} \approx \frac{2I_0R}{\Phi_0}$$

$$S_V \approx 16 k_\mathrm{B} T R \qquad S_V^{1/2} \approx 15\,\frac{\mathrm{pV}}{\sqrt{\mathrm{Hz}}} \times \sqrt{T[\mathrm{K}]\cdot R[\Omega]}$$

$$S_\Phi \approx 16 k_\mathrm{B} T \frac{L^2}{R} \qquad S_\Phi^{1/2} \approx 0.7\,\frac{\mu\Phi_0}{\sqrt{\mathrm{Hz}}} \times \sqrt{\frac{T[\mathrm{K}]}{R[\Omega]}} \times L[100\,\mathrm{pH}]$$

$$\varepsilon \approx 9 k_\mathrm{B} T \frac{L}{R} \approx \frac{9\Phi_0}{2}\frac{k_\mathrm{B}T}{I_0R} \approx \underbrace{10^{-34}(\mathrm{J/Hz})}_{\approx \hbar} \times \frac{T[\mathrm{K}]}{I_0R[\mathrm{mV}]}$$

typical values:

$S_\Phi^{1/2}$ ~ 1 - 10 $\mu\Phi_0/\mathrm{Hz}^{1/2}$

extremely sensitive to tiny changes of magnetic flux

C.D. Tesche, J. Clarke, *dc SQUID: Noise and Optimization*, J. Low Temp. Phys. **29**, 301 (1977)

dc SQUID: thermal „white“ noise

analysis based on numerical simulations (RCSJ model: solve coupled Langevin Eqs.)

including large thermal fluctuations (~ 77 K):

normalized quantities
vs. Γ and β_L (β_C=0.5)
→ factorize into

$$f(\beta_L)\cdot g(\Gamma\beta_L)$$

significantly deteriorate for

$$\Gamma\beta_L \gtrsim 0.3$$

$$L \gtrsim 0.3 L_{\rm th} \approx 100\,{\rm pH \ at \ 77\,K}$$

normalized quantities:

transfer function : $v_\phi \equiv V_\Phi \cdot \dfrac{\Phi_0}{I_0 R}$

voltage noise : $s_v \equiv S_V \cdot \dfrac{2\pi}{\Phi_0 I_0 R}$

flux noise : $s_\phi \equiv S_\Phi \cdot \dfrac{2\pi I_0 R}{\Phi_0^2}$

energy resolution : $e \equiv \varepsilon \cdot \dfrac{I_0 R}{2 k_B T \Phi_0}$

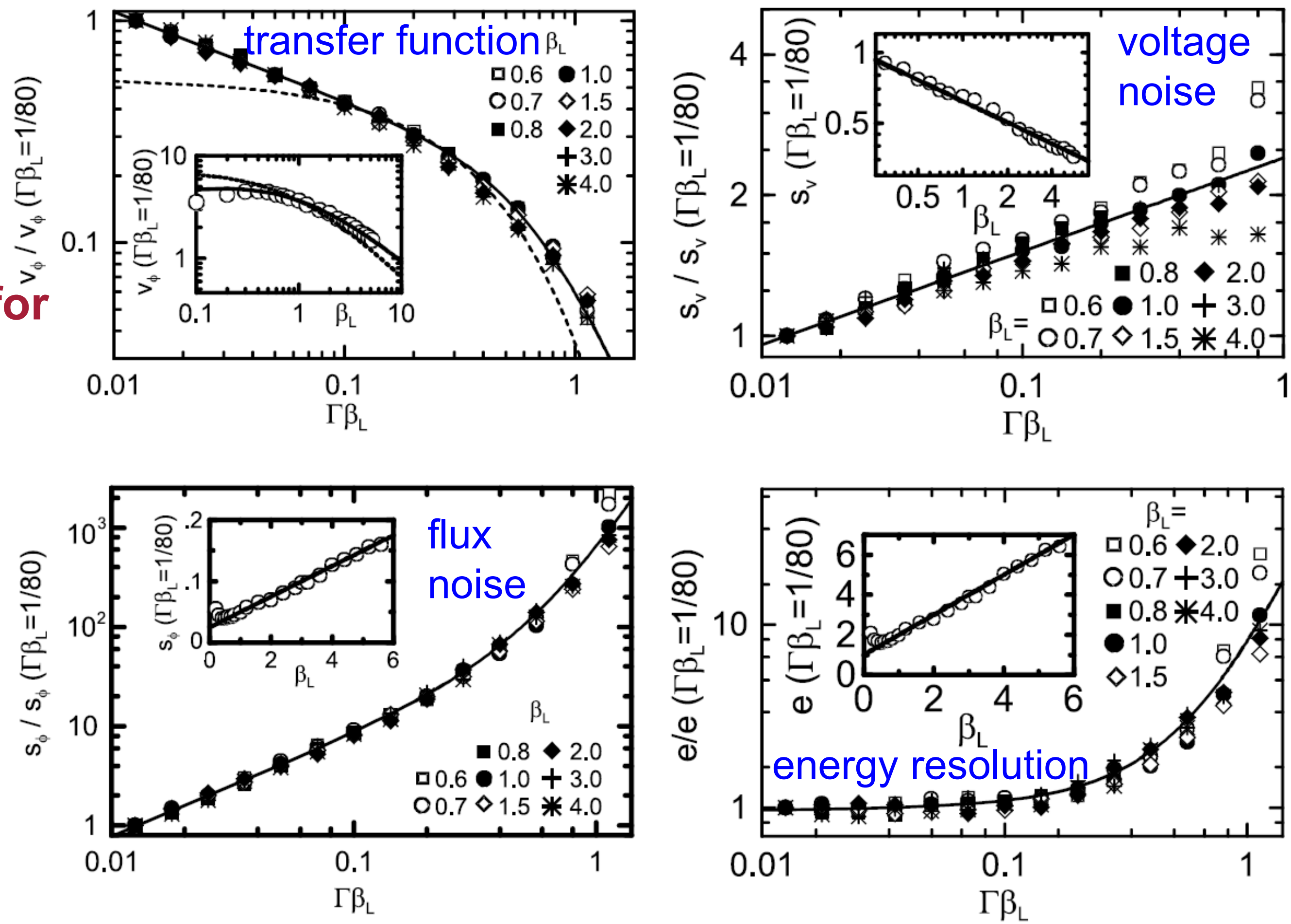

D. Koelle, R. Kleiner, F. Ludwig, E. Dantsker, J. Clarke, Rev. Mod. Phys. **71**, 631 (1999)
B. Chesca, R. Kleiner & D. Koelle, *SQUID Theory*, Ch. 2 in The SQUID Handbook, Vol. I (2004)

Outline

I. SQUIDs: Basics & principle of operation

II. Practical devices and readout

III. SQUID applications

   a. Magnetometry, Susceptometry

   b. Biomagnetism: MEG, low-field MRI

   c. Scanning SQUID microscopy

   d. magnetic nanoparticle (MNP) detection

dc SQUID Readout
Flux-Locked Loop (FLL)

voltage vs applied flux $V(\Phi_a)$

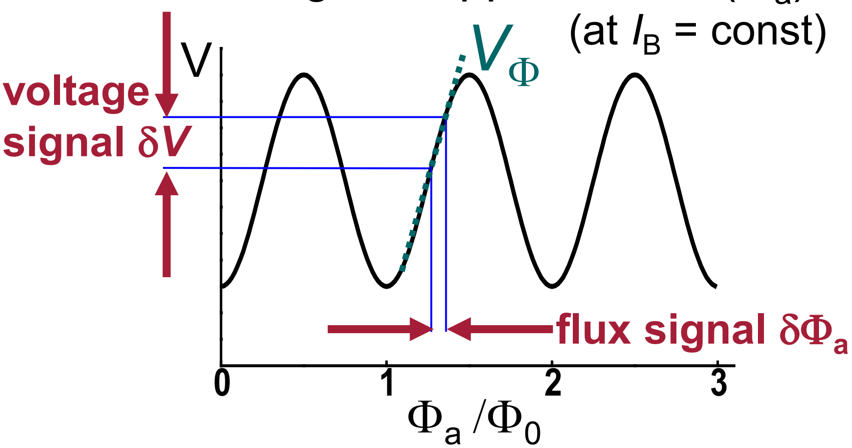

flux-locked loop (FLL)

→ linearizes output voltage

→ maintains optimum working point

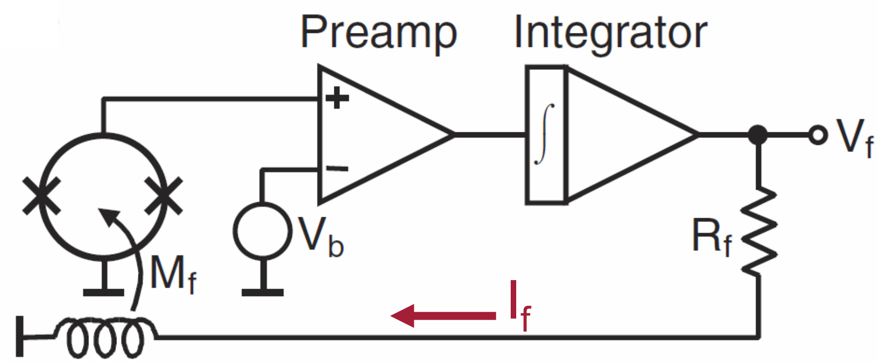

feedback flux $\Phi_f = I_f M_f$ compensates $\delta\Phi_a$

output signal: $V_f = \dfrac{R_f}{M_f}\,\Phi_f \propto \delta\Phi_a$

typical bandwidth: ~10 kHz … ~10 MHz

D. Drung & M. Mück, *SQUID* Electronics,
Chapter 4 in The SQUID Handbook, Vol. I

dc SQUID Readout
APF & ac Flux Modulation

„direct readout“

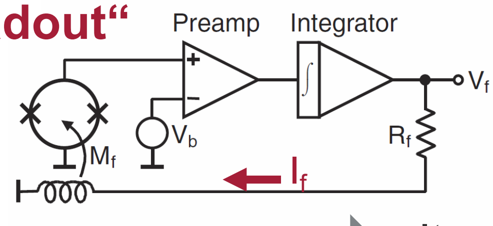

sensitivity can be limited by preamplifier (p.a.) noise

$$S_{V,\mathrm{p.a.}}^{1/2} > S_{\Phi}^{1/2} \cdot V_{\Phi}$$

alternative readout schemes:

additional positive feedback (APF)

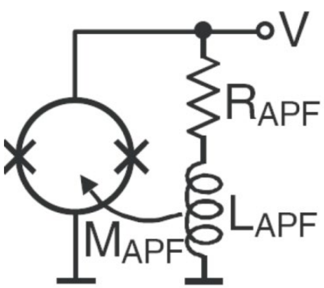

enhances V_{Φ} to overcome p.a. noise

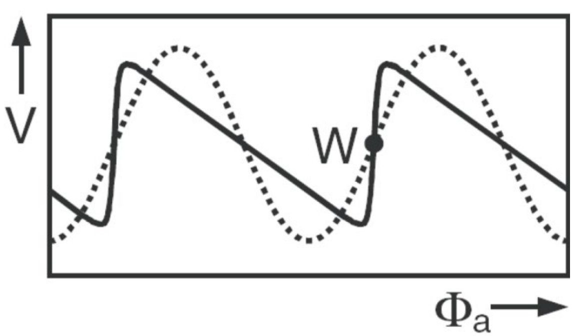

ac flux modulation

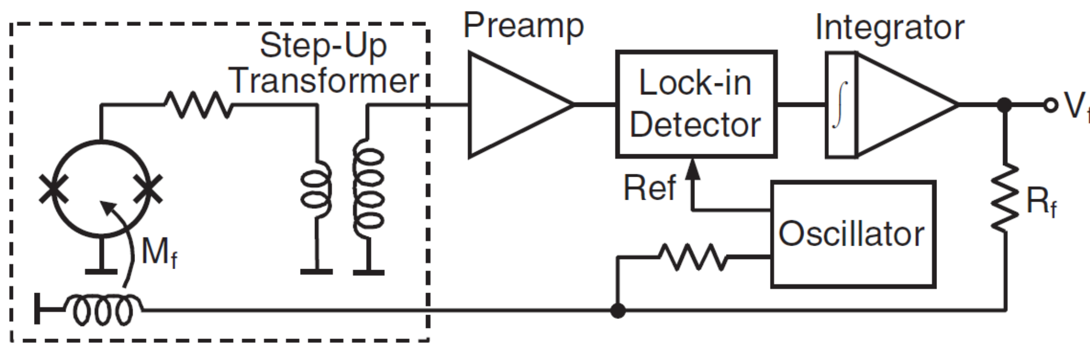

transformer enhances signal above p.a. noise level

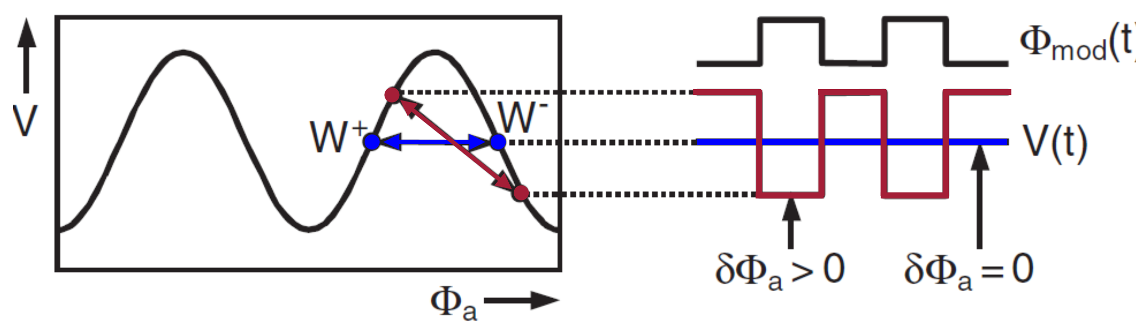

D. Drung & M. Mück, *SQUID* Electronics, Ch. 4 in The SQUID Handbook, Vol. I
D. Drung, *High-Tc and Low-Tc dc SQUID* Electronics, Supercond. Sci. Technol. **16**, 1320 (2003)

dc SQUID Readout: Bias Reversal

elimination of 1/*f* noise contribution from I_0 fluctuations

by reversing bias current (and bias flux, bias voltage) at reversal frequency f_{br} up to few 100 kHz

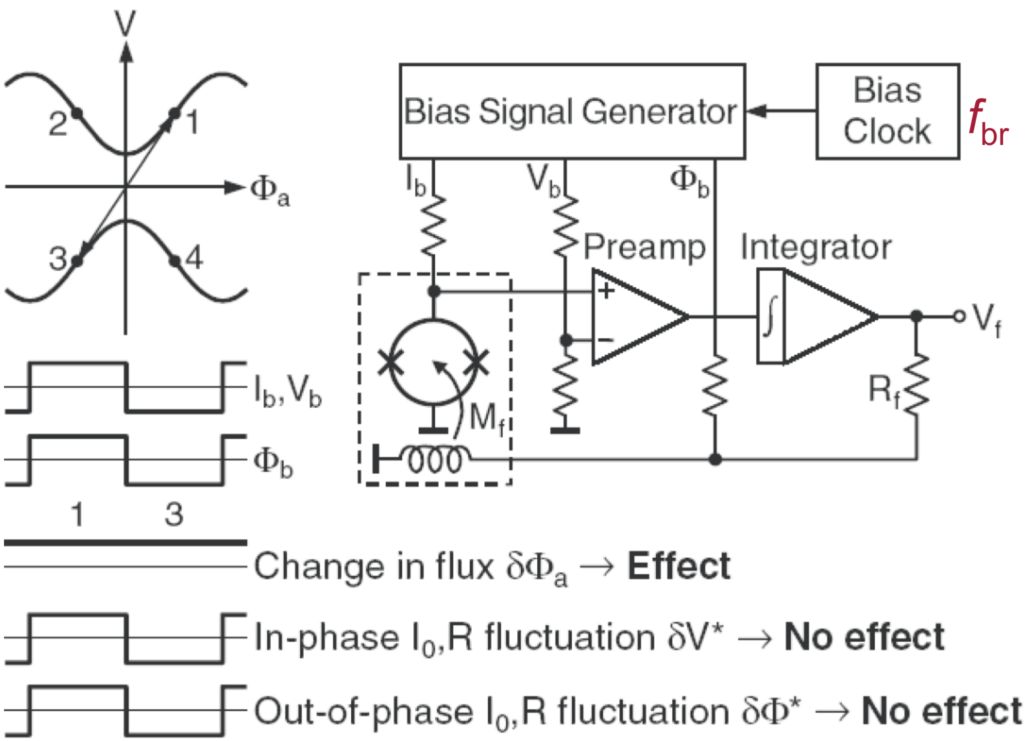

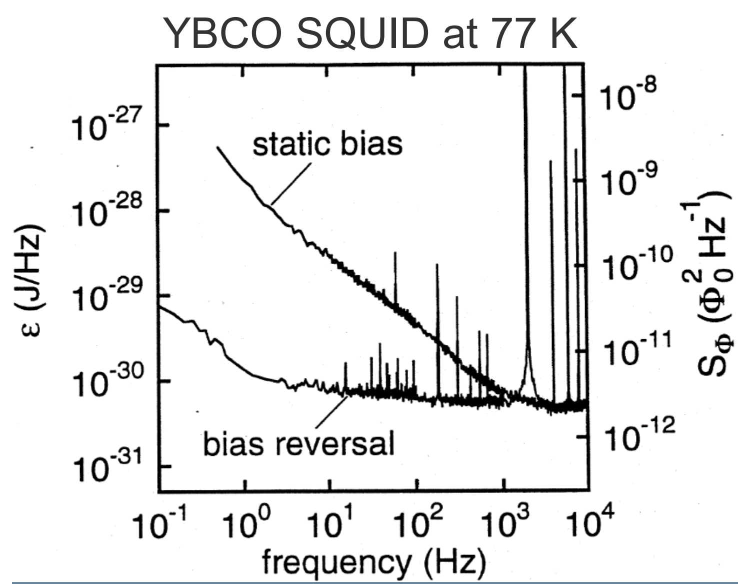

D. Drung, *High-Tc and Low-Tc dc SQUID* Electronics, Supercond. Sci. Technol. **16**, 1320 (2003)

D. Koelle *et al.*, Rev. Mod. Phys. **71**, 631 (1999)

Examples: SQUID Structures

YBCO SQUID

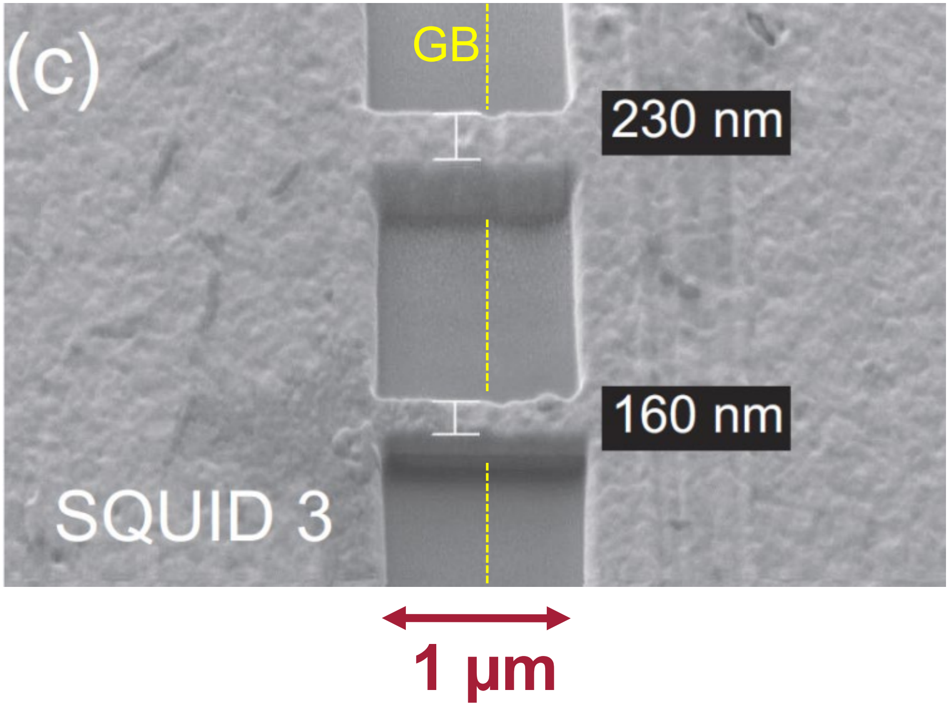

grain boundary (GB) junctions

Nb SQUID

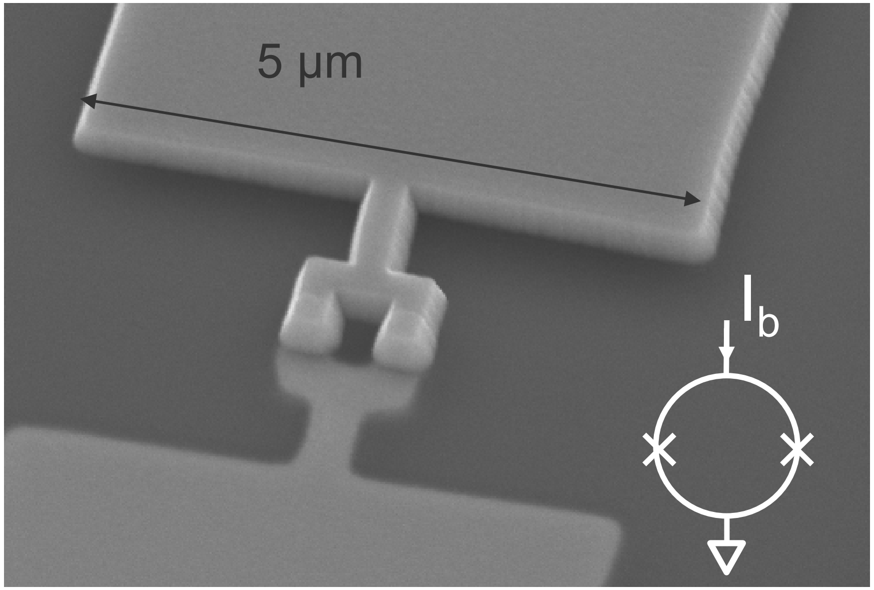

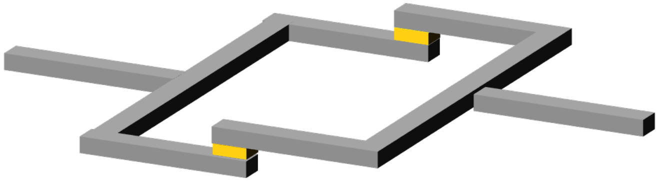

sandwich-type trilayer Nb/HfTi/Nb junctions

SQUIDs for Measurements of Magnetic Fields & Field Gradients

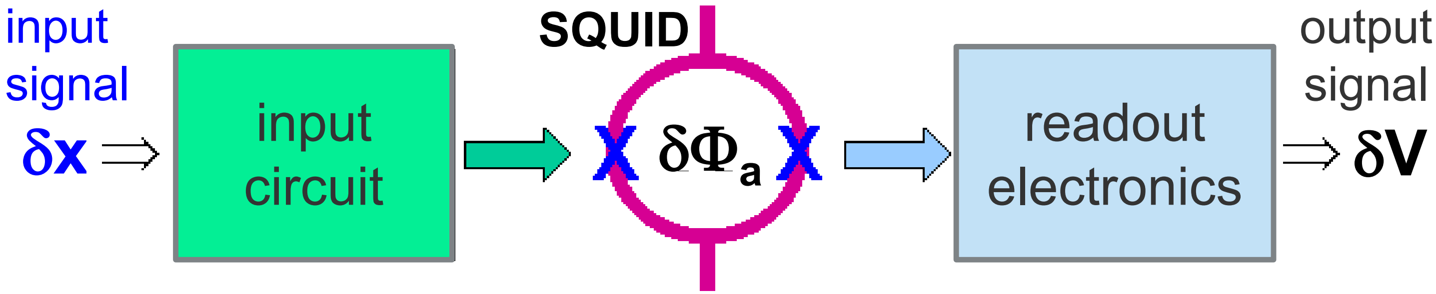

typical signal to be detected:
change of magnetic field δB → flux signal: $\delta\Phi = \delta B \cdot A_{\mathrm{eff}}$

effective sensor area ⟺ flux-to-field conversion factor

$$\frac{1}{A_{\mathrm{eff}}} \equiv B_\Phi = \frac{\delta B}{\delta \Phi_{\mathrm{a}}} = \frac{B_0}{\Phi_0}$$

magnetic field resolution:
→ rms spectral density of field noise

$$S_B^{1/2} \equiv \frac{S_\Phi^{1/2}}{A_{\mathrm{eff}}} = S_\Phi^{1/2} B_\Phi$$

experiment:
measure the homogeneous field B_0 required to induce one oscillation in $V(B)$, i.e. a flux change by 1 Φ_0

→ low field noise requires
- **small SQUID inductance L**
- **large sensor area A_{eff}**

solution: properly designed SQUID layouts and input circuit structures

EBERHARD KARLS UNIVERSITÄT TÜBINGEN

Washer SQUID

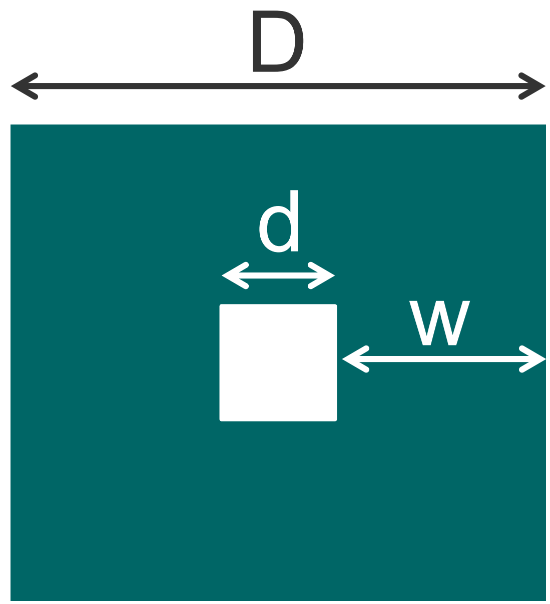

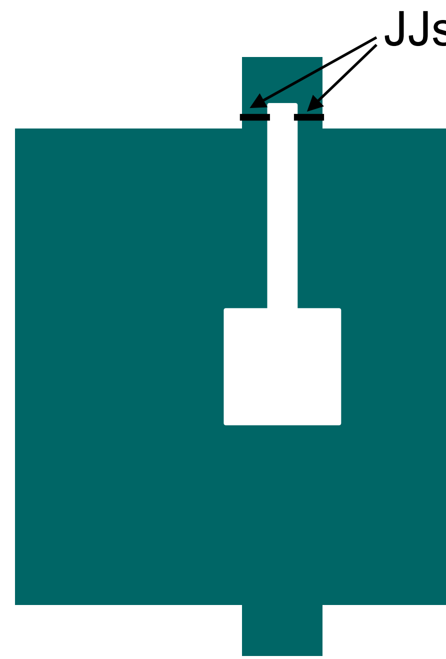

$$\boxed{\begin{aligned} A_{\text{eff}} &\approx dD \\ L &\approx 1.25\,\mu_0 d \end{aligned}}$$ (for $w \gtrsim d$)

M.B. Ketchen *et al.*, in SQUID'85, deGruyter (1985)
M.B. Ketchen, IEEE Trans. Magn. **23**, 1650 (1987)

with d = 20 μm, D = 500 μm ⇒ $A_{\text{eff}} = (100\ \mu\text{m})^2$, $B_\Phi \sim 0.2\ \mu\text{T}/\Phi_0$

with flux noise
$S_\Phi^{1/2} = 5\ \mu\Phi_0/\text{Hz}^{1/2}$

typical field noise
$S_B^{1/2} \approx 1\ \text{pT}/\text{Hz}^{1/2}$

signals < $10^{-6}\ B_{\text{earth}}$ detectable

Superconducting Flux Transformer

B induces
screening current
$$I_s = \frac{BA_p}{L_p + L_i}$$

couples flux
$$\Phi_a = MI_s$$
into SQUID

closed superconducting structure

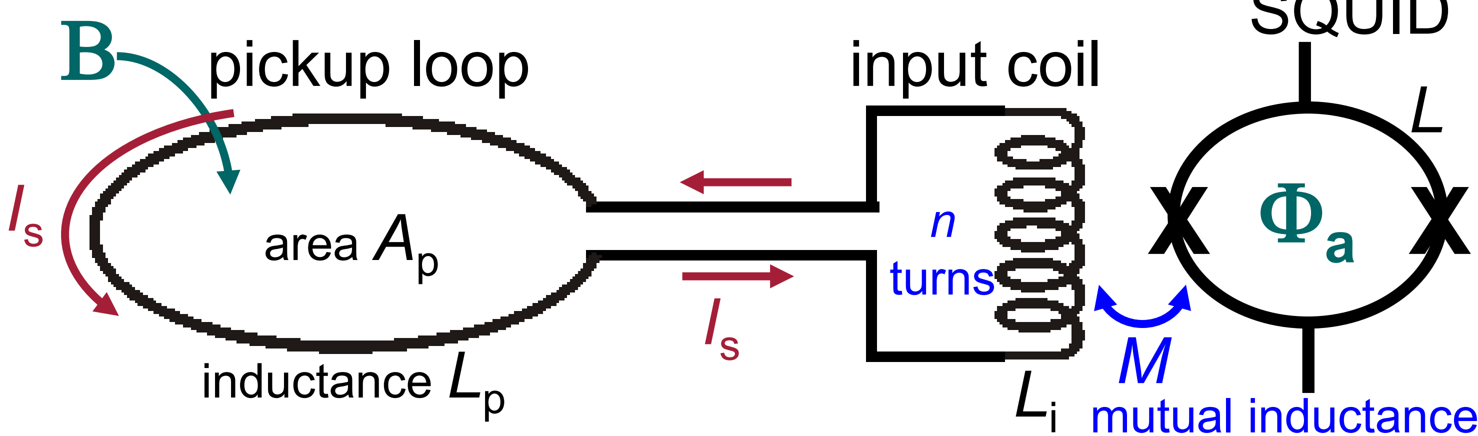

with $M = \alpha\sqrt{L_i L}$ $\quad A_{\mathrm{eff}} = \frac{\Phi_a}{B} = \frac{\alpha\sqrt{L_i L}}{L_p + L_i} A_p$

coupling factor ≤ 1

maximize A_{eff} → L_i=L_p („matched“ transformer): $A_{\mathrm{eff,mt}} = \frac{\alpha}{2}\sqrt{\frac{L}{L_p}} A_p$

adjust $L_i \approx n^2 L$ via number of turns

$$\boxed{A_{\mathrm{eff,mt}} \approx \frac{n}{2}\alpha\frac{L}{L_p}A_p}$$

significantly enhanced effective area

with A_p=1 cm², L_p=22.5 nH, L=100 pH → n=15 & α=0.75: $\mathbf{A_{eff} \approx 2.5\ mm^2}$

Inductively Coupled SQUID Magnetometer

SQUID + flux transformer = Ketchen Magnetometer

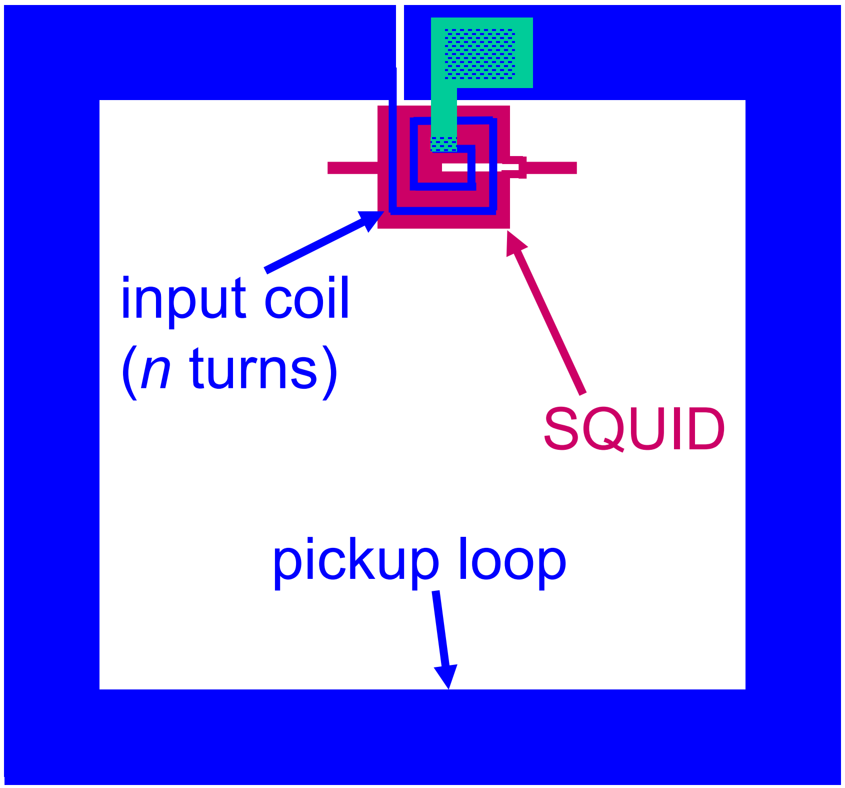

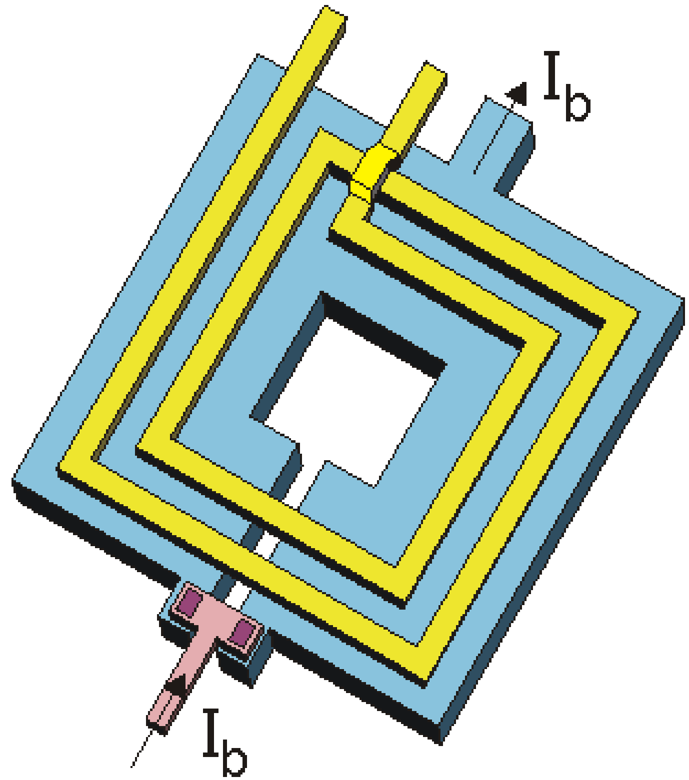

multilayer structure

EBERHARD KARLS UNIVERSITÄT TÜBINGEN

SQUID Magnetometer

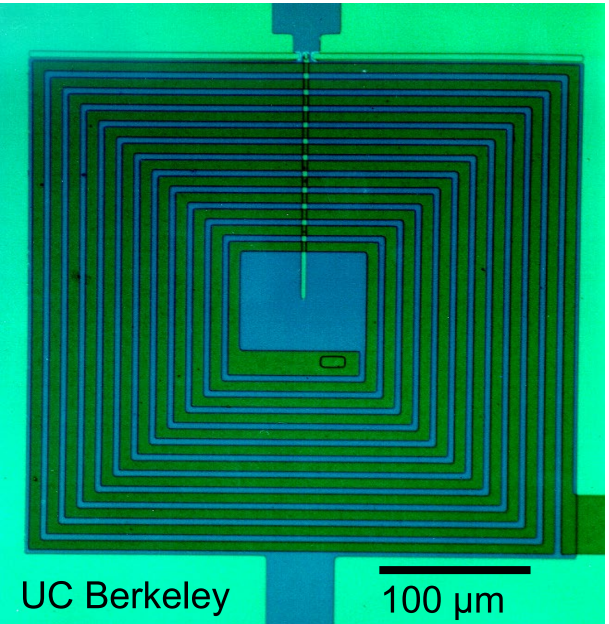

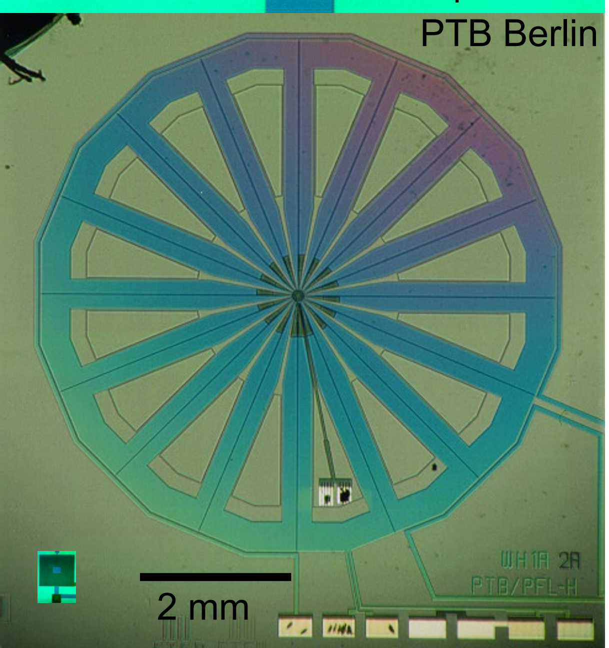

$S_B^{1/2} \sim 1$ fT / Hz$^{1/2}$ at $T = 4.2$ K

for frequencies > 1 Hz

1 fT x 60 billions = earth magnetic field

comparison in size:

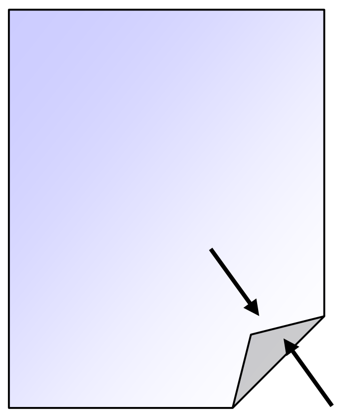

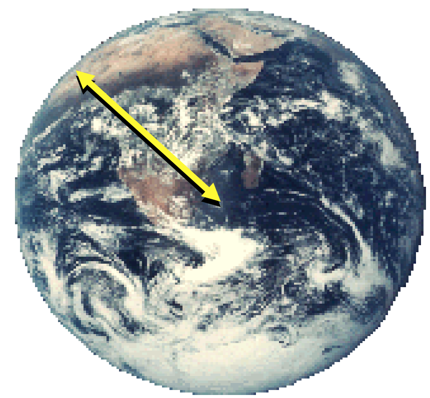

paper thickness 0.1 mm

x 60 bill. = earth radius

$S_B^{1/2} \sim 150$ aT / Hz$^{1/2}$ at $T = 4.2$ K

J.-H. Storm *et al*, Appl. Phys. Lett. **110**, 072603 (2017)

SQUID Gradiometer

magnetometer:

measures field B_z

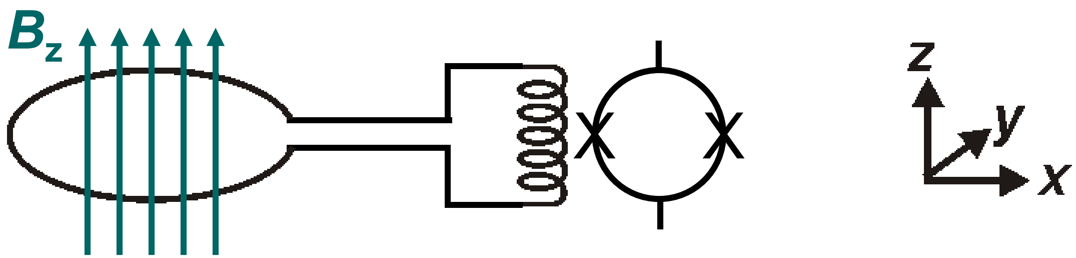

1. order gradiometer:

counter-wound
pickup-loops:

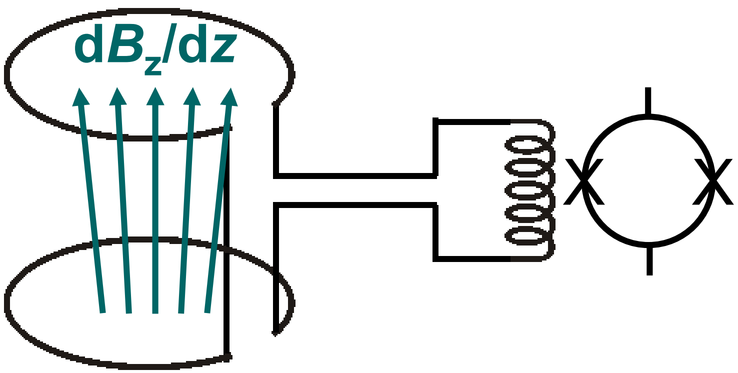

insensitive against homogeneous disturbing fields !!

measures gradient dB/dz

→ local signals at one loop

Outline

I. SQUIDs: Basics & principle of operation

II. Practical devices and readout

III. SQUID applications

a. Magnetometry, Susceptometry

b. Biomagnetism: MEG, low-field MRI

c. Scanning SQUID microscopy

d. Magnetic nanoparticle (MNP) detection

What is a SQUID good for?

<u>quantities</u>

- Magnetometry, Susceptometry
  → *materials-/geosciences, chemistry, physics* — → magnetization M
  → *magnetic nanoparticles/molecules* → nanoSQUIDs — → magnetic susceptibility χ
- Biomagnetism
  → *non-invasive imaging of brain and heart activity, ...* — → I, B, ∇B
  → *magnetic resonance imaging (MRI) at low magnetic fields* — → M
- Geophysics
  → *search for fossile or geothermal energy resources, ...* — → B, ∇B
- Non-destructive evaluation of materials
  → *cracks or magnetic inclusions (airplane wheels, -turbines, reinforced steel in bridges), ...* — → I, B, ∇B
- Metrology
  → *voltmeter, amperemeter, noise thermometer, ...* — → V_{dc}, V_{rf}, I, T
- Particle detectors (e.g. calorimeters) — → $\delta\varepsilon$, δT
- SQUID microscopy — → B,Φ(x,y,z)

IV.a Magnetometry, Susceptometry

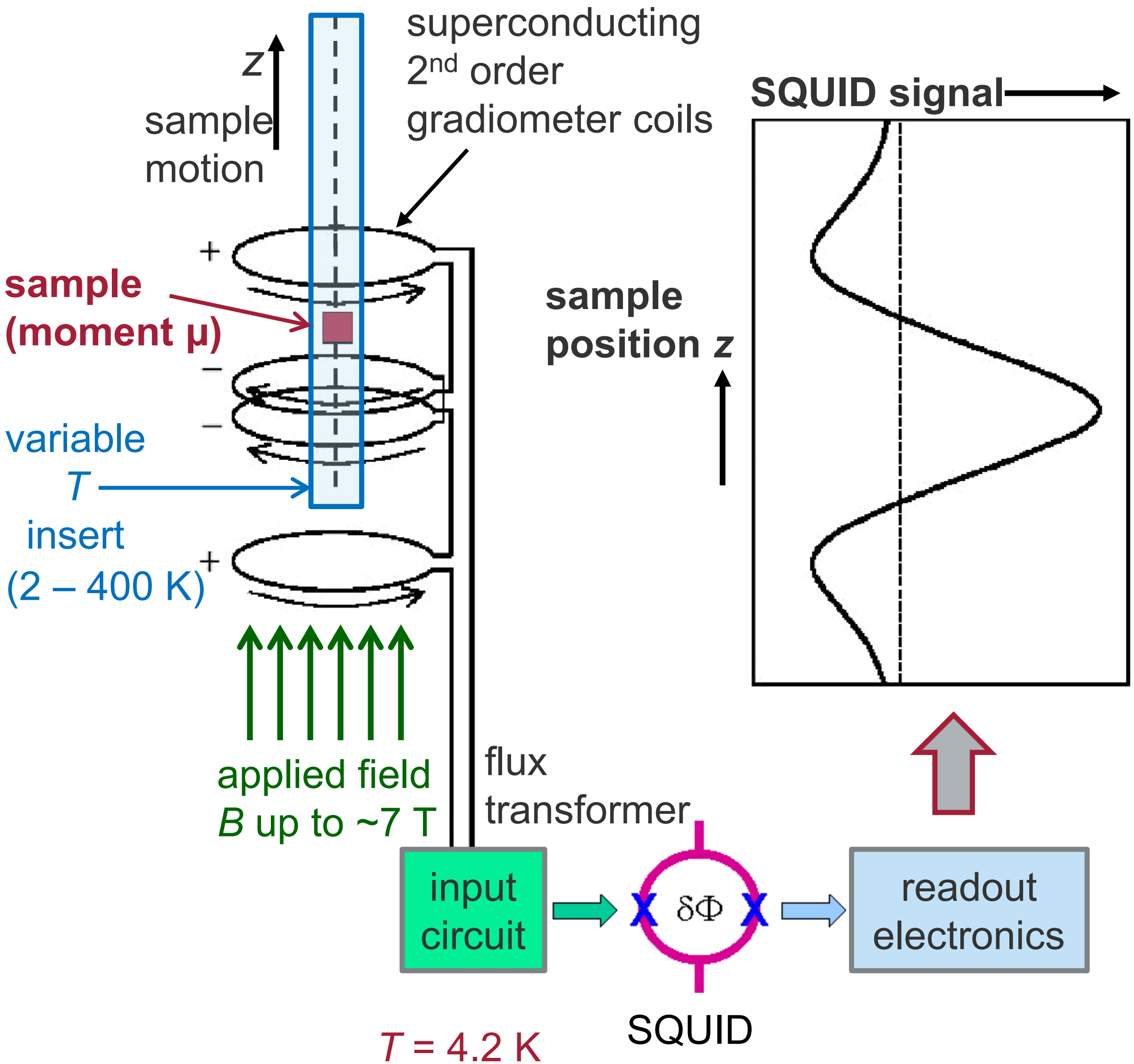

fitting routine $f(z)$

magnetic moment μ(T,B)

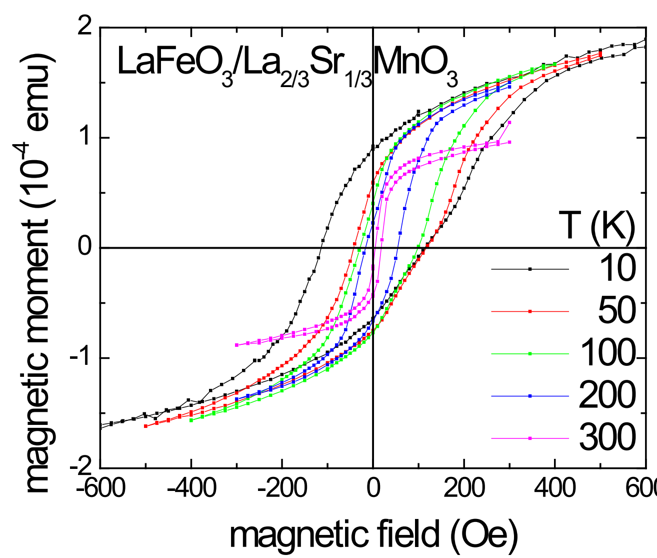

R. C. Black & F. C. Wellstood, *Measurements of Magnetism and Magnetic Properties of Matter*, Chapter 12 in *The SQUID Handbook, Vol. II*

IV.b Biomagnetism

detection of magnetic fields (currents, magnetic particles, nuclear spins) in living organisms, in particular humans

- Magneto-encephalograpy (MEG) → brain currents
- Magneto-cardiograpy (MCG) → heart currents
- Magneto-neurograpy (MNG) → action currents in nerves
- Liver-susceptometry → the only non-invasive method for quantitative determination of Fe-concentration in the liver
- Magneto-gastrography (MGG) & -enterography (MENG)
  → currents due to spontaneous activity of stomach & intestine muscles (MGG)
  → magnetic marker → mobility/transport in stomach-intestine (MENG)
- Magnetic relaxation immunoassays (MARIA)
  → magnetic relaxation of marker, coupled to antibodies
  → detection of smallest concentrations of specific stubstances (hormone, virus, …)
- Low-field magnetic resonance imaging (MRI)
  → simpler MRI systems; cancer diagnosis

J. Vrba, J. Nenonen & L. Trahms, *Biomagnetism*, Chapter11 in *The SQUID Handbook, Vol. II*

Magnetoencephalography (MEG)

Detection of brain currents → $B \sim pT - fT$

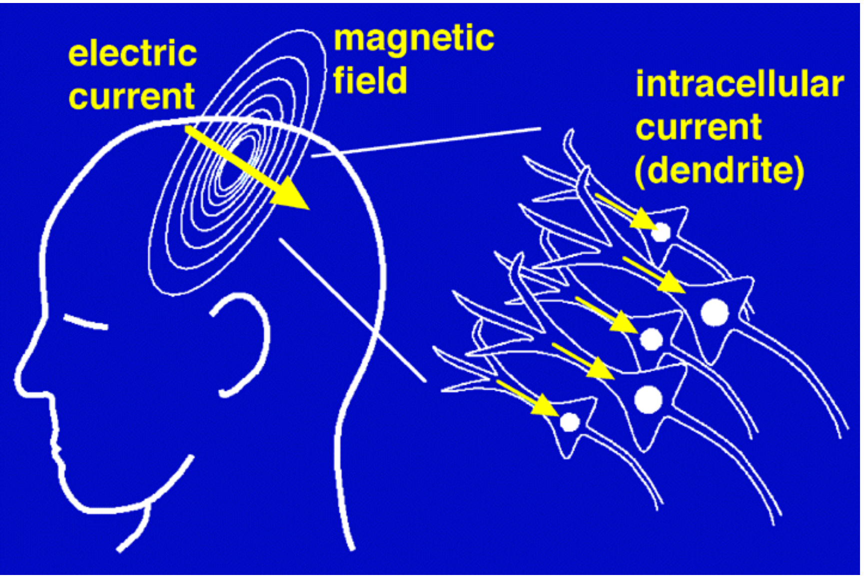

comparison:

magnetic ↔ electric

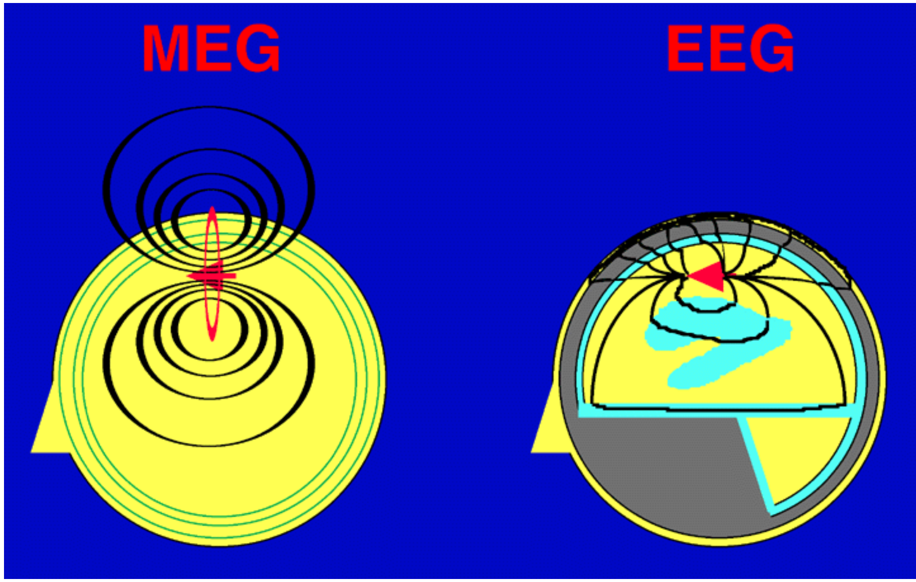

CTF Systems Inc.: MEG Introduction: Theoretical Background (2001); http://www.ctf.com

EBERHARD KARLS UNIVERSITÄT TÜBINGEN

MEG with SQUIDs

multichannel SQUID systems → imaging

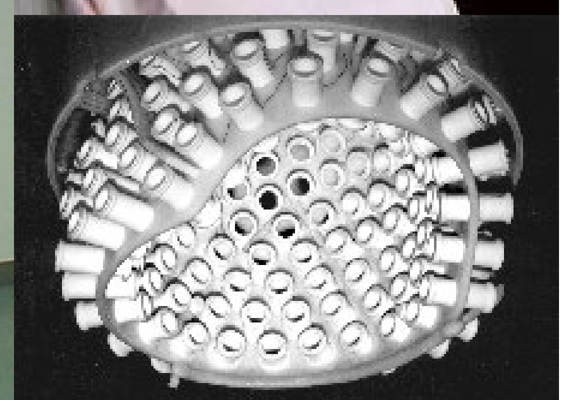

EEG (Electro~)

SQUID system:
>100 channels,
He cooling (T=4.2K)

W. Buckel, R. Kleiner, Superconductivity, Wiley-VCH (2004)

Diagnosis of Focal Epilepsy

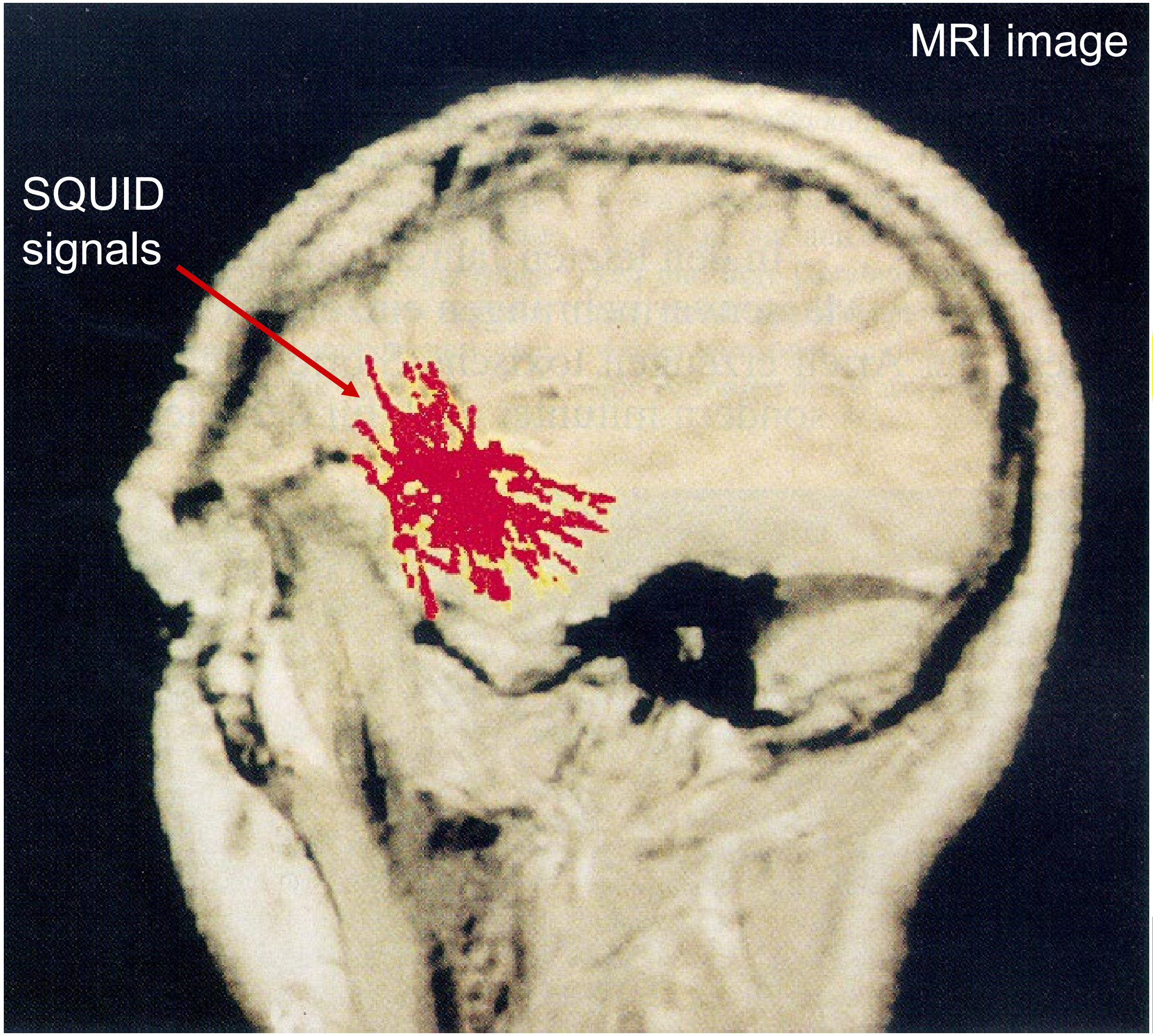

localized
neural defect

magnetic
field pulses

J. Clarke, Scientific American
08/1994

Magnetic Resonance Imaging (MRI) in Low Magnetic Fields

conventional Tesla-MRI:

detection of magnetization $M \propto \mu_p B_0 / k_B T$
(proton spins μ_p in magnetic field B_0)
at frequencies $\omega_0/2\pi = B_0 \cdot 42.6$ MHz/T
with induction coils $V \propto dM/dt \propto \omega_0 B_0 \propto B_0^2$

precession with frequency
$\omega_0 = \gamma B_0$

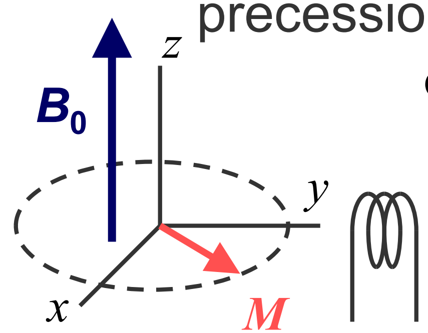

Siemens Healthcare MAGNETOM Area 1.5T

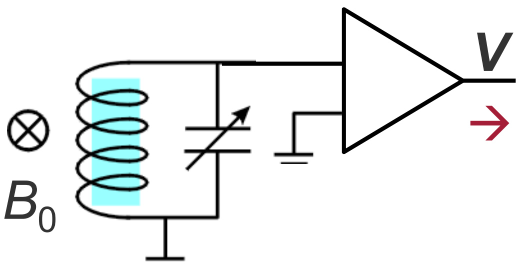

Tesla fields

→ enormously high requirements for homogeneity of B_0

SQUID-based MRI: $V \propto M \propto B_0$ (ultra-) low fields (≤mT)

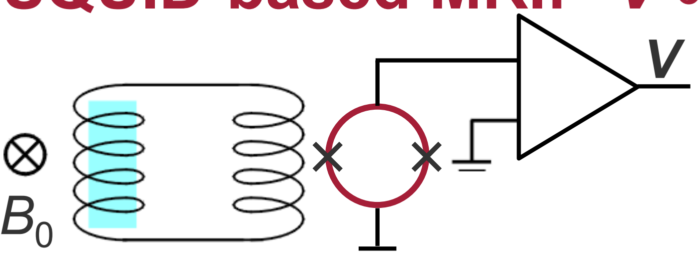

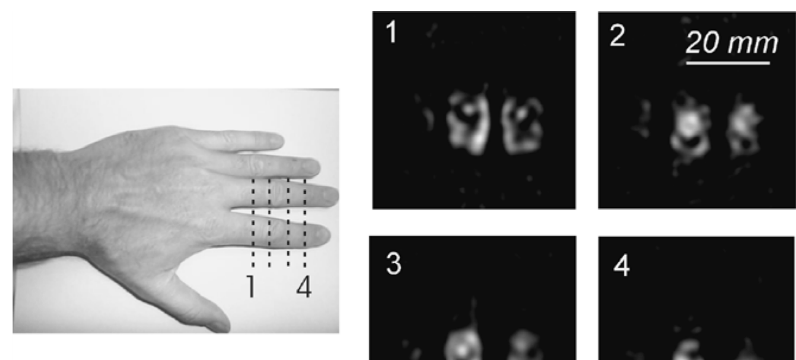

B_0 = 132 μT

prepolarization with extra coil or
hyperpolarization of spins:
→ M and V is independent of B_0

Mössle *et al.*, IEEE Trans. Appl. Supercond. **15**, 757 (2005)

Advantages of Low-Field MRI

EBERHARD KARLS UNIVERSITÄT TÜBINGEN

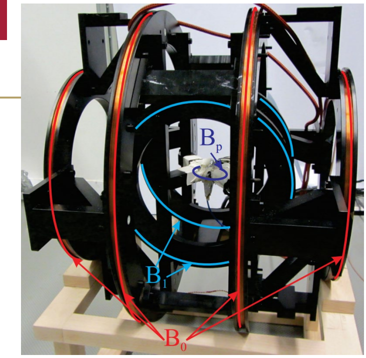

+ no superconducting coils → cheap, mobile systems

+ extremely narrow line width

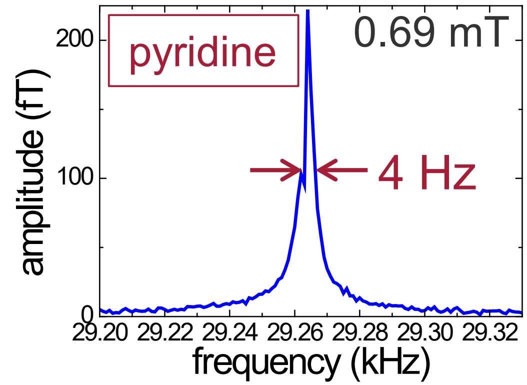

Buckenmaier *et al.*, Rev. Sci. Instr. **89**, 125103 (2018)

+ broad band readout
  → simultaneous detection of various nuclei

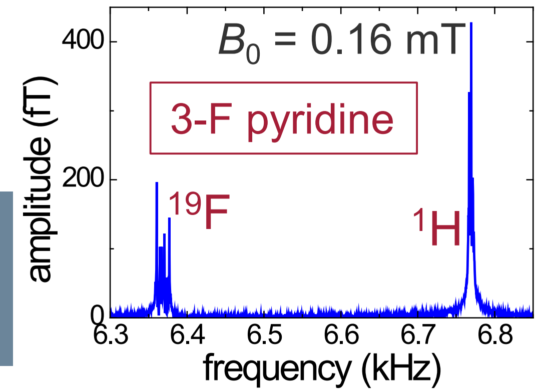

+ avoids artefacts from metals → monitoring of biopsies

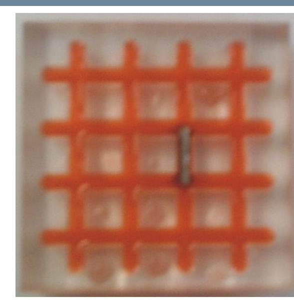

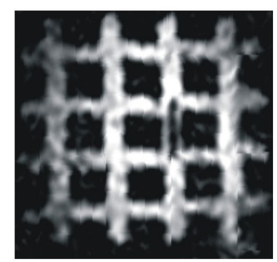

M. Mössle, UC Berkeley

+ enhanced image contrast at low fields/frequencies → cancer diagnosis

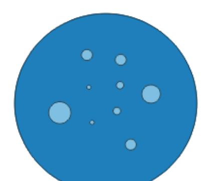

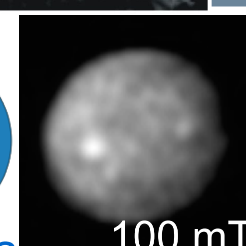

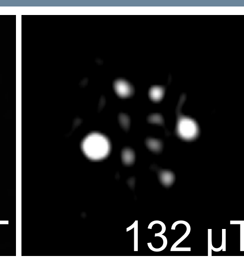

$H_2$0-columns in Agarose-Gel

+ **combine fMRI & MEG**

IV.c Scanning SQUID Microscopy

- **early results in 1990s:**

Fundamental studies on the order parameter symmetry of cuprate superconductors (Kirtley & Tsuei)

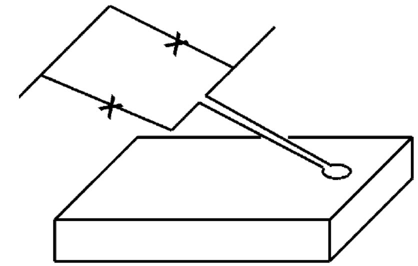

Kirtley, Physica C **368**, 55 (2002)

semifluxon in a YBCO π-loop

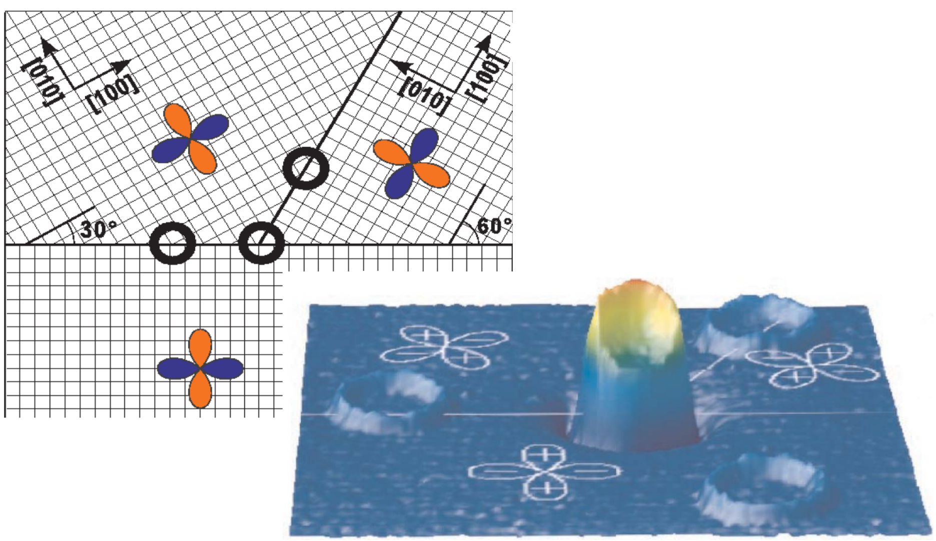

50 μm

semifluxons in YBCO/Nb 0-π junctions

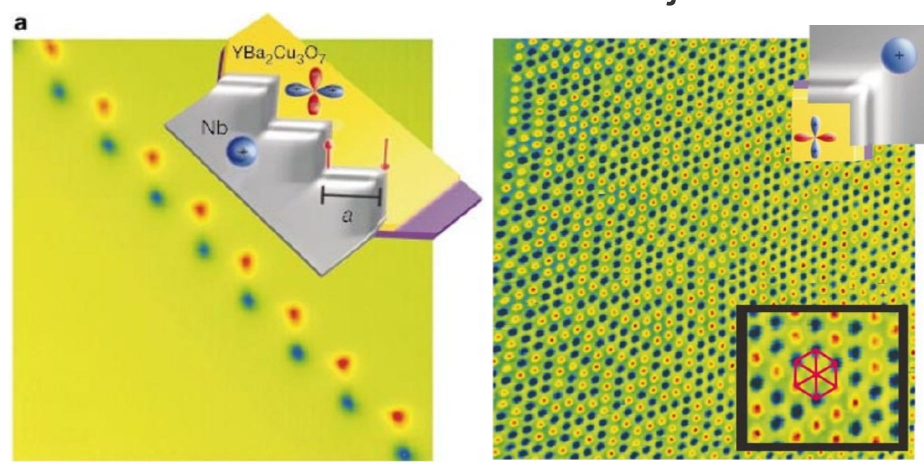

50 μm

50 μm

Tsuei &Kirtley, Rev. Mod. Phys. **72**, 969 (2000)

Hilgenkamp *et al.*, Nature **422**, 50 (2003)

IV.c Scanning SQUID Microscopy

• **today:**

investigation of fundamental properties of a wide range of novel materials

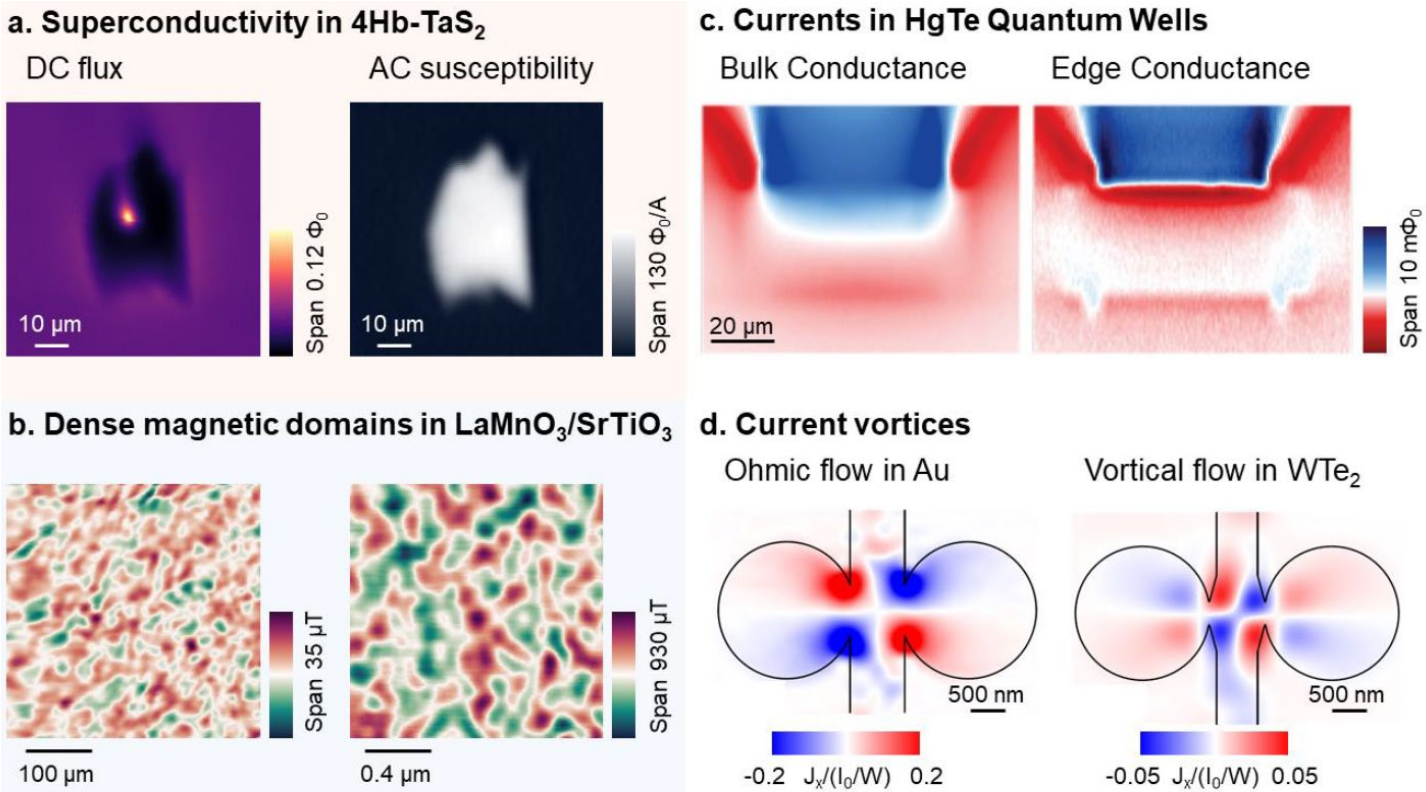

Devidas et al., Sec. 1. *Scanning SQUID Microscopy* in Christensen *et al.*, *2024 Roadmap on Magnetic Microscopy Techniques and Their Applications in Materials Science*, arXiv:2401.04793

See also: Marchiori *et al.*, *Nanoscale magnetic field imaging for 2D materials*, Nature Reviews Physics **4**, 49 (2022)

Conventional scanning SQUID *-on-tip*

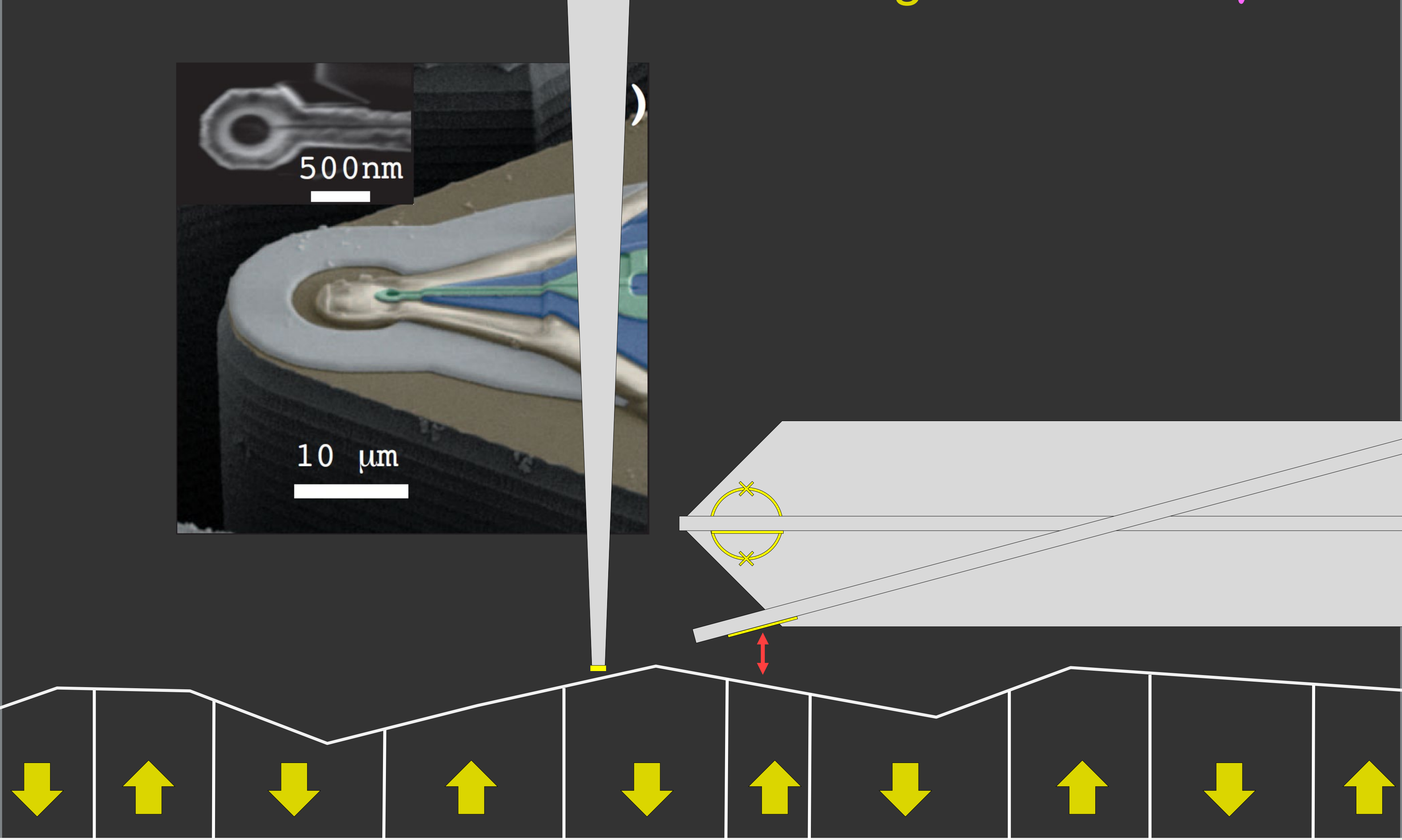

N. Koshnick *et al.*
APL **93** (2008) 243101

courtesy of J. Anahory, E. Zeldov, Weizman Inst. of Science

SQUID-on-tip (SOT)

E. Zeldov (Weizman Inst.)

Al, Pb, Nb, on apex of nanotip (quartz tube, diam. ≥50 nm) → cJJs

fabrication by 3-step shadow evaporation
→ no lithography steps required !

performance depends strongly on applied field

(no flux feedback to maintain optimum working point)

→ not easily applicable for magnetization reversal measurements

- **spin sensitivity 0.38 $\mu_B/Hz^{1/2}$**

(@ 0.5 T; for dipole @ loop center, ⊥ to loop)

- **~ 10 – 100 nm spatial resolution**

breakthrough for scanning SQUID microscopy !

also nanoscale thermal imaging !!

exploits T-dependence of I_c → sensitivity < 1μK/$Hz^{1/2}$

Halbertal *et al.*, Nature **539** (2016); Science **358** (2017)

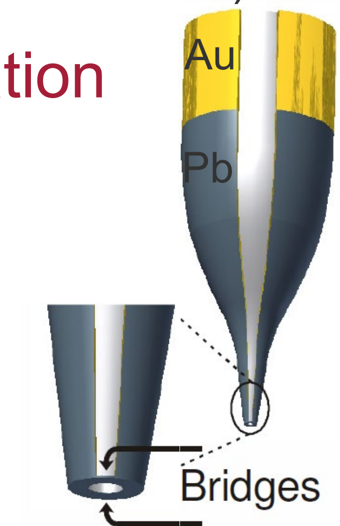

Vasyukov *et al.*, Nature Nanotechnol. **8** (2013)

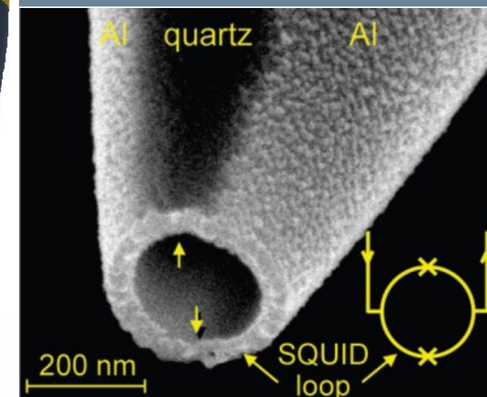

Finkler *et al.*, Nano Lett.**10** (2010)

SOT microscopy @ Basel (Poggio): Imaging FM nanotubes

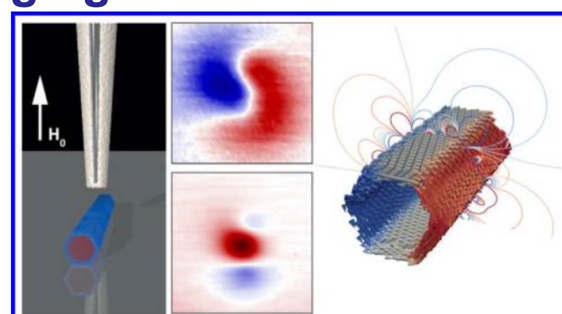

Vasyukov *et al.*,Nano Lett. **18** (2018)

EBERHARD KARLS
UNIVERSITÄT
TÜBINGEN

SQUID-on-lever

- **improve surface approach for scanning SQUID microscopy**

→ SQUID-on-cantilever: Combine topographic AFM imaging with nanoSQUID-based magnetic & thermal imaging

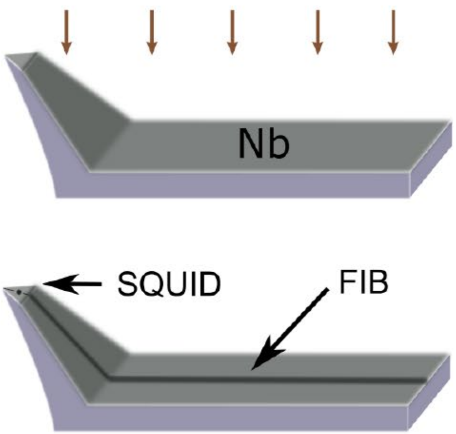

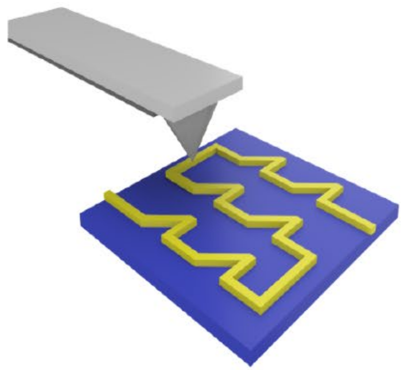

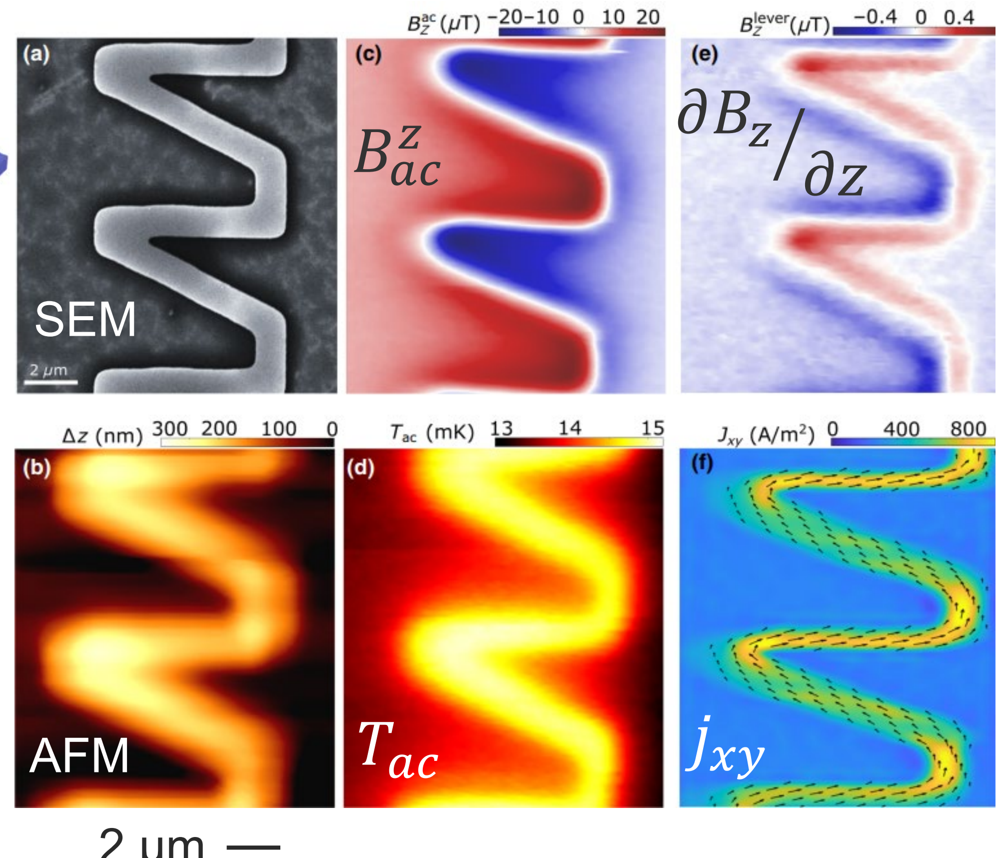

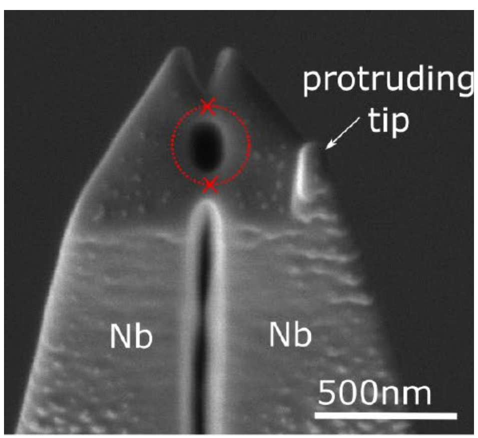

Poggio (Univ. Basel)

M. Wyss *et al.*, Magnetic, thermal, and topographic imaging with a nm-scale SQUID-on-cantilever scanning probe, Phys. Rev. Applied **17**, 034002 (2022)

IV.d nanoSQUIDs for Studies on Magnetic Nanoparticles (MNP)

strongly miniaturized SQUIDs can measure *M*(*H*) hysteresis loops of **individual** MNPs directly → pioneered by W. Wernsdorfer in the 1990s

Wernsdorfer, *Adv. Chem. Phys.* **118**, 99-190 (2001)

principle of detection:

- place particle on constriction in loop
  common approach: constriction-type JJs
- apply external magnetic field ***H***
  (in the loop plane → no flux coupled to loop)
  → switch magnetic moment ***μ***
- detect change of stray field of particle
  → magnetic flux change $\Delta\Phi$ in the loop
  → voltage change ΔV across JJs

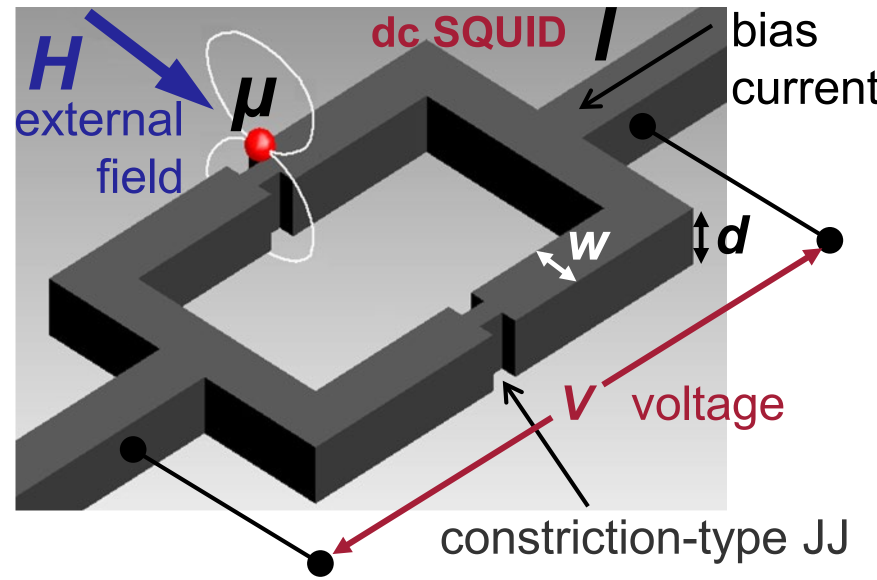

key requirements:
→ ultra-low SQUID noise
→ strong coupling
→ robust operation in strong & variable fields

nanoSQUIDs for MNP Studies: Spin sensitivity

sensitivity determined by

- **flux noise:** rms spectral density of flux noise $S_\Phi^{1/2}$ $[\Phi_0/\mathrm{Hz}^{1/2}]$
- **coupling factor** $\phi_\mu = \dfrac{\text{magnetic flux } \Phi \text{ (coupled into SQUID loop)}}{\text{magnetic moment } \mu}$ $[\Phi_0/\mu_B]$

  μ_B: Bohr magneton

  depends on particle position, orientation of moment and SQUID geometry

spin sensitivity: $\boxed{S_\mu^{1/2} = S_\Phi^{1/2} / \phi_\mu}$ **smallest amount of spin flips detectable in 1 Hz bandwidth**

units: $[\mu_B/\mathrm{Hz}^{1/2}]$

$$S_\mu^{1/2} = \frac{\mu\Phi_0/\mathrm{Hz}^{1/2}}{10\ \mathrm{n}\Phi_0/\mu_B} = 100\ \mu_B/\mathrm{Hz}^{1/2}$$

improvements in minaturization & sensitivity

$S_\mu^{1/2} < 1\ \mu_B/\mathrm{Hz}^{1/2}$ demonstrated with SOT
→ SQUID microscopy !

Vasyukov *et al.*, Nature Nano **8**, 639 (2013)

Granata & Vettoliere, Phys. Rep. **614,** 1 (2016)
Martínez-Pérez & Koelle, Phys. Sci. Rev. **2**, 20175001 (2017)

Magnetization Reversal of Co MNPs

polycrystalline Co nanopillars grown by focused electron-beam-induced deposition (FEBID)

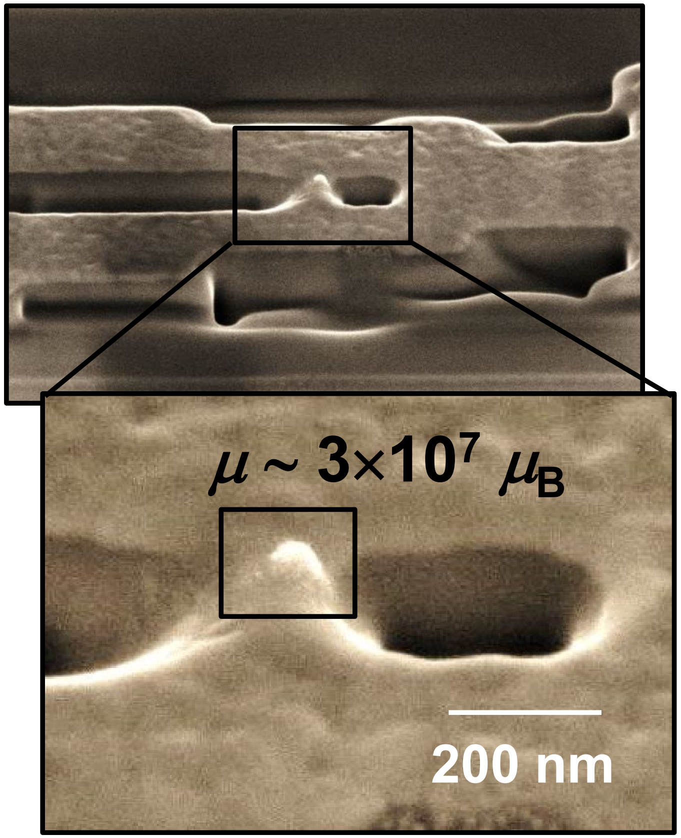

with J. Sesé (INA Zaragoza)

single & multidomain states depending on particle size

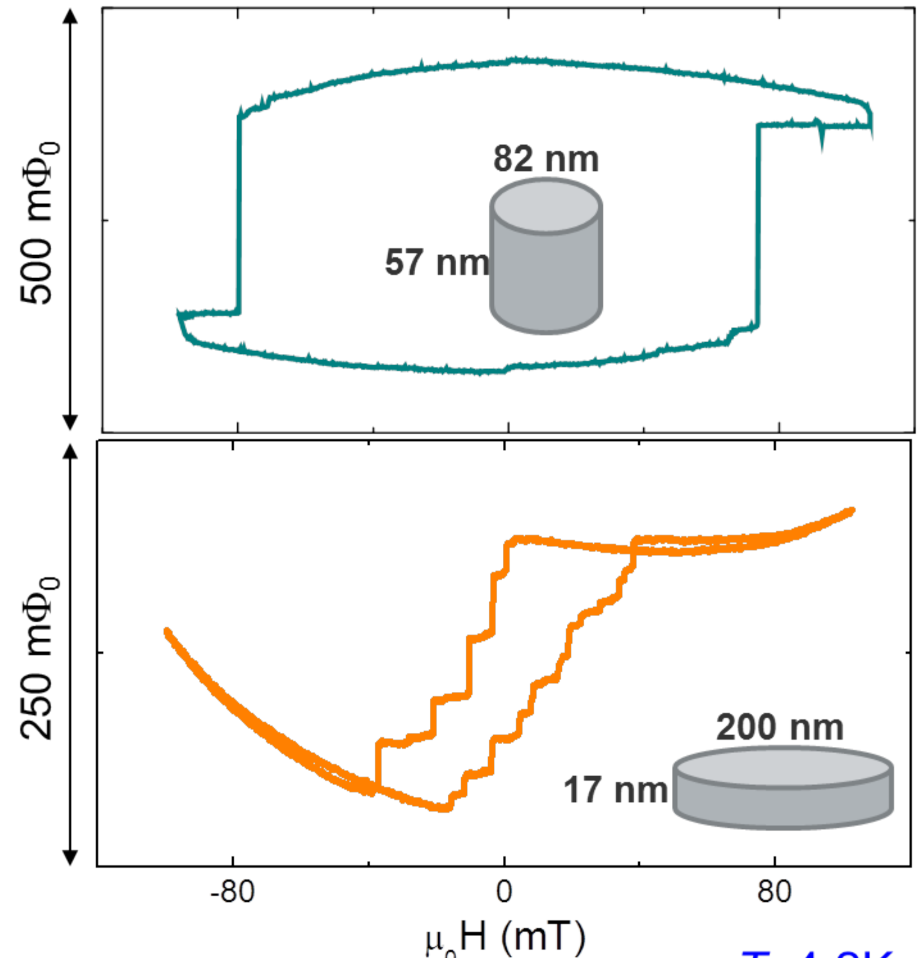

T=4.2K

Martínez-Pérez *et al.*, Supercond. Sci. Technol. **30**, 024003 (2016)

Magnetization Reversal of Co MNPs

single domain particles: *T* dependence

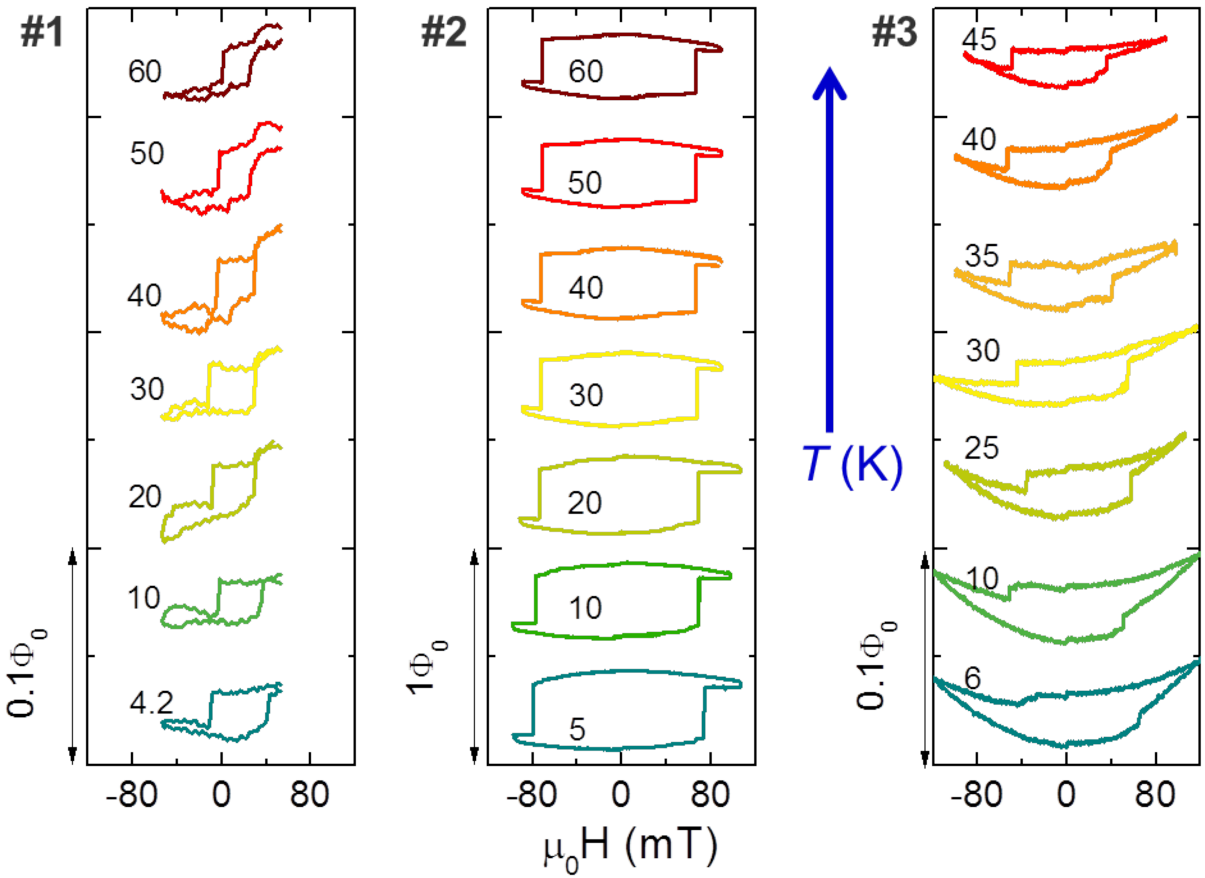

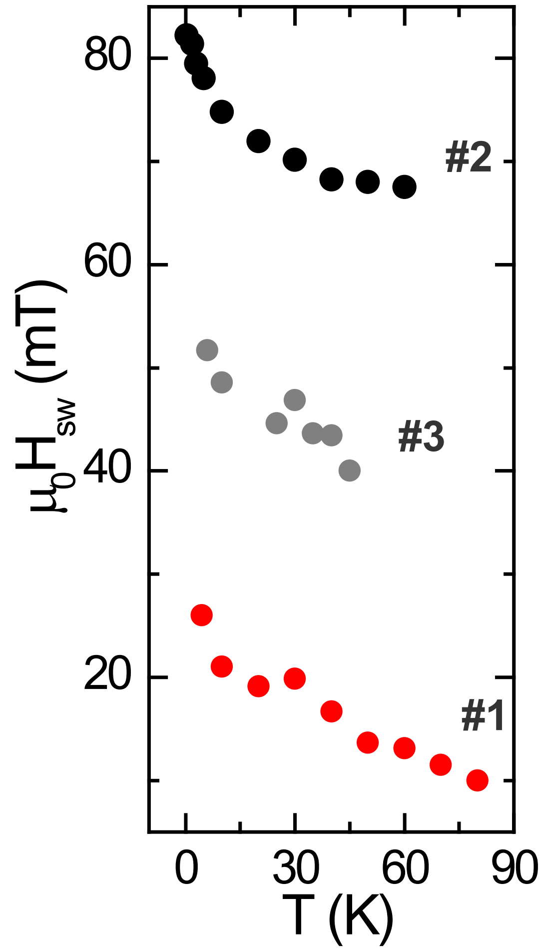

switching fields H_{sw} vs *T*

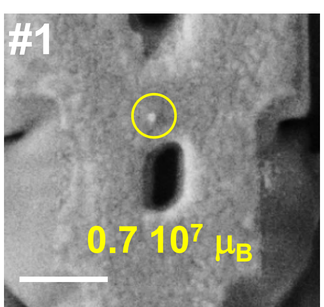

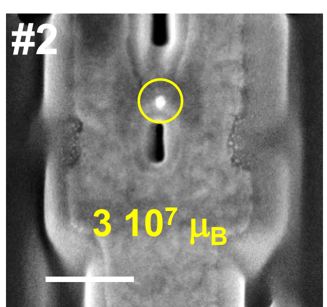

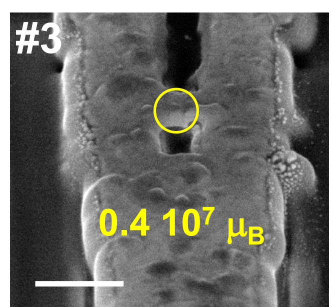

Martínez-Pérez *et al.*, Supercond. Sci. Technol. **30**, 024003 (2016)

Magnetization Reversal of Co MNPs

single domain particles: *T* dependence

classical thermally activated reversal process over energy barrier

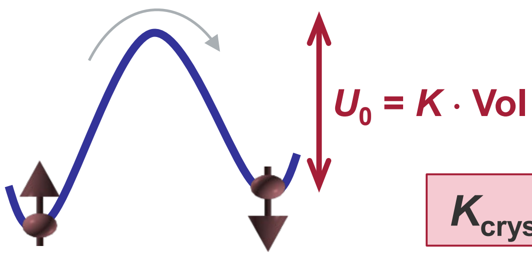

K_{crys} (bulk Co) ~ 260 kJ/m^3

$$H_{sw} = H_{sw}^{0}\left\{1 - \left[\frac{k_B T}{U_0} ln\left(\frac{k_B T H_{sw}^{0}}{2\tau_0 U_0 v(1 - H_{sw}/H_{sw}^{0})}\right)\right]^{1/2}\right\}$$

J. Kurkijärvi, Phys. Rev. B (1971)

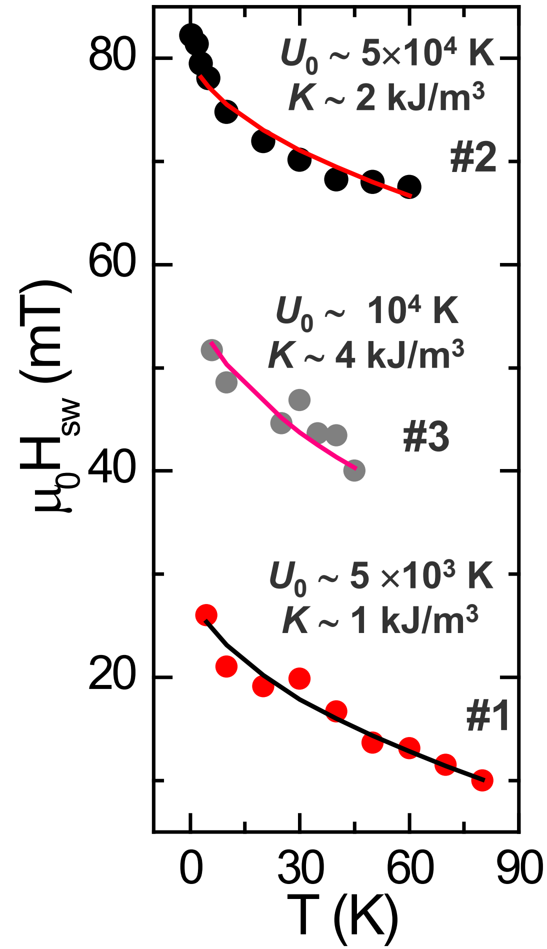

Martínez-Pérez *et al.*, Supercond. Sci. Technol. **30**, 024003 (2016)

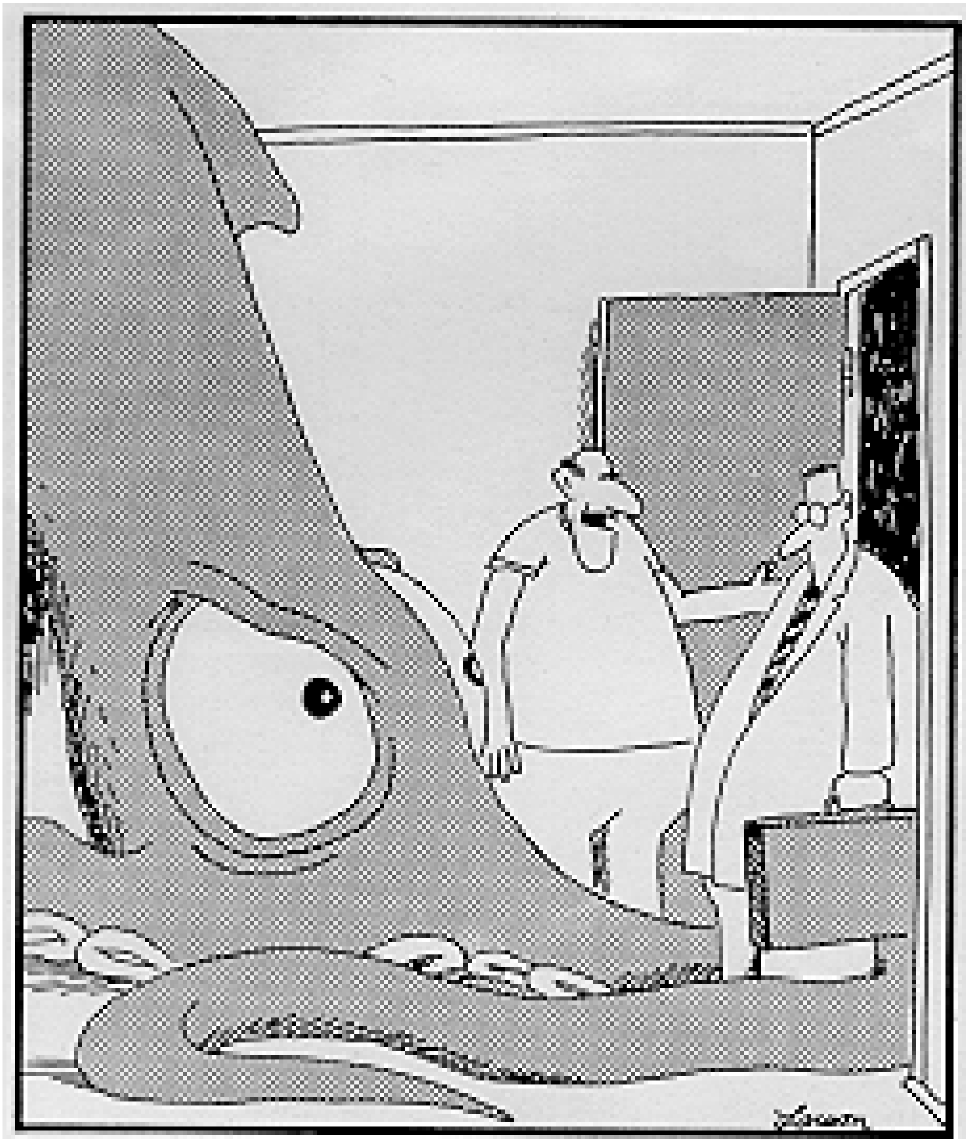

„Oh, no, he's quite harmless. ...

Just don't show any fear. ...

SQUIDs can **sense** fear.“